LAPPEENRANTA UNIVERSITY OF TECHNOLOGY
Faculty of Technology
Department of Chemical Technology

Drug loading of mesoporous silicon particles

Master's Thesis

Examiners: Professor Juha Kallas
Docent Marjatta Louhi-Kultanen

Supervisors: Docent Marjatta Louhi-Kultanen
Ph.D. Haiyan Qu

Lappeenranta 3.11.2008

Sanna Ojanen
Korpimetsänkatu 6-8 A 16
53850 LAPPEENRANTA
Finland
Tel. +358 5 621 2136

ABSTRACT

Author	Sanna Ojanen
Title	**Drug loading of mesoporous silicon particles**
Faculty	Faculty of Technology
Degree programme	Chemical Technology
Year	2008

Master's Thesis, Lappeenranta University of Technology

111 pages, 18 figures, 12 tables and 4 appendices

Examiners	Prof. Juha Kallas Docent Marjatta Louhi-Kultanen
Keywords	Mesoporous silicon, oral drug delivery, solvent selection, solvent mixtures, thermal analysis, Raman spectroscopy, indomethacin

Porous silicon (PSi) is a promising material to be utilized in drug delivery formulations. The release rate of the drug compound can be controlled by changing the pore properties and surface chemistry of PSi. The loading of a poorly soluble drug into mesoporous silicon particles enhances its dissolution in the body. The drug loading is based on adsorption. The attainable maximum loaded amount depends on the properties of the drug compound and the PSi material, and on the process conditions. The loading solvent also essentially affects the adsorption process.

The loading of indomethacin into PSi particles with varying surface modification was studied. Solvent mixtures were applied in the loading, and the loaded samples were analyzed with thermal analysis methods. The best degree of loading was obtained using a mixture of dichloromethane and methanol. The drug loads varied from 7.7 w-% to 26.8 w-%. A disturbing factor in the loading experiments was the tendency of indomethacin to form solvates with the solvents applied. In addition, the physical form and stability of indomethacin loaded in PSi and silica particles were studied using Raman spectroscopy. In the case of silica, the presence of crystalline drug as well as the polymorph form can be detected, but the method proved to be not applicable for PSi particles.

TIIVISTELMÄ

Tekijä	Sanna Ojanen
Työn nimi	**Mesohuokoisten piipartikkelien lääkelataaminen**
Tiedekunta	Teknillinen tiedekunta
Koulutusohjelma	Kemiantekniikka
Vuosi	2008

Diplomityö, Lappeenrannan teknillinen yliopisto

111 sivua, 18 kuvaa, 12 taulukkoa ja 4 liitettä

Tarkastajat	Prof. Juha Kallas Dosentti Marjatta Louhi-Kultanen
Hakusanat	Mesohuokoinen pii, oraalinen lääkeannostelu, liuotinvalinta, liuotinseokset, termoanalyysi, Raman-spektroskopia, indometasiini

Huokoinen pii (PSi) on lupaava materiaali lääkevalmisteissa käytettäväksi. Lääkeaineen liukenemisnopeuteen voidaan vaikuttaa PSi:n huokosominaisuuksia ja pintakemiaa muokkaamalla. Niukkaliukoisen lääkkeen lataaminen mesohuokoisiin piipartikkeleihin edistää sen liukenemista elimistössä. Lääkelataus perustuu adsorptioon. Saavutettavissa oleva maksimilatausmäärä riippuu PSi-materiaalin ja lääkeaineen ominaisuuksista sekä olosuhteista. Myös latauksessa käytettävä liuotin vaikuttaa olennaisesti adsorptioprosessiin.

Tässä työssä tutkittiin indometasiinin adsorptiota eritavoin pintakäsiteltyihin PSi-partikkeleihin. Latauksessa käytettiin liuotinseoksia, ja ladatut näytteet analysoitiin termoanalyysimenetelmin. Paras latausaste saavutettiin dikloorimetaanin ja metanolin seoksella latausasteiden vaihdellessa 7,7 %:sta 26,8 %:iin. Häiritsevä tekijänä latauskokeissa oli indometasiinin taipumus muodostaa solvaatteja käytettyjen liuottimien kanssa. Lisäksi PSi- ja silika-partikkeleihin ladatun indometasiinin kiinteää olomuotoa ja stabiilisuutta tutkittiin Raman-spektroskopiaa käyttäen. Silikan tapauksessa lääkkeen esiintyminen kiteisessä muodossa, kuten myös sen polymorfinen muoto pystytään selvittämään, mutta menetelmä osoittautui PSi-partikkeleille soveltumattomaksi.

CONTENTS

List of symbols and abbreviations

a	constant of Freundlich equation, -
b	constant of Langmuir equation, m^3/mol
B	constant of the Jouyban-Acree model, -
c	concentration, mol/m^3
c^0	1 mol/m^3
c_{drug}	concentration of the loading solution, kg drug / m^3
c_e	equilibrium concentration, mol/m^3
c^*	saturation concentration, kg drug / m^3
D	pore diameter, m
D_p	diffusion coefficient inside pores, m/s.
f_i	mole fraction of solvent *i* in a solvent mixture, -
k	constant of Freundlich equation, mol/kg
p_v	vapor pressure, kPa
q	loaded amount, g drug / g
q_e	adsorbed amount at equilibrium, mol/kg adsorbent
q_m	maximum adsorbed amount, mol/kg adsorbent
$q_{max,\ theor}$	theoretical maximum loaded amount, g drug / g (drug + dry adsorbent)
$q_{min,\ theor}$	theoretical minimum loaded amount, g drug / g (drug + dry adsorbent)
$q_{surface}$	surface fraction, g crystalline drug / g drug
r	radial distance from the centre of the particle, m
R	universal gas constant, 8.315 J / (mol K)
t	time, s
T	temperature, K
T_b	boiling point, K
T_g	glass transition temperature, K
T_m	melting point, K
T_0	melting point of the crystalline drug, K
V_m	molar volume, m^3/mol
V_s	pore volume, mL/g dry adsorbent
w_i	mass fraction of solvent *i* in a solvent mixture, -
x_i	mole fraction solubility in solvent *i*, -
x_m	mole fraction solubility in a solvent mixture, -
x_2	mole fraction of solute in a solution, -
γ	surface free energy, J/m^2
γ_{sl}	surface energy at the solid–liquid interface, J/m^2
δ	solubility parameter, $MPa^{0.5}$
$\overline{\delta}$	effective Hildebrand's solubility parameter, $MPa^{0.5}$
δ_d	dispersion term, $MPa^{0.5}$
δ_p	polar term, $MPa^{0.5}$
δ_h	hydrogen bonding term, $MPa^{0.5}$
ΔC_p	difference between heat capacities crystalline and supercooled liquid form at temperature *T*, J/(mol K)
ΔE_v	energy of vaporization, J
ΔH_f	enthalpy of fusion, J /kg
ΔH_{f0}	enthalpy of fusion of the crystalline drug, J/kg

ΔH_{mix}	enthalpy of mixing, J/mol
ΔH_v	enthalpy of vaporization, J /kg
ΔT	depression of melting point, K
ΔV_{mix}	volume of mixing, m^3
ε	permittivity (dielectric constant), -
ε_p	porosity of the particle, -
η	dynamic viscosity, mPa s
ρ	density, kg m^{-3}
σ	surface tension, N/m
ϕ_i	volume fraction of *i*, -

Abbreviations

API	Active pharmaceutical ingredient
CCD	Charge couple device
CED	Cohesive energy distribution
COSMO-RS	Conductor-like screening model for real solvents
DCM	Dichloromethane
DMSO	Dimethyl sulfoxide
DSC	Differential scanning calorimetry
DTA	Differential thermal analysis
EHS	Environment, health and safety
EtOAc	Ethyl acetate
EtOH	Ethanol
FT	Fourier transform
HPLC	High performance liquid chromatography
HTS	High throughput screening
ICH	Internatational Conference of Harmonization
IMC	Indomethacin
MeOH	Methanol
NIR	Near infra red
PDE	Permitted daily exposure
PSi	Porous silicon
QMS	Quadrupole mass spectrometry
QSPR	Quantitative structure property relationship
STA	Simultaneous thermal analysis
TEOS	Tetraethylorthosilicate
TG	Thermogravimetry
THCPSi	Thermally hydrocarbonized porous silicon
TCPSi	Thermally carbonized porous silicon
TOPSi	Thermally oxidized porous silicon
USP	The United States Pharmacopeia

Acknowledgements

This master's thesis is part of ComPSi-project (Composite mesoporous materials as oral drug delivery vehicles) that is a co-operation project of University of Turku, University of Helsinki and Lappeenranta University of Technology. Financial support from Academy of Finland is acknowledged (project 123037).

First of all, I would like to thank my supervisors Marjatta Louhi-Kultanen and Haiyan Qu who have been patiently advising and encouraging me. I thank professor Juha Kallas for his valuable comments.

I would also like to thank all the other participants of the ComPSi-project. I am especially grateful to Teemu Heikkilä for giving good advices for the loading experiments and for sending PSi particles and loaded samples, as well as providing us with data such as the results of nitrogen adsorption measurements. Special thanks also to Ermei Mäkilä for the production of the PSi particles.

My warmest thanks belong to Liisa Puro and Jouni Pakarinen for all the help and for the excellent collaboration of our "thermal analysis team". Together we managed to solve all the numerous problems I encountered with the TA instruments. In addition, Liisa made the calibration of DSC. I also thank Hannu Alatalo for his friendly help during my laboratory experiments and Anne Hyrkkänen for giving the opportunity to use the density meter.

I thank Mari Tiilikainen for helping me with English. I also owe thanks to all of my friends and to my parents for all the support. Finally, thanks to Mikko for love and patience.

1 Introduction

The bioavailability of poorly soluble pharmaceutical compounds can be improved using porous carrier materials. Mesoporous silicon is a promising material with several important properties advantageous to drug delivery applications. One of the most important steps in the research and development of the mesoporous silicon based drug delivery technology is the optimization of the drug loading process.

Drug loading into porous materials is typically based on adsorption from a solution. Optimization of a drug loading process involves a selection of several parameters. One of the most crucial factors affecting the drug loading is the selection of a loading solvent. Solvent selection is a demanding task, and no models or rules are yet established for predicting the loading capacities attainable using different loading solvents. Furthermore, a complete removal of the solvent is an imperative to ensure the safety of the final product.

Binary solvent mixtures are known to provide in some cases higher solubilities than either of the neat solvents. Adding a co-solvent into the loading solution may have a positive effect on the drug loading, as reported by several authors, e.g. [1, 2]. In the light of these papers, the selection of the solvents and their ratio seems quite random since the reasons for the decisions are not explained, and a further investigation into the subject is therefore needed.

In the experimental part of this work, the loading of a typical poorly soluble model compound, indomethacin, into mesoporous silicon particles is studied. Since an adsorption process is crucially dependent both on the drug compound and on the adsorbent, universal models cannot be developed based on this limited experimental data but the determination of the interactions occurring in various solvent systems will give some basis for predicting the suitability of loading solvents for other chemically related drug compounds as well. The main analysis methods utilized are thermal analysis and Raman spectroscopy.

2 Poor solubility – a challenge in drug delivery

The majority of novel innovative drug candidates suffer from poor pharmacokinetics [3] and that reduces their bioavailability, especially in oral drug delivery that is still the most common and preferable administration route. Since the problems with pharmacokinetics are usually related to the poor solubility of the drug compound, one of the main challenges in pharmaceutical industry is to find ways to enhance solubility without compromising the stability and the pharmaceutical activity.

The number of poorly soluble compounds among the pharmaceuticals under development increased rapidly in the beginning of 1990s, straight after high-throughput screening (HTS) was introduced in the drug discovery. HTS greatly intensified the generation of leads, but the drawback of this new method was that it also caused a shift towards leads with higher molecular weights and lipophilicity; properties that are typically related to low aqueous solubility. [4]

There are several different methods to enhance solubility of a crystalline compound, for instance to increase the surface area by reducing the particle size or to use a form that possesses a less ordered crystal structure. Amorphous solids, for example, may typically have 2–4 times higher solubility than the crystalline forms [5]. The use of pharmaceuticals in the amorphous state is, however, limited since the stability requirements set for pharmaceutical products are seldom met. Immobilization of the amorphous drug compounds into a porous carrier may help to overcome the stability problems.

2.1 Role of solubility in the oral absorption of pharmaceuticals

An oral absorption process includes two steps: dissolution into intestinal fluid and permeation through the intestinal membrane. Figure 1 depicts the three main causes of poor absorption with a bucket model. The bioavailability of a drug may be limited by low dissolution rate (A), by poor permeability (B), or by low solubility (C).

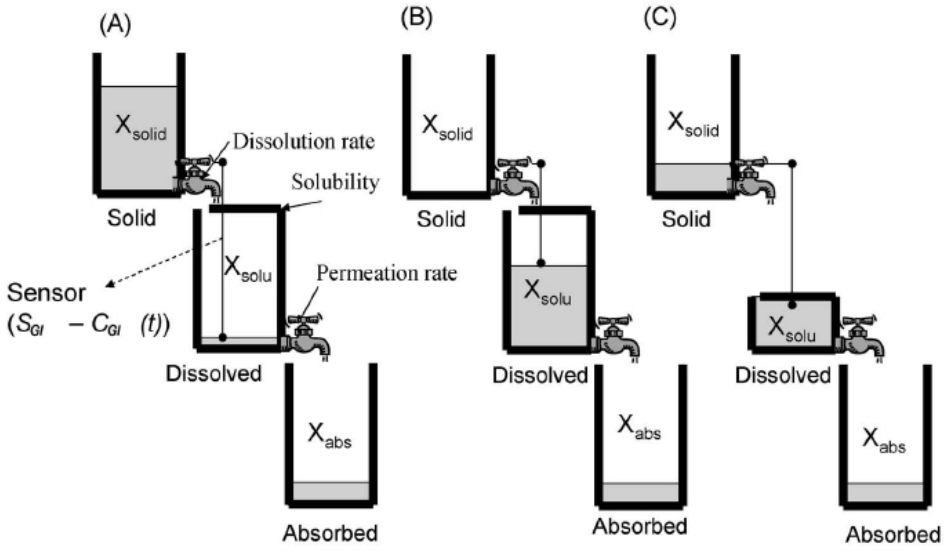

Figure 1. Limiting factors in oral absorption: (A) dissolution rate, (B) permeability, (C) solubility [6].

The permeability of an active pharmaceutical ingredient (API) is determined already at the drug discovery stage. It is dependent on the chemical structure of the drug, and thus it is difficult to improve in the drug design stage. The solubility and dissolution rates, in contrast, are also dependent on the form of the API, on the drug formulation, and on the selection of excipients [6]. An interested reader is referred to the conference report of Stegemann *et al*. [7] which gives a comprehensive review on the role of the poor solubility of a drug candidate throughout the drug development process and examples of strategies typically used for improving solubility.

It should be borne in mind that, besides the drug formulation, the conditions in the human body affect the dissolution, too. This can be exploited in controlling drug release. Drug molecules are often weak bases by nature, and their dissolution occurs through protonation in the acidic body fluids. Fasting gastric pH ranges between 1.5 and 2 for young, healthy people [8]. A malfunction called hypochlorhydria may reduce gastric acidity. This problem is encountered often among elderly and HIV patients. If the gastric acidic secretion is significantly diminished, the pH in the stomach may increase in some cases even above 5,

which obviously abates the drug dissolution [9]. Cases of this kind give an extra challenge for the development of pharmaceutics.

2.2 Porous materials as solubility enhancers

The use of a porous drug carrier may enhance the dissolution of API. The function is based on two factors: increasing the active surface area and reducing the crystallinity of the pharmaceutical substance. Decrease in crystallinity often leads to problems with stability, since the non-crystalline, disordered form has a high chemical potential and thus tends to transform to a crystalline form of a lower energy state. The porous carrier may, however, hinder or prevent these transformations by physically protecting the amorphous drug. Furthermore, loading of the drug substance into porous particles has been observed to enhance permeation [10].

The interactions occurring between the drug molecules and the surface of the carrier are of a great importance. First of all, they enable the drug loading. If there is no affinity between the drug and the surface of the pores, it is not probable that a satisfactory degree of loading can be achieved. Secondly, the interactions have also been proposed to play a key role in the stabilization of the disordered drug in the pores [11].

It has been also proposed that a small pore size is an important factor in the stabilization of the disordered drug [12]. The pores are usually small enough to restrict the formation of an organized crystal structure inside them, and thus the loaded compound is forced to stay in the amorphous form and the phase transitions upon storage are prevented. The structure of the carrier may also protect the loaded compound from external attacks by causing a steric hindrance. This kind of protection is especially needed for peptides which are vulnerable to enzymatic degradation in the body [13].

Dissolution of a drug that has been loaded into porous material is a bit more complicated process compared to that of the pure crystalline drug. If the carrier material is biodegradable, the dissolution of the drug is related to the

decomposition of the carrier. Otherwise, the mass transfer from the pores determines the dissolution rate. If the drug–carrier interactions are strong, desorption may be the rate determining step in the dissolution process in exchange to the mass transfer. If rapid dissolution is aimed at, strong interactions are not favorable. In the case of certain carrier materials, different dissolution rates can be achieved depending on surface modification and porosity. This unique feature can be exploited for controlling the drug release; either sustained or accelerated release can be attained. A model for the drug dissolution from porous particles has been presented in [14].

Surface pH of the porous material may also affect the dissolution of the pharmaceuticals that ionize within a definite pH-range. For example, calcium silicate and silica gel are known to create an alkaline local environment when moisture is adsorbed on them, and that has been observed to improve the solubility of ibuprofen, an acidic drug [15]. The effect of surface pH might explain the reduction of the pH dependency of the dissolution obtained by loading the drug compound into microparticles, which has been reported in [10, 12].

Porous materials are classified according to their poresize into microporous (pore diameter <2 nm), mesoporous (2–50 nm), and macroporous (>50 nm) materials [16]. Concerning drug delivery, the pore size range of mesoporous materials is advantageous. The mesopores are usually small enough to provide satisfactory protection of the loaded drug, but adequate mass transfer rates can be, however, achieved, which is quite important in both dissolution and drug loading.

Since the diameter of the mesopores is typically several times bigger than the size of the drug molecule, the crystallization inside the pores is not totally impossible. Even though the drug typically is in its amorphous form, it may appear as small, nanosized crystals as well. The solubility of the nanocrystals is much higher than that of the bulk material. Therefore, this form is also advantageous considering drug absorption, and the stability of the product is better than in the case of the amorphous drug. In order to obtain drug loading in a nanocrystal form, extremely careful optimization and control of the loading process is required. Nanoparticles in pharmaceutical applications, in the targeted drug release for instance, are

currently under intensive investigation, and probably some applications combining nanotechnology and porous materials will be seen in the future.

A wide variety of porous carrier materials, both polymeric and inorganic, is available. The major advantage of the inorganic drug carriers over the polymeric ones is their high stability. Application of siliceous materials in drug delivery has been intensively studied. Special attention has been paid to silica materials, especially on the ordered mesoporous silicas [17]. Recently, porous silicon (PSi) has been suggested for various biomedical applications including the oral delivery of poorly soluble pharmaceuticals. The main focus of the present work is on this new, promising drug carrier material. Other silicon based materials, mainly silica, are also shortly reviewed, as they have certain similarities with PSi.

3 Mesoporous siliceous materials and their use in drug delivery

Among the most abundant elements in the earth's crust, silicon is at the second place straight after oxygen with its share of 27.2 % [18]. In nature, silicon mainly occurs as oxygen containing compounds; never in the free elemental form due to its high reactivity with oxygen. Equation (1) presents the oxidation reaction.

$$Si + O_2 \rightarrow SiO_2 \qquad (1)$$

Silicon dioxide (SiO_2) is termed silica. Porous silica is somewhat similar material to PSi, and its use in oral drug delivery applications has been studied more widely than that of PSi. This chapter gives an overview of mesoporous silicon and silica materials.

The first mesoporous silicas, so-called M41S family, were developed in the early 1990s by the scientists of Mobil Oil Corporation [19, 20]. Before that, only microporous materials were available. The most common member of the M41S family is the hexagonally organized MCM-41 (Mobil Composition of Matter), which probably is also the most studied silica material for drug delivery applications [21-23]. Porous silica materials with different structures are presented in table I.

Porous silica molecular sieves have been mainly utilized as catalysts and as adsorbents. Porous silica is advantageous in these applications, since it possesses a high surface area (> 1000 m^2/g for MCM-41 [22]) and a uniform pore structure. Porous silicon is used in microelectronics and optoelectronics, but also in various other applications, even more being under an intensive investigation presently.

Table I Some variations of mesoporous silica [21, 24, 25].

Name	Structure
MCM-41 (Mobil Composition of Matter)	2D-hexagonal, cylindrical pores
MCM-48	3D, bicontinuous, cubic
MCM-50	Lamellar
SBA-1 (University of California at Santa Barbara)	Cage-type, cubic, spherical cavities
SBA-3	Hexagonal, cylindrical pores
SBA-11	Cubic
SBA-12	3D-hexagonal
SBA-15	2D-hexagonal
SBA-16	Cubic
KIT-1 (Korea Advanced Institute of Science and Technology)	Disordered
MSU-X (Michigan State University)	Disordered
TUD-1 (Technische Universiteit Delft)	3D, foam-like

Fabrication, properties, and biomedical applications of mesoporous silicon and silicas are next discussed. The fabrication processes of porous silicon and silica differ from each other a lot. Based on the fabrication technique, porous silicon materials are denoted as “top-down” materials, and silicas, on the contrary, as “bottom-up” materials [14]. Porous silicon is fabricated from Si substrate by etching it to form pores. Porous silica materials, on the other hand, are synthetic, and the pores are already formed upon the synthesis. Concerning the application of a material in drug delivery, chemical, physical, and also biological properties including toxicity must be taken into account. The surface chemistry of the carrier material plays a key role in the drug loading, and thus a special attention has to be paid to it.

3.1 Fabrication of mesoporous silicon

Porous silicon is fabricated by etching a silicon substrate. Porous silicon for drug delivery is not yet produced in a large scale, and thus the fabrication costs are still high. The scale-up of the production should not, however, be a problem. Due to the abundance of PSi applications in electronics, the global capacity to produce porous silicon is high, and the purity level that can be achieved is sufficient or even higher than required for biomedical applications [26].

The pore morphology of PSi is dependent on the properties of the initial Si substrate and on the fabrication parameters [27], which are discussed in chapter 3.1.1. The porosity of PSi varies typically from 40 to 80 % [28]. The possibility to control the pore formation quite easily is one of the major advantages of PSi. It allows the porous carrier matrix to be tuned for the drug molecules of certain size. Compared to porous silica, the pore size distribution tends to be slightly wider, but still satisfactory for drug delivery applications [26].

The raw materials for the production of porous silicon are presented in table II. As PSi is fabricated in laboratory, silicon substrates of the purest available grade, Si wafers, are used. As soon as the production in industrial scale starts, it is possible to shift into less expensive Si raw materials. According to Hirvonen *et al*. [14], the grade utilized for solar cells provides sufficient purity for pharmaceutical PSi. Furthermore, producing wafers from silicon ingots is not necessary: the ingots can be utilized directly.

Table II Silicon raw materials of different grades [14].

Grade of Si	**Industrial use**	**Purity (%)**	**Cost ($/kg)**	**Global production (t)**
Wafer	Electronics	99.99999	1000	5,000
Electronic	Si crystals	99.999	10–100	19,000
Solar	Solar cells	99.99	10–50	26,000
Chemical	Silicones	99.9	10	675,000
Metallurgical	Steel	97–99	1–5	1,000,000

Based on the silicon substrates, PSi materials are classified into four groups: n, p, n+, and p+. The division into n-type and p-type tells whether the function of a Si semiconductor is based on electrons or on holes. Free holes or electrons are formed upon a doping process, in which an impurity atom is added to the Si-lattice. The elements of group 13 (IIIA), e.g. P, As, or Sb, provide an electron, and are used in manufacturing n-type Si. Doping with the elements of group 15 (VA) forms p-type Si. Concerning p-type Si, one of the most used dopants is boron. Mesoporous structures obtained may vary a lot depending on the doping of the Si substrate used. Usually the low-doped n-type PSi and p-type PSi provide a finer pore structure and a larger specific surface area than the highly-doped PSi of type n+ or p+ [29].

3.1.1 Etching

Porous silicon is typically produced from Si via electrochemical dissolution HF based electrolyte solutions. Figure 2 illustrates the simplest anodization cell used in the fabrication of porous silicon. The cell is made of Teflon or some other HF resistant material, and the cathode is made of platinum. The Si substrate acts as a positive anode, and the PSi layer is formed onto its surface. Either anodic current or voltage is monitored. The use of a constant current facilitates the control of porosity and thickness and yields better reproducibility. [27]

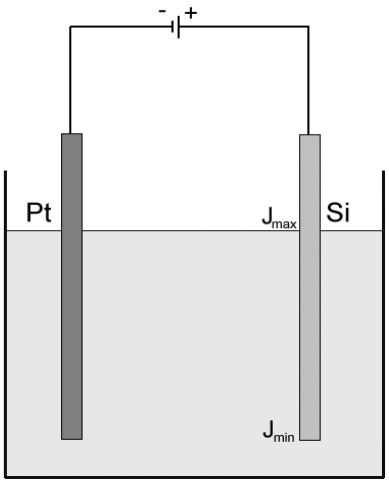

Figure 2. Simple anodization cell (reproduced from [27]).

The dissolution mechanism of Si is not completely clear yet. Two different reaction routes are, however, recognized: the indirect dissolution via oxidation or direct dissolution. The indirect dissolution is likely to occur in dilute aqueous HF solutions. The reaction equations are as follows.

$$Si + 2\ H_2O \rightarrow SiO_2 + 2\ H_2 \quad (2)$$

$$SiO_2 + 6\ HF \rightarrow H_2SiF_6 + 2\ H_2O \quad (3)$$

In concentrated HF solutions the reaction of Si follows equation (4) [18].

$$Si^0 + 2\,HF \rightarrow SiF_2 + 2\,H^+ + 2\,e^- \qquad (4)$$

Due to the polarity of the formed Si-F bonds, the Si-Si bonds are weakened and exposed to further attacks of HF. The final dissolution products will be H_2SiF_6 and hydrogen. The dissolution mechanism proposed by Lehmann and Gösele [30], is presented in figure 3.

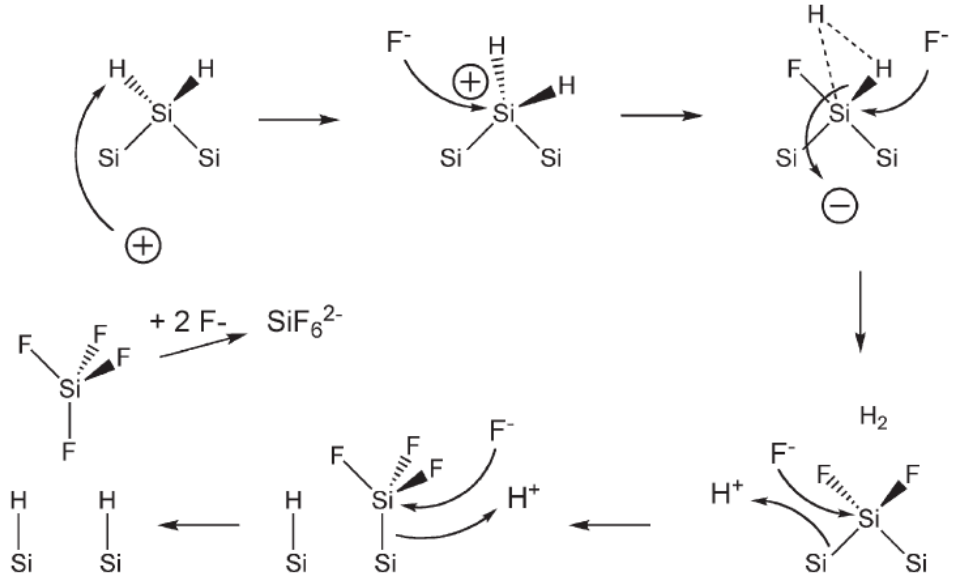

Figure 3. Dissolution mechanism of Si upon electrolysis in HF solution [28] (originally adapted from [30]).

Usually quite dilute HF solutions are used in the etching process, which favors the indirect dissolution. To improve the uniformity of the PSi layer, ethanolic solutions are preferred over aqueous [26]. Ethanol may oxidize the Si surface as water does in equation (3). Due to the lower surface tension of ethanol compared to that of water, the hydrogen bubbles formed are smaller which has a positive effect on the pore formation.

Despite the use of ethanolic solutions, uniform PSi layers are not easy to obtain when the simple anodization cell is applied. Especially if the resistivity of the Si substrate is high, non-uniformity both in the porosity and in the thickness of the formed PSi layer are likely to occur [27]. Better uniformity is obtained using installation shown in figure 4. In this so-called double-tank anodization cell, one

side of the Si substrate is the anode and the other side is the cathode [27]. Another approach is to use a conductive metal anode in contact with the Si substrate to ensure a constant current density [26].

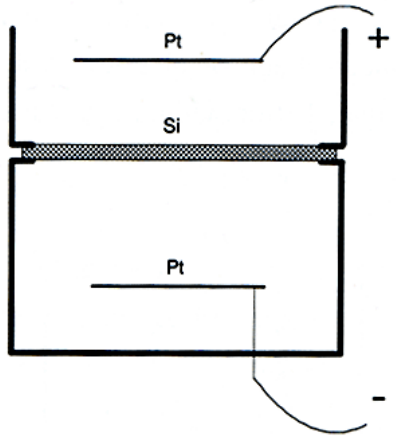

Figure 4. Double-tank anodization cell [27].

After fabrication, electrolyte has to be removed from the pores of PSi. Drying at room temperature at atmospheric pressure may cause cracking in the structure. A more sensitive method is to use supercritical CO_2. [16]

In addition to the electrochemical methods, the fabrication of PSi is also possible without electrical bias, e.g. by stain etching [31] or by photosynthesis [32]. Stain etching is basically similar to electrochemical etching, but a chemical oxidant, often nitric acid, is used instead of the electrical power supply. It is a very simple method, but it is incapable to provide as homogeneous PSi as electrochemical anodization [16]. Despite that drawback and problems with reproducibility, stain etched PSi is already commercially available [28]. Electrochemical anodization remains, however, the most common fabrication method [26].

3.1.2 Grinding

Powdered materials are typically used in oral drug delivery. To produce porous silicon microparticles, etched Si wafers are milled. The methods in use include ultrasonic fracture, lithography, and microdroplet patterning [33].

The particle size distribution is controlled by sieving. The particle size range of microparticles is 1–100 μm [28]. It is also possible to produce smaller nanoparticles. According to Salonen *et al.* [26], biomedical applications of nanotechnology are still far from practical use, in spite of the ongoing intensive study on the subject.

Grinding must be done before the surface modification, since new surface is formed during the process [14]. In some cases grinding is already performed before the etching step. The porosification of microparticles may, however, be difficult to control, at least in the case of stain etching [26].

3.1.3 Surface modification

The hydrogen terminated surface of the as-anodized porous silicon is susceptible to oxidation, and thus it does not provide the required stability without any further treatment [34]. To overcome this problem, the Si-H species on the surface are often replaced with Si-O or Si-C bonds via chemical modification [26]. Besides stabilization of the surface, the target of the surface modification may also be the biofunctionalization of the PSi surface by attaching a suitable functional group on it.

If PSi particles with larger pore sizes are desired, the pore structure can be modified prior to the surface modification by thermally annealing in inert N_2 atmosphere. This treatment reduces the overall pore volume, since it causes pore coalescence and may melt pores together. [34]

Partial oxidation is the simplest way to stabilize the PSi surface. It is typically carried out at around 300 °C. In order to obtain a completely oxidized surface the temperature has to be increased up to 900–1000 °C. Oxidation affects porosity and the pore diameter, since the formation of oxygen bridges expands the pore structure. The product obtained with this method is called thermally oxidized porous silicon (TOPSi). The TOPSi surface is similar to the silica surface, but the oxidized layer is thin and the structure of the material is different to that of porous silica. [26]

In contrast to the hydrogen terminated surface of untreated PSi, the TOPSi surface is hydrophilic [14]. That has a strong influence on the adsorption mechanisms in the drug loading process. It also improves the wetting of the particles, which is favorable to the drug release in an aqueous environment [12]. The surface is also quite reactive, which may limit its use with certain drug compounds [26].

In hydrosilylation, an alkyl terminated surface is achieved by inserting an unsaturated hydrocarbon bond into the Si-H_x-group. The reaction follows equation (5) as presented by Anglin *et al*. [28]. The reaction supplemented with the reaction mechanisms was first introduced by the research group of Buriak [35, 36]. Besides alkenes, alkynes can be used in hydrosilylation as well [35]. In that case, the obtained PSi surface is alkenyl terminated.

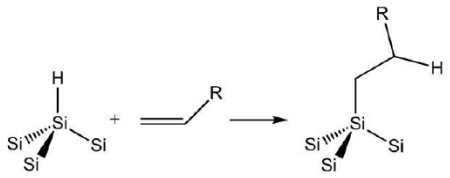

(5)

Different techniques for hydrosilylation have been introduced: it can be, for example, photochemically [37] or thermally induced, or Lewis-acid catalyzed [36]. Thermal hydrosilylation is regarded as the simplest and thus the most promising technique for drug delivery applications [26]. Since the reaction takes place in the silicon-hydride groups, the silicon has to be carefully protected from water and oxygen that would partly oxidize the surface [28]. Prior to the surface modification, the oxidized PSi surface formed during the milling process can be replaced with hydrogen termination by treating the particles with HF–EtOH solution [12].

Si-C bonds can also be produced by chemical or electrochemical grafting using, for instance, alkyl halides as reagents. One advantage over hydrosilylation is that this approach also enables the attaching of the methyl group to the PSi surface [28].

Hydrosilylation and grafting methods do not provide a complete coverage of the PSi surface; as a matter of fact, even the majority of silicon-hydride groups may remain on the modified surface [38]. This is probably mainly caused by steric restrictions. According to Lees *et al*. [38], the stability of the surface can be further improved by an additional "endcapping" step, in which the surface is electrochemically methylated. Even without the second modification step, the improvement of stability compared to the unmodified PSi is dramatic. This is supposed to be partly related to the ability of the attached hydrophobic hydrocarbon chains to exclude aqueous nucleophiles [28].

Thermal carbonization is a more effective method to form Si-C bonds onto the PSi surface than hydrosilylation or grafting. In that method the organic liquids are replaced with gaseous hydrocarbons, usually with acetylene. Acetylene molecules are firstly adsorbed on the Si surface. The interaction between the surface and acetylene molecules is so strong that the hydrogen atoms on the surface desorb more easily than acetylene when temperature is increased. At temperatures above 400 °C acetylene dissociates, and Si-C species are formed. Due to the good diffusivity of the small acetylene molecules, complete carbonization can be obtained. [26]

The nature of the formed Si-C species depends on the treatment temperature. At temperatures below 700 °C, thermally hydrocarbonized PSi (THCPSi) is formed. If treatment temperatures above 700 °C are used, no hydrogen is left on the surface, and the product is named thermally carbonized PSi (TCPSi). As far as the operating temperature is kept below 700 °C, continuous acetylene flow can be used; otherwise the acetylene flow must be stopped before the thermal treatment. [26]

The surface of THCPSi is highly hydrophobic due to the hydrogen atoms left on it and which results in poor wetting properties and makes handling of THCPSi particles difficult. The unequal wetting of the carrier particles may also lead to unequal release rate of the loaded drug. Therefore, the less hydrophobic TCPSi-particles are typically preferred to THCPSi-particles. [34]

3.2 Fabrication of mesoporous silica

Porous silica matrices are produced synthetically. The reagents include a silica precursor and a structure-directing template agent. Tetraethyl orthosilicate (TEOS), $Si(OC_2H_5)_4$, is a common precursor. Typically, a surfactant is exploited as a pore-forming template, but variations exist between different types of mesoporous silica. For example, SBA-15 is templated with neutral copolymers and MCM-41 with cationic surfactants [24].

The pore size and morphology depends on the template. In the case of surfactants, the chain length is the most critical factor but also concentration, for example, is important [20]. On the other hand, the wall thickness and stability are determined by the interactions occurring between the silica precursor and the template [24].

The synthesis procedures vary between the different types of porous silica. For instance, MCM-41 and SBA-3 are typically synthesized in alkaline conditions, as on the other hand, the production of SBA-1 involves acidic synthesis [21]. The synthesis procedure for MCM-41 has been described e.g. by Beck *et al*. [20] and by Melo *et al*. [39]. The fabrication procedure in a simplified form is presented next. This generalization is likely to cover the production of all types of porous silica.

At first, the surfactant is added with careful stirring into a homogenous mixture of the other reagents. The obtained gel is heated with stirring in an autoclave at 100 °C. The formed solid material is separated, washed, dried, and finally calcified to remove the surfactant from the pores.

The proposed mechanism of pore formation is illustrated in figure 5. In the first stage, the micelle is covered with counter ions, which may be partly exchanged with silicate ions as shown in stage 2. Heating or reduction of pH induces the silicate ions to form negatively charged pre-polymers, which are able to bound surfactant ions. As the polymerization continues, even more surfactant is bound and as a consequence, micelle-like aggregates are formed. When the charge of the polymer-surfactant complex is fully neutralized, the complex precipitates out. [40]

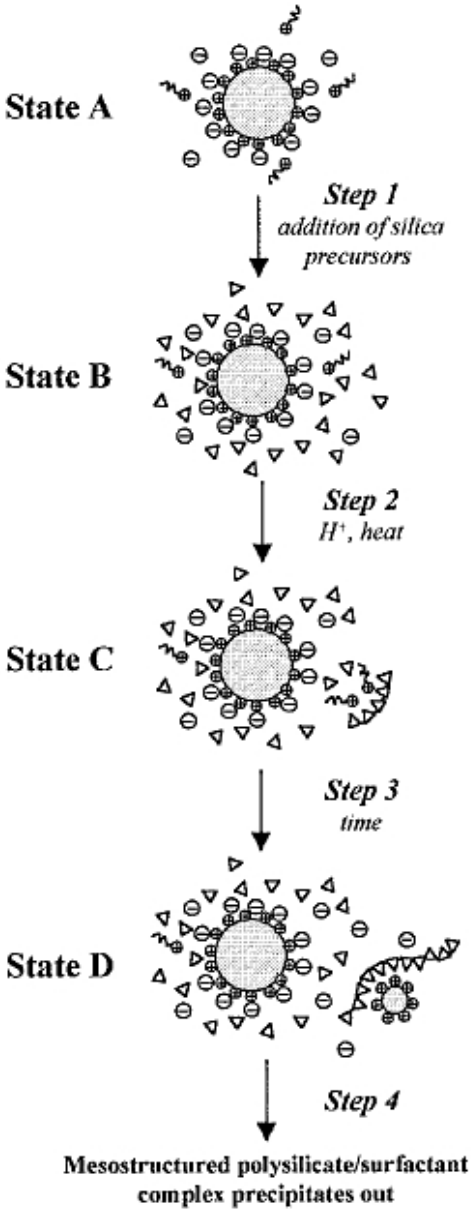

Figure 5. Formation mechanism of MCM-41. Silicate ions (illustrated as triangles) form polymers, which are able to bind the surfactant molecules. Precipitation occurs when these polymer-surfactant complexes have grown enough. [40]

New synthesis routes to produce porous silica materials are being developed. One fairly new member in the group of the porous silicas is TUD-1 (Technische Universiteit Delft), which was introduced by Jansen *et al*. [25] in 2001. The major difference between TUD-1 and the other porous silicas is that the fabrication process for the TUD-1 silica is completely surfactant-free. Instead of micelles or large organic compounds, the formation of pores is induced by aggregates of

smaller molecules [25]. This makes the process cost-effective [41]. Briefly, a mixture containing organic template (e.g. triethanolamine), silica source (TEOS), and water is aged and dried to form a homogenous gel, which is then transformed into mesostructured solid by calcination or by hydrothermal treatment [25]. The potential use of TUD-1 as a carrier for poorly soluble drugs was first investigated by Heikkilä *et al*. [41], and it was proven to provide both high capacity and favorable release kinetics.

The silica surface is satisfactory stable even without any special modification. Even though modification is not required, it is sometimes performed in order to tailor the surface for a certain drug molecule. The modification possibilities for silica surfaces are, however, more limited than those for porous silicon.

3.3 Chemistry of PSi and silica surfaces

A pure silicon surface is thermodynamically unstable, and it readily oxidizes in the presence of water. Therefore, there are always some other species present on the porous silicon surface. Surface chemistry is determined by this termination. Dependent on the termination, the surface may be either hydrophilic or hydrophobic. Since the opportunities for surface modification are wide, it is also possible to produce amphiphilic surface by attaching a suitable functional group.

A porous silicon surface is covered with hydride species (Si-H_x) immediately after fabrication. Also the hydride species are quite unstable towards oxidation, but the dissolution reaction in aqueous media is slower due to the hydrophobicity of the surface. Since HF solution is used in the fabrication, also some Si-F species may be present on the porous silicon surface. The most typical impurity is, however, oxygen. According to Salonen *et al*. [26], the impurities are probably not originated from the fabrication process but are adsorbed during the storage.

Existence of silanol-groups (Si-OH) is typical for silica surfaces. They can form hydrogen bonds acting either as donors or acceptors, or participate in ion-exchange reactions. Upon heating, the silica surface may undergo dehydration as shown in equation (6) [28]. The formed siloxane (Si-O-Si) linkages are strong and

they may coarsen the pore structure. In aqueous media the silanol groups are reversed. In temperatures above 500 °C, the siloxane linkage becomes stable [42]. It is, however, possible that part of the siloxanes can be even irreversibly hydrolyzed in the presence of moisture [43]. This will destruct the pore structure of silica.

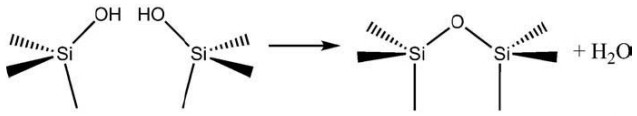

(6)

3.4 Biocompatibility

Silicon is an essential nutrient for the human body. Silicon intake in the Western diet varies between 20–50 mg/d, the major silicon sources being whole grain products, vegetables, beer, and drinking water. In food silicon exists as polymeric or phytolithic silica, which may decompose into orthosilicic acid, $Si(OH)_4$, that is the most natural form of Si and the only form in which it can be easily absorbed. In the liquid products Si naturally exists in the form of orthosilicic acid. [44]

Depending on the degree of porosity, silicon particles may be bioactive, bioinert or biodegradable [45]. Bioinert materials do not degrade in the human body, but they are not harmful, and are easily removed upon excretion [14].

In the body, also mesoporous silicon decomposes into monomeric silicic acid [14]. The dissolution is generally based on equation (7).

$$SiO_2 + 2\ H_2O \rightarrow Si(OH)_4 \qquad (7)$$

Since the pKa-value of orthosilicic acid is as high as 9.5, the fraction of the deprotonated form in body fluids is so small that it is not likely to impede protein delivery or other biological processes susceptible to pH changes [14]. The possible bioactivity of porous silicon is related to the ability of silicic acid to precipitate as bioactive inorganic silicates, which can be formed in reactions with e.g. Ca^{2+} or Mg^{2+} ions.

$$Si(OH)_4 + 2\ Ca^{2+} \rightarrow Ca_2SiO_4 + 4\ H^+ \quad (8)$$

Owing to its ability to be metabolized, porous silicon is likely to cause fewer problems in chronic use than e.g. carbon nanotubes that are more persistent [28]. Silicic acid is, however, cytotoxic in high concentrations, but apparently the removal of silicic acid from the body is efficient enough to prevent the toxic concentrations. The most hazardous form of silicon is the group of silanes, which is a series of silicon compounds including SiH_4, Si_2H_6, Si_3H_8, Si_4H_{10}, and so on [18]. To avoid formation of these highly toxic compounds, a good knowledge of the chemistry of porous silicon and toxicity tests are of an essence before the commercialization of any biomedical PSi applications.

3.5 Porous silicon based materials in drug delivery applications

Porous silicon materials in drug delivery have been researched since the turn of the millennium. The first article concerning drug loading of mesoporous silicon based material for oral delivery applications was published in 2001 [22]. Since then, the interest in the subject has been continuously increasing. The utilization of mesoporous silicon and silica in sustained drug release has also been investigated. The major advantages of porous silicon over the organic carrier materials, which are often used in drug delivery, are biochemical inertness and mechanical strength [46].

The biomedical applications of the mesoporous silicon and silica particles are not limited on oral administration. In fact, the study of porous silicon in drug delivery is mainly concentrated on implantable and injectable drug delivery applications [26] The less conventional applications include brachytherapy devices for the treatment of cancer, which have been developed by PSivida Ltd. [47]. Their product, BrachySil™, delivers a targeted dose of beta radiation straight to a tumor. The optical properties of PSi also enable monitoring of the drug release *in vivo* [28].

4 Drug loading into mesopores

In general, drug loading into a host material can be performed using various methods. The nature and the fabrication method of the carrier are, however, limiting the alternatives. As far as a “bottom-up” material such as silica is concerned, the drug may be added already during the synthesis of the carrier material. In that case, the drug is bound directly into the structure of the carrier. However, the method is not feasible for poorly soluble substances, since the occurrence of phase separation upon increasing the drug concentration limits the loading capacity [48]. Therefore, the drug loading is performed as a separate process step after the fabrication of the carrier material. Considering mesoporous silicon, a “top-down” material, that is always the case.

Drug loading can be based on different mechanisms. The mechanism has a significant effect on the release, and the controlled release. Anglin *et al*. [28] have listed the following loading mechanisms:

1. Covalent bonding
2. Physical trapping
3. Adsorption

Adsorption is a phenomenon in which a compound is attached to the surface of an adsorbent from a liquid or gaseous phase due to physical or chemical interactions. Here the term refers merely to physisorption; the type of adsorption in which only weak physical interactions are involved. Covalent bonding, on the other hand, provides stronger, chemical interactions between the drug molecule and the surface. In physical trapping, neither physical nor chemical interactions are required, since the drug is forced to remain inside the pores by physically blocking the openings of the pore channels.

As far as the target is to enhance the solubility and the dissolution rate in order to accelerate the drug absorption, adsorption is the most favorable one of the three mechanisms mentioned above. Covalent bonding and physical trapping typically

reduce the release rate, so these mechanisms are applied to obtain sustained release. Especially physical trapping may also be utilized for a fine-tuned, site-specific controlled release [17].

The most widely used drug loading process is probably the one that involves immersing the porous microparticles into a drug solution. If the interactions in the loading system are favorable, the drug is forced to move from the solution onto the pore walls and to trap into the adsorption sites located there. As the solvent is then removed by evaporation, the drug substance will remain in the pores.

If the drug concentration near to the adsorbent surface exceeds the saturation concentration, e.g. during the drying step, the drug may start to crystallize on the external adsorbent surface. Since this crystalline surface fraction may have completely different dissolution properties than the amorphous solids inside the pores, its formation is not favorable. If crystalline solids are formed on the surface, they can be removed by washing the loaded particles. Unfortunately, the washing process is difficult to control. Therefore, the aim is to totally prevent the formation of the surface fraction at first hand by controlling the loading process. [26]

It is also possible to infuse the drug solution into the pores by an impregnation method, which is based on the capillary action. In the case of highly expensive pharmaceuticals, the impregnation method may be preferred. The uniformity of drug loading is, however, much more difficult to control than upon loading from a solution. Furthermore, a crystalline surface fraction is more likely to appear in the case of impregnation loading. [26]

Different approach is the hot melt method, in which the drug is heated along with the adsorbent to a temperature above the melting point of the drug and the quench cooled [15]. Kinoshita *et al.* [49] have also developed a continuous process for the melt adsorption. A prerequisite for using this method is that both the adsorbent and the drug have sufficient thermal stability, which excludes all of the pharmaceuticals that are known to decompose upon melting. Another solvent-free method that has been used is physical blending. As far as the even distribution of

the drug in the carrier matrix is one of the main targets, the applicability of these methods is doubtful.

Since the solution immersion seems to be the most feasible one of the all drug loading methods described above, the use of that method is the main assumption in the further discussion of the chemical and physical phenomena occurring during the loading process. The loading system is determined to consist of the loading solution and the adsorbent particles.

4.1 Adsorption process and the interactions in the loading system

The maximum amount of drug that can be loaded in the mesopores is basically determined by the adsorption thermodynamics. In equilibrium, the chemical potential of the adsorbed drug equals to that of the drug in the solution phase.

Adsorption isotherms are often used for describing the thermodynamics of the adsorption. They illustrate the adsorbed amount in equilibrium state as a function of the concentration (in the case of adsorption from liquid phase) or pressure (adsorption from gas phase). The most common isotherms are Langmuir isotherm and Freundlich isotherm, which are presented by equations (9) and (10), respectively. Adsorption isotherms always include certain simplifying assumptions, and thus they are not valid to describe every system. Therefore, many more sophisticated models and variations to the basic equations have been developed and presented in literature. In most cases it is, however, quite easy to fit an equation of either Langmuir or Freundlich type to the adsorption data.

$$q_e = \frac{bq_m c_e}{1 + bc_e} \tag{9}$$

q_e adsorbed amount at equilibrium, mol/kg adsorbent
b constant, m^3/mol
q_m maximum adsorbed amount, mol/kg adsorbent
c_e equilibrium concentration, mol/m^3.

$$q_e = k\left(\frac{c_e}{c^0}\right)^a \tag{10}$$

k constant, mol/kg

c^0 1 mol/m^3

a constant, -.

If the loading time is not sufficient for achieving the equilibrium state, the kinetics must be taken into consideration. The adsorption itself is typically very fast. The rate determining step in the adsorption processes is the mass transfer onto the adsorbent surface and, in the case of a porous adsorbent, the mass transfer in pores. Diffusion in a spherical porous particle can be described, for example, using equation (11).

$$\left(\frac{\partial c}{\partial t}\right)\left[\varepsilon_p + (1-\varepsilon_p)\left(\frac{\partial q}{\partial c}\right)\right] = \frac{1}{r^2}\frac{\partial}{\partial r}\left[r^2 \varepsilon_p D_p \left(\frac{\partial c}{\partial r}\right)\right] \tag{11}$$

t time, s

ε_p porosity of the particle, -

r radial distance from the centre of the particle, m

D_p diffusion coefficient inside pores, m/s.

Both the adsorption kinetics and the equilibrium are determined by various different physical and chemical interactions that occur simultaneously in the loading system. In the case of a simple pure binary solution and a homogeneous adsorbent, the interactions can be classified into five groups:

- solute–surface,
- solute–solvent,
- solute–solute,
- solvent–solvent, and
- solvent–surface interactions.

In addition, three-body interactions are also possible, even though their occurrence is less probable than that of the two-body interactions. If impurities or degradation products are present, the number of the interactions will increase rapidly. Detecting and understanding all the interactions occurring in the system is essential for the optimization of a drug loading process. Affinity of the drug molecule toward the adsorbent surface is considered the most important interaction. It should be, however, also borne in mind that there are also other phenomena that have a significant effect on the drug loading. Some examples of those are given next.

Solute–solute interactions may lead to multilayer adsorption and thus increase the loaded amount. It is, however, also possible that solute–solute interactions hinder the drug loading. It is common that the solute molecules exist as dimers, and breaking the dimer may be a prerequisite for adsorption.

As far as adsorption from the liquid phase is considered, the solvent has a crucial role in the adsorption process. Firstly, a compound may have varying diffusivities in different solvents. Secondly, the drug molecules may form complexes with the solvent. This phenomenon is called solvation, and as it stabilizes the solution, it may hinder the adsorption. On the other hand, the solvent may also repel the solute, which improves adsorption. The drawback is that these repelling forces are also likely to result in a very low solubility. The worst situation is when the solvent induces the degradation of the API.

Typically the interactions in the adsorption process are of electrostatic nature. In drug loading, specific interactions such as hydrogen bonding often have an important role. Since the interactions are always case-specific, it would not be reasonable to try to give an extensive overview of the nature of the interactions herein; the case-example of indomethacin loadings presented in the experimental part of this work will give some perspective to the issue instead.

One more fact that could be emphasized is that besides the chemical nature of the adsorbent and the other components of the loading system, also physical factors such as pore size and the shape of the pores have an influence on the mass transfer

in the loading system. It has been also proposed that the pore structure of the carrier matrix itself would have an effect on the drug affinity [50]. Further study on this subject might be needed to develop a carrier material with an optimal pore structure for each purpose.

4.2 Control of surface fraction

The crystallization of the drug may hinder or totally stop the drug loading, since it tends to cause blocking of the pores. It is likely that the formation of the surface fraction is induced by the occurrence of a concentration gradient in the loading solution. If a rapid transfer of drug compound driven by strong attraction and repulsion forces is followed by a slow diffusion inside the narrow pores, the drug will accumulate near to the surface. As the concentration exceeds the saturation concentration, crystallization may occur, especially if any crystalline seeds are present.

Concentration gradients should be avoided by using sufficient mixing intensity. In some cases, especially when scaling-up the process, the crystallization cannot be avoided simply by mixing. If the concentration of the loading solution is near to the saturation concentration, the formation of the surface fraction is more plausible. Therefore, the solubility should be taken into consideration when selecting the initial concentration of the loading solution. This increases the importance of the solvent selection. If the solubility of the drug in the solvent is low, the concentration range at which the loading process can be operated is narrow.

The effect of the carrier material itself and its surface modification on the tendency for formation of the surface fraction has also been verified empirically [51]. Since the properties of porous silicon can be easily controlled and modified, this opportunity can also be exploited for reducing the surface fraction.

Optimal drying temperature may also decrease the fraction of the crystalline drug. If the drug in the pores is completely melted after heating up to certain temperature, but the surface fraction remains crystalline, capillary forces may

suck the drug from the surface into the pores. Salonen *et al*. [52] have reported on this kind of behavior, which they had also observed in DSC measurements.

5 Solvent selection

Solvent selection is one of the most essential tasks in the optimization of a drug loading process. It requires a deep understanding of the interactions in the complex multi-component system.

The first prerequisite for a loading solvent is a sufficient solubility of the drug in it. The optimal solvent for the loading process might not be the one in which the solubility is the highest. It is often a sign of strong attractive interactions between the solvent and the solute [53], and it may cause the solute to prefer staying in the solution phase to adsorption onto the carrier. Another inauspicious situation in drug loading is the competitive adsorption; if the solvent possesses attractive interactions with the adsorbent, it will compete on the adsorption sites with the solute.

Besides the affinities among the solute, solvents and adsorbent surface, also the possible degradation of the API in the solvent must be taken into account. Even if the API would not decompose, it may re-crystallize from the solution as a different polymorph or as a solvate. Observation of that kind of behavior is important, since the conservation of the right polymorph is often essential both for the stability and for the pharmaceutical action [54]. Solvents that induce the degradation of the API must be avoided. In addition, the use of many solvents is limited by their toxicity or too low or too high volatility. If the solvent is too volatile, vacuum filtration cannot be successfully used in separation [55]. On the other hand, extremely low volatility will hamper the drying process.

Binary solvent mixtures have been often proven to provide better solubility than either of the solvents alone [56]. In addition, the degradation, which occurs in pure solvents, can be sometimes prevented by adding a cosolvent. The challenge is that the extra solvent will make the system even more complex: when shifting from a single solvent to a binary solvent mixture, the number of binary interactions will increase from five to 12.

5.1 Solubility

In the absence of all attractive or repulsive interactions or steric restrictions, the solution will freely fill the pores of the adsorbent material, and the concentration inside the pores will be equal to that of the bulk solution. When the sample is filtered and dried, the drug compound present in the solution inside the pores can be assumed to stay in the pores and thus contributing the loaded amount. In this theoretical case, the loaded amount of drug can be calculated using equation (12). The value obtained using this equation can also be termed a minimum loaded amount.

$$q_{\min}^{theor} = \frac{c_{drug} V_s}{1 + c_{drug} V_s} \qquad (12)$$

$q_{min,\,theor}$ theoretical minimum drug load, g drug / g dry adsorbent + drug

c_{drug} concentration of the loading solution, g drug / mL solution

V_s pore volume, mL/g dry adsorbent.

The problem with poorly soluble drug substances is that even if a saturated solution is used, the concentration is low and therefore the loaded amount calculated using equation (12) will also be low. If the concentration of the loading solution can be increased by changing the solvent, the loading capacity might be enhanced. In addition, higher solubility into the loading solution facilitates the determination of adsorption isotherms. If the saturation concentration is low, the isotherm becomes very narrow.

In drug loading, the highest possible solubility of the drug in the loading solution cannot be assumed to offer the highest loading performance. An optimal solvent or solvent mixture would provide high solubility but the affinity between the solute and adsorbent surface should be still the strongest one of the attraction forces occurring in the loading system.

Solubility is a function of temperature. By increasing the loading temperature, the solubility of a drug can be increased. On the other hand, increase in temperature may also accelerate the degradation of drug or evaporation of the solvent, and the temperature also affects the adsorption rate and equilibrium. Therefore, the elevated loading temperature may not always enhance the drug loading capacity and the adsorption rate.

Several mathematical models have been developed for solubility prediction, and some of these models are represented in chapter 5.1.3. These models may provide useful information on the molecular interactions between solvents and solutes. Furthermore, these models could possibly be extended and applied also to predict the drug loading capacities that can be achieved using different loading solutions. A probable requisite for modeling the drug loading of PSi is the better characterization of the PSi surface.

5.1.1 Thermodynamics of solutions

Solubility is defined as the maximum amount of a compound, which is generally termed a solute, that remains in the solution in the given amount of the given solvent. In the saturated solution of a crystalline compound, the solid solute is at equilibrium with solute in the solution. Solubility is dependent on temperature and pressure, and also on the crystal form of the compound. The real thermodynamic solubility always refers to the solubility of the most stable crystal form which has the lowest lattice energy and, as a consequence, the lowest solubility. The solubility of an ionizable solute has also a strong pH-dependency. [57]

Dissolution is driven by intermolecular forces between the solvent and the solute. These forces have to overcome the solute–solute and solvent–solvent interactions. The former includes e.g. overcoming the lattice energy and the latter refers to the cavitation energy needed to accommodate the solute among the solvent molecules [57]. In general, dissolution increases the system entropy despite the possibly increased local order resulted by solvation. In some cases the driving force of the dissolution is not the overall enthalpy change involved in the dissolution process, but the increase in the system entropy.

The solution process of a solid solute can be divided into two hypothetic sub-processes: melting of the solute and mixing [58, 59].

Solute (s) → Solute (l) → Solute (solution)

Perlovich *et al*. have taken another approach to the solution process by dividing it into the sublimation of the solute and mixing [60, 61].

Solute (s) → Solute (v) → Solute (solution)

In an ideal solution, each component obeys Raoult's law over the whole range of composition. As a result, enthalpy of mixing ΔH_{mix} and volume of mixing ΔV_{mix} both equal to zero. In the case of an ideal solution, equation (13) is valid.

$$\ln x_2 = -\frac{\Delta H_f (T_0 - T)}{R T_o T} + \left(\frac{\Delta C_p}{R}\right)\left[\frac{T_0 - T}{T} + \ln\left(\frac{T}{T_0}\right)\right] \qquad (13)$$

ΔC_p difference between heat capacities crystalline and supercooled liquid form at temperature T, J/(mol K)

In practice, determination of ΔC_p is difficult, and since ΔC_p is relatively small, it is often neglected by assuming that ΔH_f is independent on temperature. Equation (13) will be then reduced to

$$\ln x_2 = -\frac{\Delta H_f}{R}\left(\frac{1}{T} - \frac{1}{T_0}\right) \qquad (14)$$

In reality, solutions are often far from ideal, and activity coefficients are required to correct the solubility equations. Very dilute solutions are exceptions, and the equations for ideal solutions are usually applicable for them. In infinite dilution, the solute molecules are completely surrounded by solvent molecules and thus no solute-solute interactions occur.

It has to be borne in mind that some of the methods used in solubility measurements, e.g. turbidity-based solubility determination, do not give the true thermodynamic solubility values but a kinetic solubility. Especially in the case of poorly soluble substances, it may take a very long time to reach the equilibrium state [62], and thus the measurement of thermodynamic solubility is time-consuming. The rate limiting step is often the formation of crystals from the precipitated amorphous material and the crystal growth [63]. The kinetic methods are rapid, but the results are often over-estimating the solubility and cannot be directly compared with the thermodynamic solubility values. Kinetic solubility data is valuable e.g. in studying dissolution in the intestinal tract due to the short transit time through it.

5.1.2 Solubility parameters

The concept of solubility parameter δ was first introduced by Hildebrand. The solubility parameter of a substance is a square root of its cohesive energy density (CED). The cohesive energy is the net energy which holds the substance together; it includes all the interaction between molecules or atoms, e.g. covalent and ionic bonds, electrostatic interactions, hydrogen bonds, and van der Waals forces.

$$\delta = (CED)^{0.5} = \left(\frac{\Delta E_v}{V_m} \right)^{0.5} = \left(\frac{\Delta H_v - RT}{V_m} \right)^{0.5} \qquad (15)$$

ΔE_v Energy of vaporization, J

V_m Molar volume, m^3/mol

ΔH_v Enthalpy of vaporization, J/kg

R Universal gas constant, 8.315 J / (mol K)

T Temperature, K

The cohesive energy is determined as the energy of vaporization per unit volume, as can be seen from equation (15). The solubility parameter can be thus determined experimentally by measuring the enthalpy of vaporization. Another approach is to use the surface free energy γ as the basis of calculation (see

equation (16)), and there are also other experimental methods for determination. Often the solubility parameters are, however, calculated based on the molecular structure of the compound. For a simple molecule the solubility parameter can be calculated based on the group increments, which can be found in literature. For more complicated molecules it is more convenient to use software developed for computing solubility parameters.

$$\delta = \left(\frac{\gamma}{V_m^{1/3}} \right)^{n/2} \tag{16}$$

The original application of solubility parameters was predicting the miscibility of liquids by comparing their δ values. The use of solubility parameters can be extended into prediction of solubility of solids or gas in a certain solvent.

Improvements to Hildebrand's solubility have been based on dividing the solubility into several terms each corresponding to certain type of interactions. This enables more detailed characterization of the compound and the forces that determine its compatibility with other substances. Hansen's solubility parameter, for instance, consists of dispersion term δ_d, polar term δ_p, and hydrogen bonding term δ_h.

$$\delta_t^2 = \delta_d^2 + \delta_p^2 + \delta_h^2 \tag{17}$$

Solubility parameters are widely applied in the design of pharmaceuticals. The use of solubility parameters in pharmaceutical dosage form design has been reviewed by Hancock *et al*. [64]. The main use is in prediction of interactions in multi-component mixtures and compatibilities of excipients. Also, the wetting of powders can be predicted using solubility parameters.

Since the solubility parameter is a liquid phase property, it is independent of the polymorph form. It is, however, well known that the apparent solubility varies among the different polymorphs due to the difference in the lattice energy.

5.1.3 Cosolvency

Enhanced solubility in solvent mixtures is has been observed and attempts to explain the phenomenon has been made already in the 1950s [65, 66]. The first approach was based on the Hildebrand solubility parameters. In brief, the solubility parameter represents the polarity of a compound, and by selecting a proper solvent mixture, the polarity of the solvent can be fixed to match the polarity of the solute.

For solvent mixtures the solubility parameter is obtained as sum of the parameters for the components weighted by their activity coefficients. For ideal solvent mixtures, the solubility parameter is a linear function of the composition. The solubility of a drug is usually (but not always) higher in the binary solvent system than in pure solvents if its solubility parameter is between those of the two solvents [56]. The intersection point of the solubility parameters can be used to predict the optimal ratio of the solvents in order to obtain the highest solubility. Equation (18) presents the effective Hildebrand parameter $\overline{\delta}$ which is volume-wise proportional to the Hildebrand parameters of the components in the mixture.

$$\overline{\delta} = \frac{\sum_i \phi_i \delta_i}{\sum_i \phi_i} \tag{18}$$

ϕ_i volume fraction.

If the volume fraction of the solute is very small, the effective Hildebrand parameter for a binary solvent mixture is

$$\overline{\delta} = \phi_i \delta_i + \phi_j \delta_j . \tag{19}$$

It is notable that in some cases solubility in a binary solvent mixture may be higher than in either of the pure solvent even if the solubility parameters of the two solvents were both either higher or lower than that of the solute. This “chameleonic effect” reflects that polarity alone does not account for solubility.

The solubility enhancement can be explained with the increase in entropy due to the loss of solvent structure as a co-solvent is added. The resulting solubility profiles with two maxima have been reported, for example, for caffeine [67] and oxolinic acid [68]in ethyl acetate–ethanol and water–ethanol mixtures, and it is observed to be typical especially for compounds with a high solubility parameter ($\delta \geq 25$ MPa^{½}) [69] or many polar functional groups [67].

A variety of factors may affect the solubility in a solvent mixture due to the complicity of the dissolution mechanisms, e.g. changes in the solid phase, cavity formation, and specific and non-specific solvation [70]. Specific interactions, e.g. hydrogen bonding, have an essential role in the dissolution of many pharmaceuticals. One viewpoint to the co-solvency assumes that the solvent composition around the solute differs from the bulk mixture, and the solvent preferentially dissolves in one of the solvents [71].

Owing to the special co-solvent effect, solvent mixtures bring numerous possibilities for solubility enhancement in pharmaceutical design. One should, however, remember that the solvents are recommended to be selected in a way that their solubility parameters do not differ too much; otherwise there will be two separate liquid phases in the loading solution, which will complicate the system. Not only solid–liquid but also liquid–liquid equilibrium has to be hence considered.

5.1.4 Solubility prediction

A lot of work has been done to create mathematical models for predicting solubility in order to reduce the number of required solubility measurements. At least in the pharmaceutical industry, the experimental determination of solubility is expensive, since it is time-consuming and requires a high amount of solute. Furthermore, reproducibility of solubility measurements is not good and the results may vary between laboratories despite the use of a standard method [72].

Use of solvent mixtures increases the amount of solubility experiments required and thus makes the use of predictive models even more favorable. In addition, the

models could be extended to predict the loaded amount from different loading solutions. Modeling of solubility is, however, a demanding task due to the complicity of multi-component systems and the diversity in the molecular structures of both solutes and solvents. Furthermore, reasons for solubility enhancement in solvent mixtures are not fully understood yet and there are several different theoretical approaches into the co-solvency phenomenon.

Comparison of the solubility parameters is the simplest way to estimate whether the use of solvent mixtures is reasonable or not. Nevertheless, the reliability of the method is not very good due to the numerous exceptions and the errors in estimation of solubility parameters. Furthermore, this approach does not, however, give any quantitative information about the amount that will be dissolved. Thus also solubility measurements are still required.

Recently, numerous empirical, semi-empirical, and theoretical models have been developed for predicting the solubility in solvent mixtures. Theoretical models are preferred, since they fulfill the purpose of the mathematical modeling, i.e. truly predicting and minimizing the number of required experiments [73]. Furthermore, they can improve understanding of the molecular interactions. A couple of models for solubility estimation are described below, and more models have been reviewed in [74, 75].

One of the simplest mathematical models is the log–linear model which can be written for a single solute in a binary solvent mixture as follows [76]:

$$\ln x_m = f_1 \ln x_1 + f_2 \ln x_2 \qquad (20)$$

x_m mole fraction of the solute in the solvent mixture
f_1, f_2 mole fraction of solvent in the mixture
x_1 mole fraction of the solute in the pure solvent.

The log-linear model is not applicable in cases when the solubility in a binary mixture exceeds the solubilities in both of the neat solvents. Better fit can be

achieved with the models that include additional terms, e.g. the Jouyban–Acree model [73] presented in equation (21), but the drawback is that more experimental data is usually required to quantify the model coefficients for each compound. The additional term in eq. (21) is based on the Redlich–Kister activity coefficient model. The model constants B_j represent formation of dimers and multimers in the mixture. The use of the model can be extended to more complex multicomponent systems as described in [77].

$$\ln x_m = f_1 \ln x_1 + f_2 \ln x_2 + f_1 f_2 \sum_{j=0}^{2} B_j \left(f_1 - f_2\right)^j \qquad (21)$$

Attempts have been made to create models for calculating the model constants based on the numerical descriptors of the solvents and solutes, which are available in literature or can be computed using commercial software. Some of the models use physicochemical properties such as the melting point of the solute, which partly compromises the benefit of these models since the empirical determination of these properties is often required, at least in the case of newly developed pharmaceuticals.

At the early stage of drug development, models based on the molecular structure of the solute are useful. One subtype of these quantitative structure property relationship (QSPR) models are the group contribution methods, e.g. UNIFAC and its modified version UNIFAC(Dortmund) which are actually databases of thermodynamic data [78]. The drawback of group contribution methods is that even a large database may miss some essential fragments, which limits its application for complicated molecules [58].

One alternative to the group contribution methods is the conductor-like screening model for real solvents (COSMO-RS) that is based on quantum chemical calculations. The method has been presented by Klamt [79], and its applicability in solvent screening has been demonstrated by Eckert and Klamt [80]. COSMO-RS model is relatively new method, and not yet developed to a highly sophisticated level. It shows quite large absolute errors, and especially the accuracy of predictions for the solubility of simple compounds is worse than that

of UNIFAC predictions. COSMO-RS is, however, very promising, since it is a general method that can be applied for any kind of system.

As the computing power is continuously increasing, the possibilities for solubility prediction are growing, and computationally demanding methods such as those exploiting 3D-structure of the molecule are becoming realistic.

5.2 Common solvents in drug loading

Water is an unsuitable solvent for drug loading, since majority of the drug compounds to be loaded are practically insoluble in water. Thus organic solvents have to be used. In the case of poorly soluble pharmaceuticals, it may be difficult to find a solvent that dissolves a sufficient amount of the drug. It might be attractive to use a "super solvent" such as dimethyl sulfoxide (DMSO) which dissolves practically all pharmaceutical substances and is therefore typically used in the initial drug discovery screening [7]. Despite its high solvating power, DMSO is not a favorable solvent for drug loading, since it is an oxidant that affects the pore structure of PSi [81]. Furthermore, the removal of DMSO after loading would be problematic due to its extremely high boiling point.

Hexane has shown to provide high loading amounts of ibuprofen on porous silica (up to 59 % with MCM-41 [23]), but it is highly toxic and therefore preferably replaced by another solvent. Drug loading is often carried out from an ethanol solution. It usually provides satisfactory loading amounts in the case of ibuprofen. The applicability of ethanol is, however, limited for loading more poorly soluble drugs by their extremely low solubility in it.

The use of binary solvent mixtures in drug loading of silica particles has been reported e.g. by Ambrogi *et al.*, who have made loading experiments onto MCM-41 using a mixture of acetonitrile and dichloromethane for piroxicam [55] and a mixture of ethanol and dichloromethane for carbamazepine [1]. A binary mixture was advantageous in these experiments, since it provided better loading capacity than ethanol or acetonitrile, and pure dichloromethane would have been too volatile for the experiment procedure used, which included vacuum filtration.

5.3 Environmental and safety aspects

Pharmaceutical industry in general utilizes enormous amounts of solvents. At the API synthesis stage, the solvent use accounts for 80–90 % of the total mass utilization [82]. If large amounts of solvents are needed at the further production stages too, the atom efficiency of the final product will be very low. Minimizing the amount of solvents needed is preferable from the environmental and safety aspects, as well as from the economic aspect. Therefore, finding an optimal solvent for each purpose is essential. Additionally, the separation of solvents and possible re-use must also be considered. Use of solvent mixtures may set extra requirements for the separation of the solvents, especially if the solvents form an azeotrope.

Environment, health and safety (EHS) issues are very important in the solvent selection. Firstly, it is important to minimize the environmental impact of processing and the risks for the employees who are exposed to the chemicals. Secondly, one has to remember that possible solvent residuals in the final product may cause a serious health risk to the end users. It is advisable to keep these factors in mind already at a preliminary screening for solvent selection. In an article concerning solvent selection, Gani *et al*. [83] have pointed out that once a suitable solvent has been found and already successfully applied in the laboratory experiments, it is often considered too risky and demanding to replace that with a new, potentially better solvent. In most cases, however, the solvent has to be changed during the development, since the EHS issues are not in a key role in the solvent selection at the early stage.

There are certain regulations and recommendations concerning chemicals and methods used in pharmaceutical industry. ICH (International Conference of Harmonisation) guideline Q3C [84] deals with residual solvents. It gives recommendations for using less toxic solvents and presents toxicologically acceptable levels for harmful solvents. Solvents are classified into three groups according to their safety. Class 1 solvents are the most hazardous ones, and they should always be avoided. These solvents are [85]

- benzene
- carbon tetrachloride
- 1,2-dichloroethane
- 1,1-dichloroethane
- 1,1,1-trichloroethane.

The solvents belonging to class 2 (Table III) are less harmful, but their use should be limited. The solvents in class 3 are those for which no significant toxicity has been noticed, and they are preferable for all applications. In addition, there are some class 4 solvents for which adequate toxicological data is not available.

Table III Class 2 solvents and the permitted daily exposures (PDEs) for them [85].

Solvent	**PDE (mg/d)**
Acetonitrile	4.1
Chlorobenzene	3.6
Chloroform	0.6
Cyclohexane	38.3
1,2-Dichloroethene	18.7
Dichloromethane	6.0
1,2-Dimethoxyethane	1.0
N,N-Dimethylacetamide	10.9
N,N-Dimethylformamide	8.8
1,4-Dioxane	3.8
2-Ethoxyethanol	1.6
Ethyleneglycol	6.2
Formamide	2.2
Hexane	2.9
Methanol	30.0
2-Methoxyethanol	0.5
Methylbutyl ketone	0.5
Methylcyclohexane	11.8
N-Methylpyrrolidone	5.3
Nitromethane	0.5
Pyridine	2.0
Sulfolane	1.6
Tetrahydrofuran	7.2
Tetralin	1.0
Toluene	8.9
1,1,2-Trichloroethene	0.8
Xylene	21.7

Recently the use of green solvents has been a hot topic. Organic solvents can be replaced with supercritical carbon dioxide. Its successful use in drug loading onto silica has been reported recently [86]. When supercritical carbon dioxide is used,

the loading arrangement becomes more complex. The apparatus needed is illustrated in figure 6.

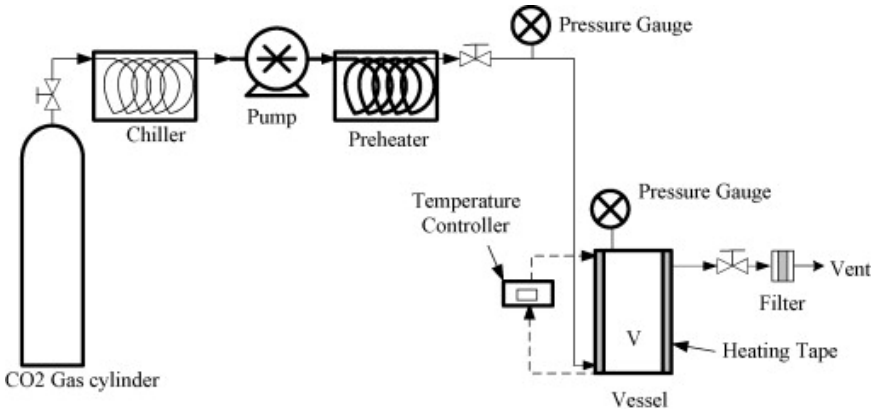

Figure 6. A flow chart of a drug loading system which utilizes supercritical CO_2 [86].

6 Analysis methods

Various analysis methods are utilized in the research and development of porous materials for drug delivery of poorly soluble drugs. Firstly, the properties of the porous material, especially the pore morphology, have to be investigated. Secondly, the analysis of the loaded amount and certain other factors are required in the optimization of the drug loading. Finally, dissolution tests are carried out in order to determine whether the utilization of a carrier really has enhanced solubility in simulated gastrointestinal fluid. In addition, *in vivo* and *in vitro* toxicity tests are required to ensure the biocompatibility.

Like Salonen has stated, the determination of the quantification of the loaded drug is a problematic issue, and the use of several analysis methods is recommended for verifying the reliability of the results [26]. The analysis methods used in drug loading experiments are described briefly herein. A little more attention is given to the two most important ones: Raman spectroscopy and thermal analysis.

The loaded amount is usually determined using thermal analysis or high performance liquid chromatography (HPLC). Other alternatives are the nitrogen sorption method and pycnometry. It is recommended to use several parallel methods, since none of the methods is completely reliable due to the complexity of the sample.

HPLC is based on the different retention times of the substances in the chromatography column. The detection can be done e.g. by a UV detector. The main challenge in the HPLC analysis is to find a solvent, which is able to dissolve the drug material completely without causing any degradation [14].

The nitrogen sorption method is based on the difference between the pore volumes before and after the loading. The main problem is that the results will be distorted if the drug molecules block the pores. It is also possible that the drug adsorbs in a way that it increases the internal surface area, which may cause underestimation of the drug load. [26]

An alternative method to the nitrogen sorption is pycnometry [26]. The volume of the sample is measured using pressurized He in order to determine its density. One of the drawbacks of pycnometry is the possible trapping of He into the smallest pores, which distorts the results [87].

Vibrational spectroscopy is a useful tool in investigation of interactions between the drug molecule and the adsorbent surface. If these interactions are clear and well-known, also a quantitative analysis is possible, but it requires the development of a calibration model. For a qualitative analysis of the loading uniformity, Raman spectroscopy is also a good method.

An in-line or on-line monitoring of the loading process would be useful especially in the study of adsorption kinetics. The concentration in the liquid phase during the loading process is often monitored in-line with a UV detector. A small amount of the loading solution is pumped through a filter to analysis. The retention time in the circulation is minimized. This method provides, however, no information about the possible nucleation or crystallization of the substance onto the adsorbent surface, so the straight evaluation of the loaded amount based on this method may be misleading. Better results could be obtained if both the solid and the liquid phase could be monitored simultaneously e.g. with methods of vibrational spectroscopy. The development of this kind of monitoring system for the small scale used in loading experiments is, however, demanding, and so is the generation of calibration models, too.

6.1 Raman spectroscopy

Raman spectroscopy detects molecular vibrations like IR spectroscopy, and therefore they are often grouped together. It is a relatively fast, non-destructive analysis method. Furthermore, only little or no sample preparation is required, which is especially advantageous in the study of polymorphism, since the sample preparation, e.g. grinding, might induce solid state transitions [54]. A difference to IR spectroscopy is that, instead of absorption, the basis of Raman spectroscopy is inelastic scattering of monochromatic light. Because of this difference, the

selection rules for the Raman effect differ from those for the IR spectrum. Raman spectroscopy provides information on the symmetric vibrations and non-polar groups, which are usually IR-inactive.

The scattered photons polarize the electronic cloud of the molecule, and the molecule undergoes a transition to a virtual excited state. Usually the transition back to the ground state happens very quickly. There is no energy change between the scattered photons and the incident photons, and thus they radiate at the same frequency. This elastic scattering process is called Rayleigh scattering, and it is illustrated in figure 7, which compares different transitions in the vibrational state of a molecule.

If energy is absorbed or emitted during the process, the wavelength of the scattered light will differ from that of the incident light. This occurs if part of the energy is turned into the nuclear motions. Vibrational mode changes the polarizability of the molecule, and the scattering becomes inelastic. This phenomenon is the Raman effect. The molecule may be promoted either to a higher energy level (Stokes scattering) or if it is already at an elevated level it may return to the ground state (anti-Stokes scattering). The intensity of the Stokes scattering is much higher than that of anti-Stokes scattering, and thus it is preferred in conventional Raman spectroscopy.

Fluorescence may interfere with the Raman signal. If the sample fluoresces in the range of optical, i.e. if electrical transitions occur, the Raman spectrum may be totally undetectable due to its low intensity.

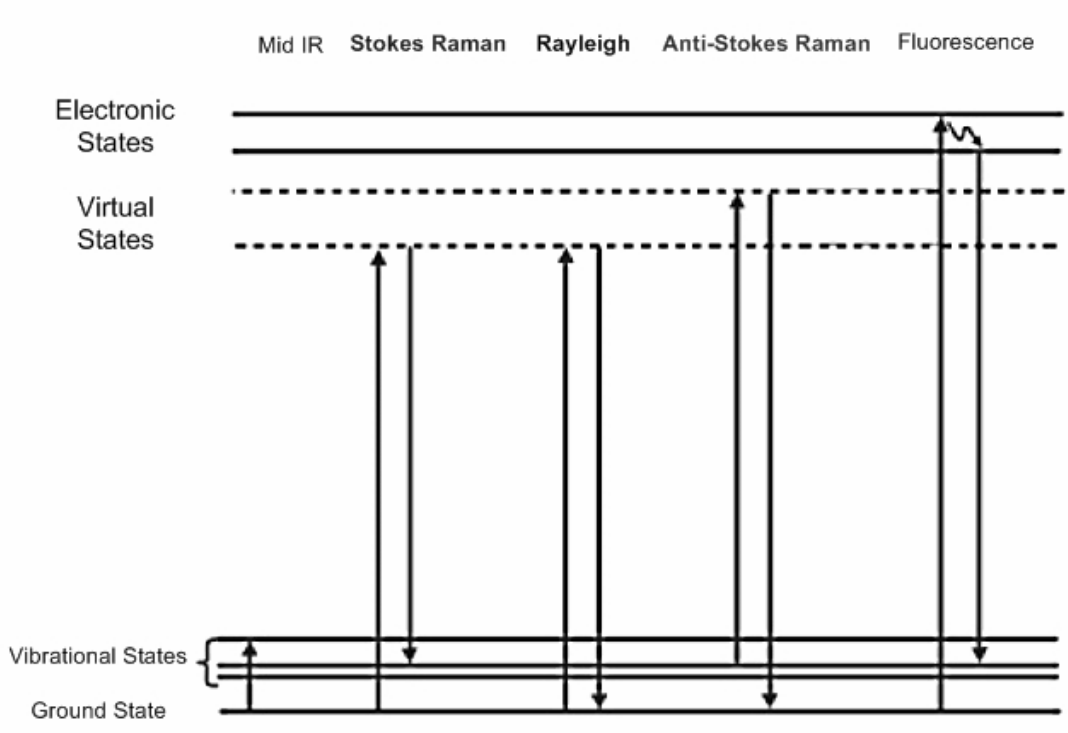

Figure 7. Changes in the molecules energy levels (adapted from Horiba Jobin Yvon [88]).

Since only about 0.1 % of the light is scattered and the elastic Rayleigh scattering is the dominant scattering process, the probability to obtain Raman scattering is very small. The Raman intensity is less than 10^{-7} of the intensity of the incident light. In order to get satisfactory intensity level, a laser source is used as the incident light. The sensitivity depends on the laser wavelength. In general, shorter wavelength provides higher intensity. Nevertheless, the intensity cannot be limitlessly increased by shortening the wavelength, since decreasing the wavelength into too low level may promote fluorescence or burn the sample.

The most commonly used Raman instruments are dispersive and Fourier transform (FT) spectrometers. A Raman instrument consists of an excitation source, a sample illumination system, wavelength selector, and detector. The most commonly used detector is a charge couple device (CCD). The scattered light is collected using a sampling angle of 90° or 180°. The collected light is then filtered. The purpose of the filtering is to reject all light at the incident laser frequency, which would add a large background in the spectrum. The detector

discriminates the different wavelengths, and finally the spectrum of the sample will be obtained. FT Raman system usually employs a NIR laser emitting at 1064 nm, an interferometer, and a special software which Fourier transforms the signal to generate the spectrum. FT Raman spectrometers are typically applied in routine measurements.

Raman microscopy or Micro-Raman spectroscopy is a technique in which the laser beam is focused on the sample using a microscope objective. Micro-Raman is a valuable method in detecting the spectra of molecules adsorbed on surfaces. The microscope also helps to select the measurement points if it is necessary to avoid sample inhomogeneities [89].

A single measuring point does not give much information of the sample. To improve the statistics of the data, it is recommended to collect spectra from several points and take the average of them as a result. As the uniformity of the sample is of an interest, the average is not used but the spectra from the multiple measurement points are compared.

The application of fiber optic probes enables in-line monitoring of processes. As can be seen in figure 8, the laser light is transmitted to the fiber optic probe via an optical fiber, and another fiber (or several fibers) collect and transmit the spectral signature to the detector.

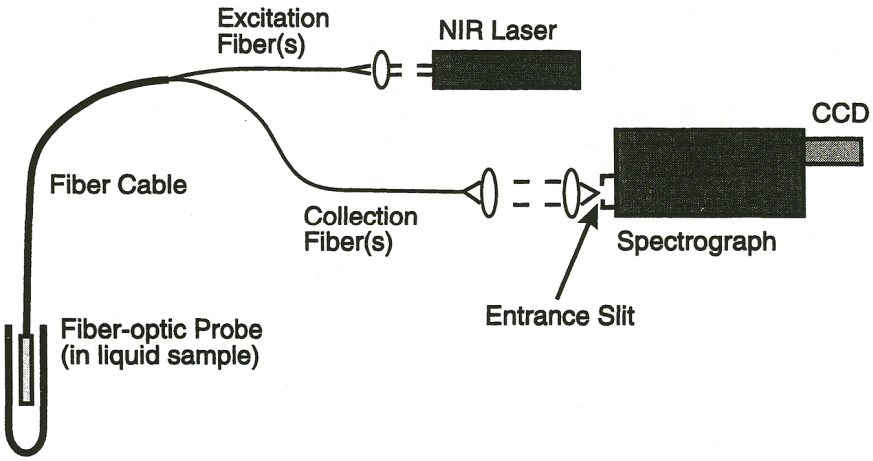

Figure 8. Schematic of a fiber optic remote Raman spectrometer [90].

In laboratory scale measurements fiber optic remote Raman spectrometers provide excellent results, but problems may arise as the length of the probe is increased. In the case of highly scattering samples, filtered Raman probe is required to reduce the Raman background caused by silica. [90]

Raman spectroscopy is nowadays widely applied in pharmaceutical research. The advantage of Raman spectroscopy in the study of pharmaceutical products is that usually the spectra of the API containing benzene rings is much stronger than that of the simpler excipient molecules in certain wavelength range. Because the Raman scattering of water is weak, also water solutions can be easily studied. Furthermore, *in vivo* measurements are possible. An excellent book of the pharmaceutical applications of Raman spectroscopy [91] has been published recently. The ability to determine the solid state form and the uniformity of the sample with Raman imaging will be exploited in the experimental part of the present work.

6.2 Thermal analysis

Thermal Analysis (TA) is the general denomination for a group of analysis methods that are based on the changes occurring in certain property of the sample upon forced temperature alteration [92]. By combining these techniques, a lot of information is obtained from a small sample. In pharmaceutical industry, TA is

widely used in research and development as well as in quality control. One important application area is the study of polymorphism of pharmaceuticals.

Thermogravimetry (TG) measures the mass change of the sample. TG is a suitable method for determining the amount of the loaded drug quantitatively. Upon heating the sample, the medicine will decompose and vaporize. This can be observed as a mass loss in the TG curve. Problems in the analysis arise if the degradation products do not vaporize completely or if the compound reacts with the carrier material upon heating. Also solvent residuals on the sample may distort the results. An improvement to this is achieved by analyzing the evolved gases e.g. with a coupled mass spectrometer, which may help to detect the solvent residuals or traces of water in the sample.

Besides measuring the total amount of the loaded drug, it is also essential to determine, whether the drug is in an amorphous form as desired, or if it has partially crystallized onto the external surface. The possible surface fraction can be detected using Differential Scanning Calorimetry (DSC), which detects all the reactions and phase transitions which are associated with enthalpy changes. If any crystalline particles exist on the surface, they appear as a melting endotherm on the DSC scan. The method also gives quantitative information, as the degree of crystallinity can be calculated based on the enthalpy of fusion. The mass fraction of the crystalline drug on the adsorbent surface $q_{surface}$ can be calculated with equation (22).

$$q_{surface} = \frac{\Delta H_f}{\Delta H_{f,0}} \tag{22}$$

ΔH_f enthalpy of fusion of the sample
$\Delta H_{f,0}$ enthalpy of fusion of crystalline drug.

Sometimes small nanocrystals may be formed inside the pores. These crystals can be detected with DSC, even if they are too small to be observed using X-ray powder diffraction. The melting peak of the crystals located inside the pores differentiates from that of the surface fraction, since the presence of amorphous

form causes the depression of the melting point and broadening of the melting peak. [14]

Unlike with TG, direct determination of the loaded amount is not possible with DSC, since it only provides the value for decomposition energy. If the drug compound in the pores was completely in a crystalline form, the loaded amount could be calculated based on thermoporometry using Gibbs–Thomson equation:

$$D = \frac{4V_m T_0 \gamma_{sl}}{\Delta H_f \Delta T} \qquad (23)$$

D	pore diameter, m
V_m	molar volume, m^3/mol
T_0	melting point of the crystalline drug, K
γ_{sl}	surface energy at the solid–liquid interface, J/m^2
ΔH_f	specific heat of fusion, J/mol
ΔT	depression of melting point, K.

Thermoporometry is based on the dependence of melting point depression on the pore size. Equation (23) is usually applied to determine the pore size distribution. As the amount of loaded drug is the main interest, the surface energy term can be neglected. [52]

The thermoporometric approach is not applicable in practice, since the drug is at least partly amorphous. Estimates of loaded amount can, however, be obtained if calibration is first performed using the results from nitrogen sorption or from density measurements [52].

7 Drug loading experiments

The aim of this study is to find ways to improve the drug loads of mesoporous silicon particles in order to investigate the effect of loading parameters on the drug loading process. In the case of poorly soluble drug compounds, sufficiently high drug loads are not readily obtained. The main focus of this work is in the solvent selection. In the case of poorly soluble drug compounds, the concentration of the drug in the loading solution is limited, since the solubility of these compounds in the common loading solvents such as ethanol is quite low. Thus even the theoretical minimum drug load remains low. By changing the loading solvent to one in which the solubility is higher, slightly higher drug loads might be obtainable. Different binary solvent mixtures will be selected for the experiments in order to enhance the solubility of the drug and thus increase its concentration in the loading solution.

Furthermore, loading experiment using different loading solvents and the comparison of PSi particles with different surface modifications (TOPSi, TCPSi) may give information on the affinities and the repulsive forces between the components in the loading system. Determination of these interactions helps in prediction of the advantageous loading parameters and development of PSi particles with optimal surface chemistry and porous properties.

Use of porous silicon particles as oral drug delivery vehicles is still on quite early development stage. At this stage of the development, it is important to prove the feasibility and performance of the product by using a representative model drug compound. Indomethacin (IMC) is suitable for this purpose due to its low solubility and good availability.

Before the actual loading experiments, solubility of IMC has to be investigated, since the published works on the subject are scarce. Especially little is known about indomethacin solubility in mixed solvents. The solubility data helps in the decision of the composition of the solvent mixture and the concentration of the

drug in the loading solution. The tendency of indomethacin to form solvates makes the determination of solubility more challenging.

The selection of the loading solvents will be based on the solubility measurements. The drug loading will be investigated using the selected solvents and two different PSi materials. Loaded amount will be determined using thermal analysis. In addition, indomethacin loaded PSi and silica particles are studied using Raman spectroscopy.

7.1 Materials

Two PSi materials with different surface modification were compared in the drug loading experiments. The number of model drug compounds had to be limited to one. Indomethacin was selected as a model compound, since it is quite well-established and its aqueous solubility is very low compared to, for example, that of ibuprofen, which is maybe the most commonly used substance in the drug loading experiments. In addition to PSi-particles, also drug loaded silica particles were studied.

7.1.1 Mesoporous silicon particles

The mesoporous silicon particles were fabricated in the Laboratory of Industrial Physics in the Department of Physics at University of Turku. Thermally oxidized and thermally carbonized PSi-materials with the same particle size fractions were compared. The surface modification and characterization of the PSi particles were also carried out at the University of Turku. BET-nitrogen adsorption isotherms were determined in order to characterize the pore properties, and the results are presented in table IV. The pore size distributions were calculated according to the method of Barrett, Joyner and Halanda (BJH) and the results can be found in appendix A.

Table IV Properties of the PSi materials used in the experiments.

Type	Particle size, µm	BET surface area, m^2/g	Pore volume, cm^3/g	Average pore diameter, nm
TOPSi	53–75	240	0.811	14.8
TCPSi	53–75	283	1.207	17.8

7.1.2 Indomethacin

Indomethacin (IMC), 1-(4-chlorobenzoyl)-5-methoxy-2-methyl-1H indole-3-acetic acid, of analytical grade was purchased from Hawkins, Inc. IMC is a non-steroidal anti-inflammatory drug. Its chemical structure is shown in figure 9. As can be seen, indomethacin has several functional groups, which may contribute to the interactions influencing the loading process. Among these groups, the carboxylic acid group is likely to play an essential role. Carboxylic acid groups are able to form cyclic acid-acid dimers or chains via hydrogen bonding [93], and hydrogen bonding may naturally occur with any suitable functional groups of e.g. solvent molecules as well. The carboxylic acid group may also react e.g. with alcohols in esterification reactions. According to Watanabe *et al*. [94], esterification reaction may occur also with silanol groups upon grinding of IMC with silica. In alkaline conditions IMC exists in ionic form. The pK_a value of IMC is 4.5 [95].

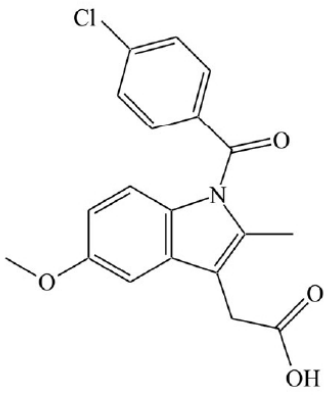

Figure 9. Molecular structure of indomethacin [96].

Three IMC polymorphs have been isolated. The most stable form is the form γ (also denoted as form I). The γ-form constitutes a monotropic system with α-form

(form II) [96]. Despite the thermodynamic metastability of the α-form, it may persist over 18 months at room temperature without transforming into the γ-form [97]. The third polymorph of IMC is the metastable δ-form (form IV) [98]. According to Legendre and Feutelais, a fourth polymorph has also been proposed in an article by Borka [96].

The polymorph form of IMC depends on the crystallization solvent. IMC is also known to form solvates with various solvents, for instance with propanol, dimethylether, dichloromethane, benzene, chloroform, acetone, methanol, and t-butanol [97, 99, 100]. These pseudo-polymorphs are generally denoted as β-form. Solvate formation may distort the results of solubility measurements and affect the drug loading process, so it must be taken into account. IMC crystallization studies in solvent mixtures have not been reported.

Indomethacin is vulnerable to photolytic degradation, so the samples have to be protected from light during all the experiments. Furthermore, both basic and acid hydrolysis reactions are feasible [101, 102]. A typical degradation route is via hydrolysis of the amide linkage [103]. Photolysis of IMC in methanol may produce methyl ester and γ-lactone derivatives [104-106]. The degradation of IMC can be observed from the Raman spectra mainly due to increased fluorescence [107].

7.1.3 Solvents

The initial screening of solvents was based on comparison of solubility parameters. Solvents were selected in a way that one of them has a higher Hildebrand solubility parameter value and the other a lower one than that of IMC. The calculations were based on the IMC solubility parameter values reported by Liu *et al*. [108], who have calculated them using the group contribution method. The reported value for overall solubility parameter is 24, which is higher than those reported by Forster *et al*. [109] (22.3 and 21.9). Since the value of the solubility parameter may vary depending on the method used in its measurement or calculation, the values may not be very accurate, but they probably give, however, quite good estimates.

Mixture of methanol and dichloromethane has been proven to provide high IMC solubility and it has been used successfully in the drug loading of PSi, too [2]. Since both methanol and dichloromethane are classified to the solvent class 2 in IHC guideline [85], the target of this study was to find out whether these solvents could be replaced with less hazardous ones: methanol with ethanol and DCM with acetone or ethyl acetate. Ethanol was selected since it is very much similar to methanol and it has been applied in drug loading experiments. Selection of acetone and ethyl acetate, on the other hand, was based on their good availability and their solubility parameters, which are quite near to that of DCM, even though the molecular structures are rather different. The Hansen solubility parameters for the selected solvents and for IMC are presented in table V, and some other properties of the solvents in table VI.

Table V Hansen solubility parameters of the selected solvents and IMC. δ_d is the dispersion term, δ_p the polar term, and δ_h the hydrogen bonding term.

Compound	δ, $MPa^{-1/2}$	δ_d, $MPa^{-1/2}$	δ_p, $MPa^{-1/2}$	δ_h, $MPa^{-1/2}$	Ref.
Indomethacin	24.0	21.4	5.8	9.2	[108]
DCM	20.3	15.3	6.1	3.9	[56]
Acetone	20	15.5	10.4	7.0	[56]
Ethyl acetate	18.1	15.8	5.3	7.2	[56]
Methanol	29.6	15.1	12.3	22.3	[56]
Ethanol	26.5	15.8	8.8	19.4	[56]

Table VI Properties of the selected solvents: molar volume V_m, density ρ, boiling point T_b, vapor pressure p_v, dynamic viscosity η, dielectric constant ε, and surface tension at liquid–air surface σ.

Solvent	V_m, [a] $cm^3\ mol^{-1}$	ρ, [a] $g\ cm^{-3}$	T_b, [b] °C	p_v, [c] kPa	ΔH_{vap} [d] $kJ\ mol^{-1}$	η, [e] mPa s	ε, [e] -	σ, [e] $mN\ m^{-1}$
DCM	55.4	1.316	39.64	61.3	28.9	0.411	8.93	27.2
acetone	74.0	1.075	56.07	30.9	30.5	0.303	20.56	22.7
ethyl acetate	98.5	0.894	77.06	12.9	35.6	0.426	6.02	23.1
methanol	40.7	0.786	64.54	17.0	37.7	0.551	32.66	22.3
ethanol	58.5	0.785	78.65	7.6	42.4	1.083	24.55	21.9

[a] Ref. [56]
[b] Ref. [110]
[c] Ref. [111], T = 24–30 ºC
[d] Ref. [112]
[e] Ref. [113]

According to Slavin *et al*. [97], all of the selected solvents are capable of forming IMC solvates. In the case of IMC crystallization from a solvent mixture, it is likely that a mixture of several solvate forms and polymorphs will be obtained. Furthermore, chemical reactions of the solvents must be taken into consideration. Acetone and alcohol may also react forming a hemi-ketal or further a ketal. Due to these side products, the binary solvent mixture may, in fact, include multiple components. The formed compounds might be problematic to remove in the drying stage, since they are slightly less volatile than the original solvents.

The solvents that were used in the experiments were of analytical grade, except methanol which was of HPLC grade (LiChrosolv), and ethyl acetate which was of synthesis grade (>99.5 %). DCM was stabilized with ca. 0.5 % of methanol, which was not taken into account in the calculations. Acetone, ethyl acetate and methanol were purchased from Merck, ethanol (ETAX Aa 99.5 %) from Altia, and DCM from Orion. All the solvents were used as received.

7.1.4 Indomethacin loaded silica particles

Indomethacin loaded SBA-15 and MCM-41 silica particles were studied using Raman spectroscopy. The characterization of the particles and drug loading had been carried out in the Laboratory of industrial physics of the University of Turku.

The physical properties of the original silica particles determined by nitrogen sorption method are presented in table VII. The sample names in the first column refer to the identifications of the loaded samples.

Table VII Properties of the SBA-15 and MCM-41 silica particles: particle size d_p, particle size below which 90% of the volume of particles exists D_v90, BET surface area S_{BET}, average pore diameter D_{BJH}, pore volume V_p, and porosity ε. (by T. Heikkilä, University of Turku)

Sample	**d_p, μm**	**D_v90, μm**	**S_{BET}, m^2/g**	**D_{BJH}, nm**	**V_p, cm^3/g**	**ε, %**
SBA+indo(5)	100–125	117.4	597	5.9	0.880	67.1
SBA+indo(6)	45–63	54.0	535	5.3	0.709	62.1
MCM+indo(3)	100–125	161.3	935	3.4	0.789	64.3
MCM+indo(4)	45–63	72.4	909	3.5	0.785	64.2

All of the samples were loaded with similar method except that the concentration of IMC in the loading solution was a bit higher in the case of MCM-41. The loading solvent was hot ethanol (68 °C). IMC was added to the pre-heated solvent so that the concentration of the loading solution was 180 mg/mL for the SBA-15 particles and 250 mg/mL for the MCM-41 particles. The silica particles were added to the clear solution. The loading time was 2 h. After the loading the particles were separated by vacuum filtration (Versapor filter, pore size 1.2 μm) and dried at 65 °C for 24 h. The particles were protected from light and stored in a dry silica exsiccator prior to the analysis.

Due to the scarce sample materials, the samples used in the Raman analysis were already used in Tristar analysis. These Tristar samples had been analyzed using Tristar nitrogen sorption method in which the sample is exposed to the temperature of liquid nitrogen (-196 °C). The possible changes in the sample during this treatment were studied by comparing an original sample SBA+indo(5) and a Tristar measured sample SBA+indo(5)-TRISTAR. Furthermore, the stability of the drug loaded into the silica particles was studied by analyzing stressed samples that had been aged for 3 months at the temperature of 30 °C and relative humidity (RH) of 60 %.

The drug loads were determined in the University of Turku using TG (PerkinElmer TGA-7) and DSC (PerkinElmer Diamond). The determined drug loads for both the original and the stressed samples are presented in table VIII. In the TG measurements, the sample was heated from room temperature to 850 °C in a Pt-crucible. Al-pans with a pierced lid were used in DSC and the final temperature was 200 °C. Both TG and DSC measurements were carried out in inert N_2 atmosphere. Heating rates in the TG and DSC measurements were 10 K/min and 20 K/min, respectively. The high heating rate used in the DSC measurements may have caused overlapping of the small melting endotherms of the two IMC polymorphs, α and γ, which impedes the specification of the solid form and may result in small error in the calculated crystalline surface fraction.

Table VIII Drug loads of the IMC loaded silica samples determined using TG and DSC (by T. Heikkilä, University of Turku).

Sample	**Total payload, w-%**	**Amorphous drug, w- %**	**Crystalline drug, w-%**
SBA+indo(5)	37.6	36.3	1.3
SBA+indo(5) stressed	36.4	35.9	1.3
SBA+indo(6)	35.3	32.4	2.9
SBA+indo(6) stressed	27.3	22.5	4.8
MCM+indo(3)	23.8	21.5	2.3
MCM+indo(3) stressed	24.0	23.3	0.7
MCM+indo(4)	24.5	22.7	1.8
MCM+indo(4) stressed	24.7	23.7	1.0

7.2 Setup and procedure

The first step of the experiment procedure was the determination of the solubility of IMC in the binary mixtures of solvents described in chapter 7.1.3. The solvent mixtures providing the highest IMC solubility were selected for the loading experiments based on these solubility measurements. The methods used and the experiment procedure are next described in detail.

7.2.1 Solubility measurements

The solubility of IMC in solvent mixtures with different compositions was determined gravimetrically. The solvent mixtures with different composition were prepared. IMC suspensions were prepared by adding IMC in small amounts until

an excess of solid was observed. The solutions in sealed flasks were kept under magnetic stirring in a temperature-controlled bath at the constant temperature of 25 °C. After the equilibration time of 24 hours, the solids were let to settle and clear solution samples was taken using a syringe equipped with a filter unit (Whatman Spartan 30 regenerated cellulose filter unit, pore size 0.2 μm). The solid phase was separated by vacuum filtration using an ashless filter paper. The clear solution was weighed and dried at 36 °C under vacuum for three days. Heinz *et al*. [114] have reported of using the same drying temperature for crystallized IMC. The precision of the balance used in the solubility measurements was 1 mg.

The physical forms of the IMC re-crystallized upon drying of the clear solution and the solid filtered from the solid–liquid suspension were both analyzed with Raman spectrometer. The excitation source used was a far-red laser operating at 785 nm. The spectrometer slit was set to 150 μm and the confocal hole to 400 μm. The sample exposure time was set to 2 s with two accumulations. The measurements were performed in duplicate. The spectra were collected using a wave number range from 200 to 1750 cm^{-1}. Baseline correction was carried out using LabSpec software.

The solvent–solvent interactions were investigated using an immersion Raman probe. The sample exposure time of 60 s and two accumulations per one measurement were selected for the liquid samples. The wave number region studied ranged from 200 to 1750 cm^{-1}.

The samples from the pure solvents and a part of the samples from solvent mixtures were also analyzed with combined TG-DTA in order to investigate the desolvation. The samples were heated from the room temperature up to 200 °C with a heating rate of 10 °C/min in an Al_2O_3 crucible under He atmosphere.

The constants of Jouyban-Acree model for each solvent pair were determined by fitting equation (21) to the solubility data using least squares method. Matlab and MS Excel were used in the mathematical data handling.

7.2.2 Loading experiments

Prior to the loading experiments, PSi particles were dried in vacuum at 100 °C for 2 h in order to remove moisture from the pores. After this treatment, the particles were let to cool in a desiccator. The loading solutions were prepared by mass. The IMC concentration in the solutions was selected to be 0.8 times the saturation concentration. The solutions were kept at 25 °C in a thermostated water bath under magnetic stirring for 2 h to ensure the total dissolution of IMC. The density of each solution was measured using a density meter (Anton Paar DMA 4500) for the determination of the minimum drug load. In order to avoid the photolytic degradation of IMC, the solutions as well as the loaded samples were protected from light as much as possible.

For the loading experiments, 30 mg of porous silicon was weighted and 3 mL of loading solution was then added. Loading time was selected to be 2 h. A magnetic stirrer bar was used for mixing.

After the loading, the solids were separated with vacuum filtration using a PTFE membrane (Pall Life Sciences TF-200, pore diameter 0.2 μm) as a filter media and dried at 85 °C for 1 h. The temperature was selected to enable desolvation of the possibly formed solvates. According to Joshi [98], IMC should not decompose at the selected temperature. After the drying, the samples were let to stabilize in a desiccator at least for 3 days prior to the analysis.

7.2.3 Analysis of loaded samples

The loaded samples were analyzed with a TG-DTA instrument Netzsch STA 449C. The samples (1–6 mg) were heated in open Al_2O_3 crucibles from 25 °C to 850 °C with a heating rate of 10 °C/min under dynamic helium (flow rate 70 mL/min). Temperature and sensitivity calibration had been carried out with 5 calibration standards (In, Sn, Zn, Ag, Ni) and mass calibration with a standard mass of 2 g. According to the manufacturer, the measuring uncertainty is 0.012 mg.

For comparison, the theoretical maximum and minimum loadings were calculated using equations (24) and (12), respectively. The maximum value tells the amount of the drug that could physically fit into the pores. The IMC density value used in the calculations is 1.457 g/mL, which has been reported by Chieng *et al*. [115] for amorphous IMC produced by milling.

$$q_{\max}^{theor} = \frac{\rho_{drug} V_s}{1 + \rho_{drug} V_s} \tag{24}$$

$q_{max,\,theor}$	theoretical maximum loaded amount, g drug / g
ρ_{drug}	density of the drug, g/mL
V_s	pore volume, mL/g PSi.

The presence of surface fraction was investigated using Netzsch DSC 204 F1. Closed Al-pans with pierced lids were used. The samples (1–3 mg) were heated from 20 °C to 200 °C, with a heating rate of 10 °C/min under nitrogen purge (flow rate 40 mL/min). An empty Al pan was used as a reference. Calibration was performed in conditions equal to those used in the measurements using standard materials (Hg, In, Sn, Bi, Zn, and CsCl). The calibration was validated with In prior to analysis. The baseline was corrected by removing the background that was measured with an empty crucible using the same temperature program. Netzsch Proteus software was used for data handling.

The uniformity of drug loading and the solid form of the loaded drug was studied using a Horiba Jobin Yvon LabRam 300 Raman microscope equipped with a liquid nitrogen cooled CCD detector. A laser with a wavelength of 785 nm was employed. Preliminary experiments revealed that Raman spectroscopy is not applicable in the analysis of loaded PSi-particles. In the analysis of PSi materials it is necessary to use a filter to reduce the laser power; otherwise the spectrum will reach the saturation level. The filtering will, however, reduce the intensity in such a way that the loaded IMC cannot be detected at all. On the other hand, in the case of drug loaded porous silica Raman spectroscopy is applicable analysis method, since the reduction of the laser power is not required.

In the analysis of the indomethacin loaded silica particles, the spectrometer slit was set to 100 μm and the confocal hole to 1000 μm. The sample exposure time was set to 15 s. Accumulation was performed in duplicate in order to reduce the noise level. In order to get information of the uniformity of the drug load, Raman mapping was used. In the mapping mode, altogether 576 spectra at different points were collected systematically so that the distance between adjacent measurement points was about 100 μm. Baseline correction was carried out using LabSpec software and Matlab was used for further data handling and for visualization of the data.

8 Results and discussion

The results of the IMC solubility tests and the loading experiments of TOPSi and TCPSi microparticles are presented in this chapter. Higher solubilities were observed in binary solvent mixtures than in single solvents. The strong tendency of IMC to form solvates impeded the interpretation of solubility data and affected the adsorption into PSi particles.

8.1 Solvent selection and characterization of indomethacin

The solubility of IMC was studied in solvent mixtures in order to maximize the IMC concentration in the loading solution. Solubility measurement and analysis of the solid phase gave also information about the behavior of IMC in the solvent mixtures used. The solubility curves can be found in appendix B.

8.1.1 Solubility of IMC

The solubility of IMC was determined in various binary solvent mixtures but in order to determine the solubility enhancement in solvent mixtures over pure solvents, the solubility of IMC was determined in neat solvents, too. The results of the solubility in pure solvents are presented in table IX. Solvates were formed in all of the pure solvents except in ethanol. The true solubility values were calculated by taking into account the desolvation based on the mass loss determined with TG.

Table IX IMC solubility in pure DCM, acetone, ethyl acetate, methanol, and ethanol.

Solvent	Experimental solubility, g/100 g solvent	Desolvation mass loss, m-%	True solubility, g/ 100 g solvent	Mole fraction of IMC
DCM	5.44	1.11	5.38	0.0126
Acetone	12.55	3.74	12.08	0.0192
Ethyl acetate	4.60	3.84	4.43	0.0108
Methanol	2.41	6.19	2.26	0.0020
Ethanol	2.79	0	2.79	0.0036

In the light of the results of the solubility measurements in neat solvents, IMC is sparingly soluble in pure alcohols and soluble in the less polar solvents studied. When comparing the results with the scarce IMC solubility data available, they agree quite well; the experimental value for the solubility in pure ethanol was 2.79 g IMC / 100 g solvent and the literature value is 25 mg/mL (3.18 g / 100 g solvent) [116]. The highest solubility was determined in acetone, probably due to the absence of intramolecular association in acetone [117]. The solubility in ethyl acetate was closest to the ideal solubility of IMC (x_2 = 0.0101). The ideal solubility value was calculated using eq. (14) and the values of melting point and enthalpy of fusion reported by Legendre and Feutelais [96] were used.

The solubility of IMC increased significantly as solvent mixtures were used. The solubility curves in each solvent mixture are presented in appendix B. The solvent mixtures that yielded the solubility maxima and the saturation concentrations of IMC in them are presented in table X. The values overestimate the solubility slightly since the mass of the solvent present in the solvates has not been diminished.

Table X The mixtures of the studied solvent pairs providing highest IMC solubility, and the calculated effective Hildebrand's solubility parameters and the IMC saturation concentrations in the mixtures. w_1 is the mass fraction of solvent 1 in the solvent mixture.

Solvent 1	Solvent 2	w_1, w- %	$\bar{\delta}$, $MPa^{-0.5}$	c^*, g/100 g solvent
DCM	Methanol	80	23.03	34.69 ± 0.43
DCM	Ethanol	70	22.89	27.40 ± 0.01
Acetone	Methanol	75	23.00	24.08 ± 0.14
Acetone	Ethanol	80	21.66	21.81 ± 0.05
Ethyl acetate	Methanol	75	21.26	14.95 ± 0.06
Ethyl acetate	Ethanol	70	20.86	13.49 ± 0.10

Higher solubilities are obtained in methanol mixtures than in ethanol mixtures, probably due to its higher hydrogen bonding ability. High solubility may also be a result of acid–base interaction between the solute and the solvent. Since methanol is a stronger Lewis base than ethanol, the acid–base interactions between methanol and acidic IMC are more favorable than in the case of ethanol. Interestingly, the solubility of IMC in pure ethanol is, however, a bit higher than

that in pure methanol, probably because ethanol molecules are not bound to as ordered net structure as small methanol molecules, which is favorable to the cavity formation. The higher solubility in ethanol than in methanol is also in agreement with the smaller difference between the solubility parameters of IMC and ethanol.

DCM seems to be the most powerful co-solvent. This will probably result from its lower polarity and small molecular volume, which allows it to effectively break the highly ordered chain structure of alcohols that is presented in figure 10. Due to the low hydrogen bonding ability of DCM, it does not compete on the hydrogen bonding sites with IMC.

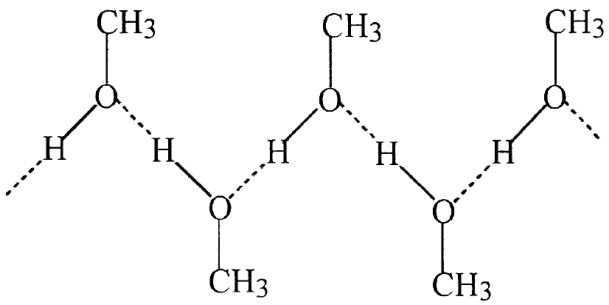

Figure 10. The hydrogen bonding network in pure methanol [118].

The Raman spectra of the solvent mixtures did not reveal any significant solvent–solvent interactions. As an exception, a small new peak appeared in one of the acetone–ethanol mixtures (a mixture containing 70 % acetone) in the wave number range from 540 to 550 cm^{-1}, which might be a sign of the hemi-ketal formation.

Figure 11 illustrates the solubility profile of IMC, i.e. solubility vs. the effective Hildebrand solubility parameter of the solvent. In an ideal case, the solubility parameter value of the optimal solvent mixture is equal to the solubility of the solute, and thus independent on the composition of the solvent mixture. The solubility profile (Fig. 11) of IMC shows, however, deviation among the solubility parameters of the solvent mixtures providing the solubility maxima. Moreover, all of the values are below the reported solubility parameter of IMC (δ = 24.00)

[108]. Romero *et al.* [119] have observed similar deviation between the experimental solubility parameter and the value calculated with the group contribution method, and according to them, the possible reason is that the group contribution method overestimates the effect of the aromatic ring to the molar volume.

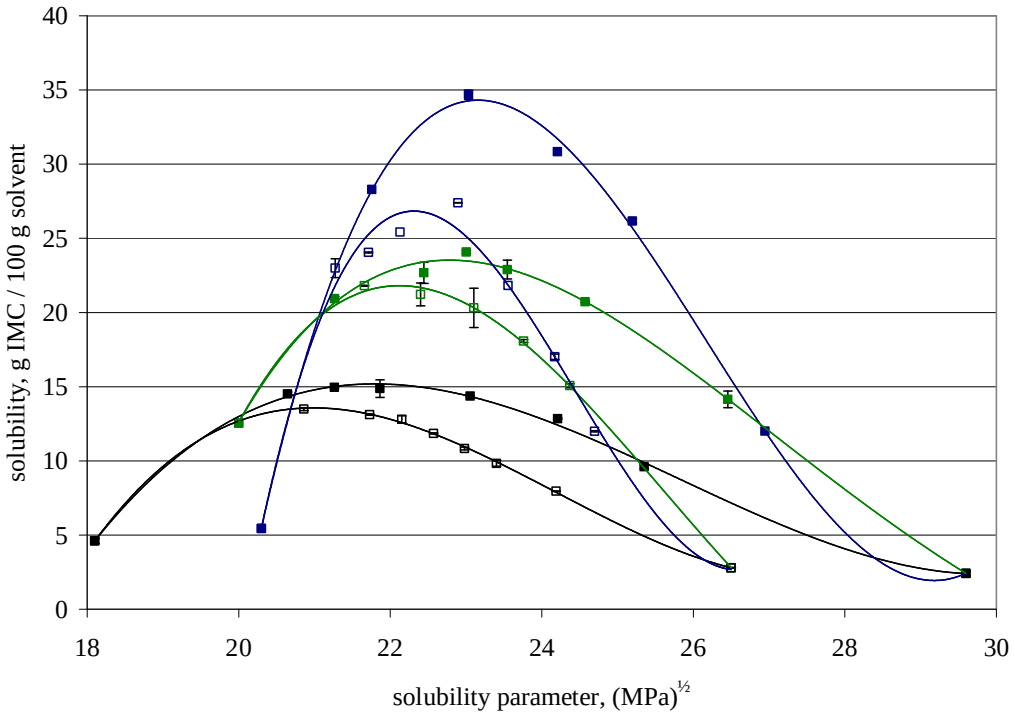

Figure 11 The solubility of IMC as a function of the solubility parameter of solvent mixture. DCM–MeOH mixtures: closed blue symbols, DCM–EtOH mixtures: open blue symbols, acetone–MeOH: closed green symbols, acetone–EtOH: open green symbols, EtOAc–MeOH: closed black symbols, EtOAc–EtOH: open black symbols. The fitted polynomial curves are only guides for eyes.

Romero *et al.* [119] and Teychene *et al.* [120] have also used equation (25) proposed by Lin and Nash for calculating the experimental solubility parameter. The equation is based on the experimental solubilities in three pure solvents and the solubility parameters of these solvents. The obtained value depends on the solvents selected. If equation (25) is extended by including all the data points obtained from the solubility measurements, the solubility parameter of IMC is 22.77.

$$\delta = \frac{\sum_i x_{2,i}\delta_i}{\sum_i x_{2,i}} \qquad (25)$$

In order to get better understanding of the nature of the solubility of IMC in solvent mixtures, it is favorable to examine the solubility data from several viewpoints. In figure 12, the solubility has been presented as a function of the molar composition of the solvent mixture. The figure reveals that, independently of the solvents, the solubility maximum is obtained with the alcohol fraction around one third. Another observation that can be done from figure 12 is that the mole fraction solubilities obtained in mixtures with EtOH and MeOH are approximately the same in the case of acetone and EtOAc, but DCM–MeOH mixtures show higher solubilities than the mixtures of DCM and EtOH.

It is notable, that the mixture that contains 30 w-% of ethanol in ethyl acetate and shows the highest IMC solubility is an azeotrope [121]. The molar ratio of EtOAc and EtOH in the mixture is 2:1. The solubility maximum observed in acetone–methanol mixtures was also close to the azeotropic point (acetone mole fraction 0.783 [122]). DCM and methanol, on the other hand, form an azeotrope with DCM mole fraction 0.846 [123] and the solubility maximum was showed by the mixture with a mole fraction of 0.706. Correlation between the solubility maximum and the azeotropic point has also been reported by Teychene *et al*. [120]. According to them, the presence of solute in the mixture increases non-ideality of the mixture. This might explain the difference from the azeotropic point in the case of DCM–methanol mixtures, where the amount of dissolved IMC is higher. Also the possible impurities in the solvents may shift the equilibrium.

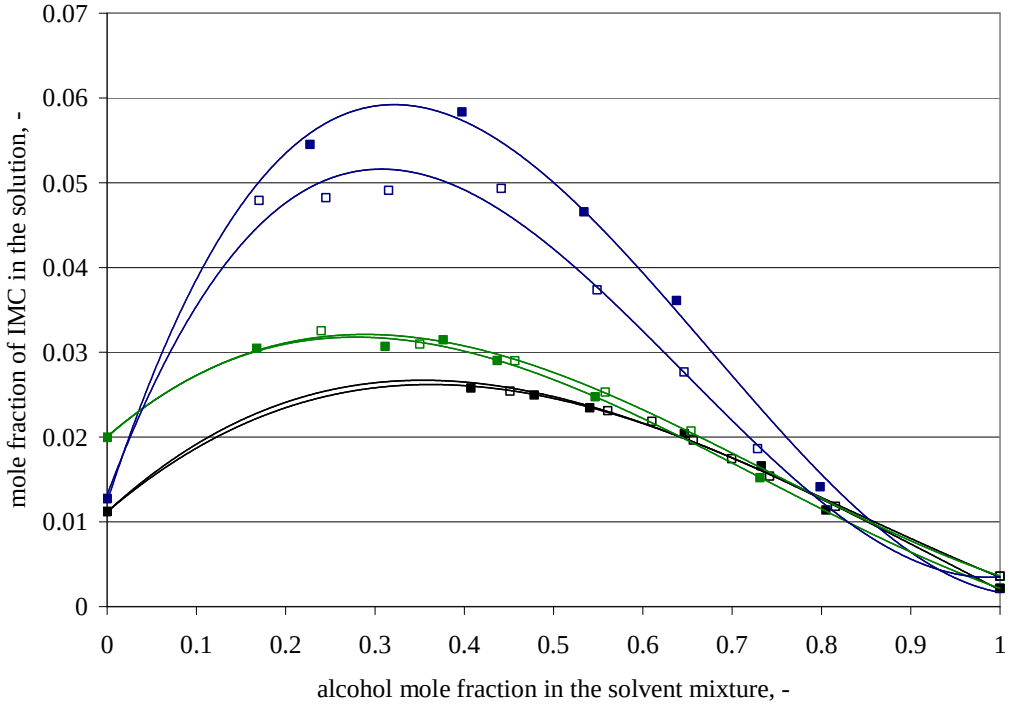

Figure 12 Solubility of IMC in binary solvent mixtures with varying mole fraction of alcohol. DCM–MeOH mixtures: closed blue symbols, DCM–EtOH mixtures: open blue symbols, acetone–MeOH: closed green symbols, acetone–EtOH: open green symbols, EtOAc–MeOH: closed black symbols, EtOAc–EtOH: open black symbols. The fitted polynomial curves are as a help for eye.

The Jouyban–Acree model parameters were determined by fitting the experimental solubility data, and the model constants obtained are presented in table XI. As can be seen from the values of mean percentage deviation and from the fitted curves, which are presented in appendix B, this nearly ideal binary solution model defines the solubility of IMC in the studied solvent mixtures well.

Table XI The fitted model constants of the Joyban–Acree model and the mean percentage deviation *MPD* of the experimental and fitted solubilities.

Solvents	B_0	B_1	B_2	R^2	*MPD*, %
DCM-MeOH	8.966	0.300	4.581	0.991	5.07
DCM-EtOH	7.212	1.889	3.801	0.933	6.21
Acetone-MeOH	5.636	-1.593	2.404	0.991	1.25
Acetone-EtOH	4.684	-0.849	2.429	0.994	1.08
EtOAc-MeOH	6.436	-1.802	3.493	0.997	1.51
EtOAc-EtOH	5.447	-0.760	1.298	0.999	0.76

The solubility in the mixtures of EtOAc and EtOH gave the best fit; thanks to the absence of solvates in the solid phase. Since the standard deviation of the duplicate measurements was also lowest in the EtOAc–EtOH mixtures, it can be concluded that the best accuracy of the experimental solubilities was obtained with this solvent pair. One of the key factors behind the accurate results is probably the low vapor pressures of EtOAc and EtOH. Evaporation of the solvent is often an essential error source in the solubility measurements.

The model constants could be applied in determination of the two-body and three-body interactions in the solvent mixture. It is, however, risky to draw conclusions of these interactions due to the scarcity of comparable values. It was neither reasonable to develop the model further, since the current dataset was not adequate for the development and evaluation of a sophisticated model.

8.1.2 Polymorphs and solvates of IMC

Three different polymorphs (α, γ and δ) of IMC were obtained as IMC was recrystallized from different solvents. Furthermore, IMC formed solvates with all of the solvents studied. The solvate formation was strong with acetone, methanol and DCM, but solvates with ethanol and ethyl acetate were observed only in single samples. The characterization of the different forms of IMC was based on thermal analysis and Raman spectroscopy. In order to facilitate the interpretation of the results, the structures and thermodynamic properties of the IMC polymorphs and solvates are first briefly reviewed.

The interactions of IMC with the solvent molecules affect its molecular orientation upon crystallization and thus lead to certain morphology. Therefore, the polymorphic form is determined by the crystallization solvent. In addition, the conditions, especially the supersaturation level, have a significant effect on the formed product as shown by Slavin *et al*. [97] who have studied crystallization of IMC in various solvents at high and low supersaturation levels. It is typical that metastable forms are obtained at high temperatures, i.e. above the glass transition temperature T_g of IMC (45 °C) [124].

The molecular orientation in the crystal structure of α and γ IMC is illustrated in figure 13. In α form, three molecules form a chain via hydrogen bonding between the carboxylic acid groups and between carboxylic acid and amide [116]. The chain structure explains the needle-like shape of the crystals. γ IMC, on the other hand, consists purely of carboxylic acid dimers, which results in the rhombic plate morphology [97]. The reactive carboxylic acid groups are shielded by hydrophobic groups which probably plays the key role in the stability of the γ form [125]. The structure of δ IMC has not been identified [126], and also the structures of the majority of IMC solvates remain unknown.

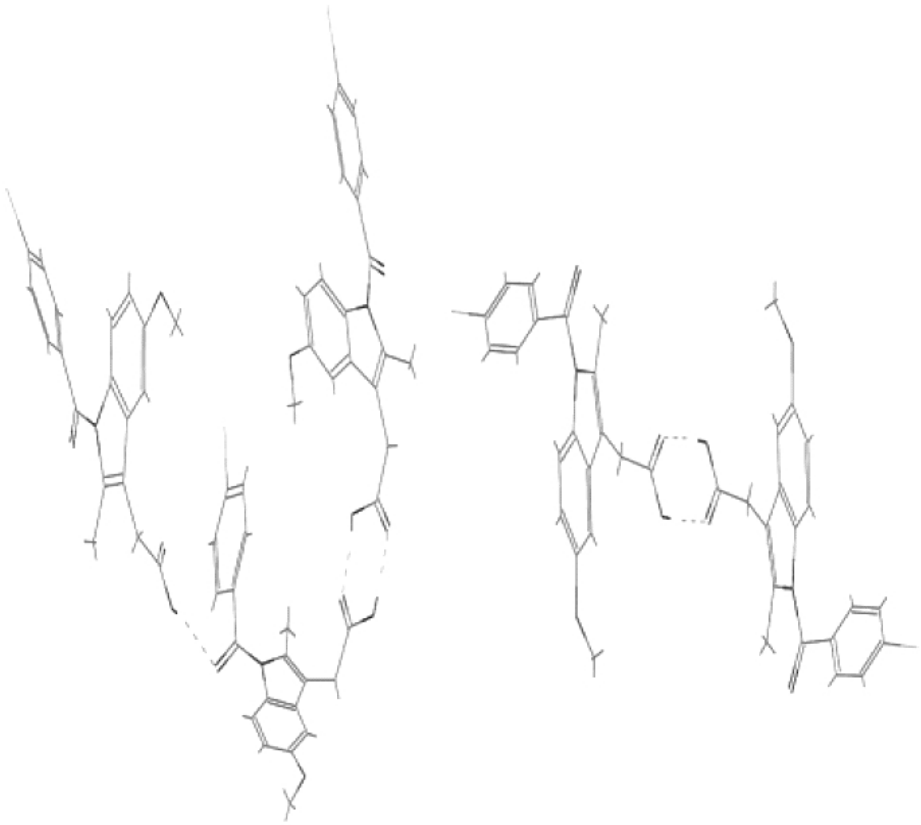

Figure 13. The hydrogen bonded IMC molecules in the α form (on the left) and in the γ form (on the right) [116].

According to Joshi [98], the DCM and acetone solvates of IMC are non-stoichiometric, and probably also the ethyl acetate and ethanol solvates belong to the same category. Strictly speaking, these compounds are not real solvates due to their non-stoichiometric composition. The solvent is not bound in to the crystal structure, more like adsorbed or occluded, which might explain why these solvates

are mainly formed only at high supersaturation levels as reported by [97]. However, a composition involving 0.5 moles of solvent per one mole of IMC has been proposed [97].

IMC methanolate has a stoichiometric 1:1 composition for which two defined structures have been proposed (Figure 14). The second hydrogen bonding arrangement is actually the mirror image of the first one, but it results in a plate-like crystal shape, not the needle-shaped crystals that are related to the first arrangement. [98]

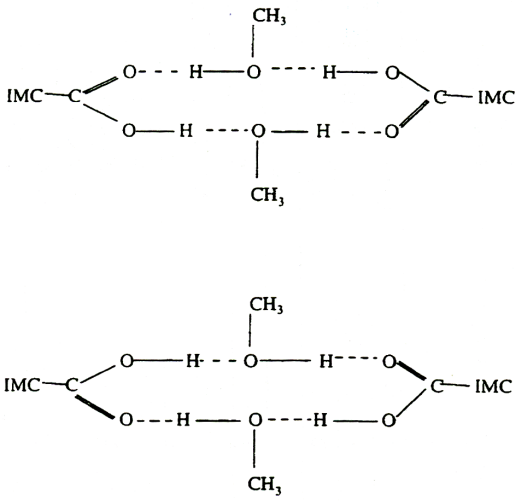

Figure 14. H-bonding in IMC methanolate [98]

A hydrogen bonding arrangement akin to the one presented in figure 14 is also characteristic for the t-butanol solvate of IMC [98]. The structure results in columnar crystal morphology [97]. The peculiarity is, however, that other alcohols do not produce the same solvate structure. In the light of this fact, it could be proposed that the formation of the presented hydrogen bonding arrangement necessitates a solvent with symmetric structure and relatively small molecule size.

A simple method to determine the amount of solvent in the solvate is to measure the mass loss accompanied with the desolvation using TG. In the present study,

the observed mass loss upon desolvation of IMC solvates (Table IX) was often much lower than the theoretical mass loss calculated presuming unimolar methanolate composition and the 1:0.5 IMC:solvent compositions for all the other solvates. The mass loss values for DCM and acetone solvates agree quite well with the results of Hamdi *et al*. [99]. On the other hand, in their study the crystallization of IMC in ethanol and methanol did not yield solvates at all.

The variation in the observed desolvation mass losses can be thought to confirm the non-stoichimetric composition of the IMC solvates. On the other hand, the used experiment conditions and methods have a crucial effect on the results, which impedes the comparison.

Desolvation temperature is higher than the boiling point of the solvent. This holds true also for non-stoichiometric solvates, since even if the solvent molecules are not strictly bound into the crystal lattice, there are certainly attractive interactions, e.g. van der Waals forces, between the solvent molecules and the parent compound. Desolvation of IMC solvates occurred mainly in the temperature range of 70–100 °C.

The drying of the DCM solution saturated with IMC yielded pure α form of IMC. On the other hand, the filter cake, i.e. the excess solids, included both α and γ forms as well as DCM solvate. The desolvation of the DCM solvate of IMC occurred between 65 °C and 110 °C. The mass loss observed was only about 1 %. Desolvation was followed by an exotherm in the DTA curve, probably due to the re-crystallization of IMC.

Acetone solvate was present in the cake sample only when pure acetone was used as a solvent, but upon drying the filtrate samples solvate was also formed in acetone–alcohol mixtures. Similarly to the case of the DCM solvates, IMC was re-crystallized after desolvation. The re-crystallization phenomena have also been reported by Hamdi *et al*. [99].

Based on the thermal analysis, IMC methanolate was present only in the sample taken from the dried filtrate, not in the one from the filter cake. This observation

can be explained by the different supersaturation levels during crystallization. Slavin *et al*. [97] have reported that IMC methanolate is only formed at low supersaturation conditions which are typical to the slow drying of the saturated solution at low temperature.

The onset temperature of IMC methanolate desolvation was 82.9 °C and the mass loss of 6.19 % was observed. The desolvation temperature is exactly the same as reported by Crowley and Zografi [100]. δ-, α- and γ-forms were all present in the samples, the first one being the dominating polymorph. According to Joshi [98], δ IMC is formed upon desolvation of IMC methanolate. Interestingly, metastable δ IMC was also present in the cake samples, even though no methanolate was present in them. Another surprising result was the presence of δ form in some samples crystallized from DCM–ethanol mixtures. This can be, however, easily explained by the reason that the DCM used contained a small amount of methanol as a stabilizer.

The carbonyl stretching region is the most interesting part of the Raman spectra of different IMC forms. Taylor and Zografi [93] have presented Raman spectra for the α, γ and amorphous forms of IMC, and Hédoux *et al*. [126] have complemented the spectral data to include also the spectrum of δ IMC. In addition, Joshi [98] has presented FT-Raman spectra of α, γ and δ IMC and methanol and t-butanol solvates. The Raman spectra of the three polymorphs and amorphous IMC are presented in figure 15.

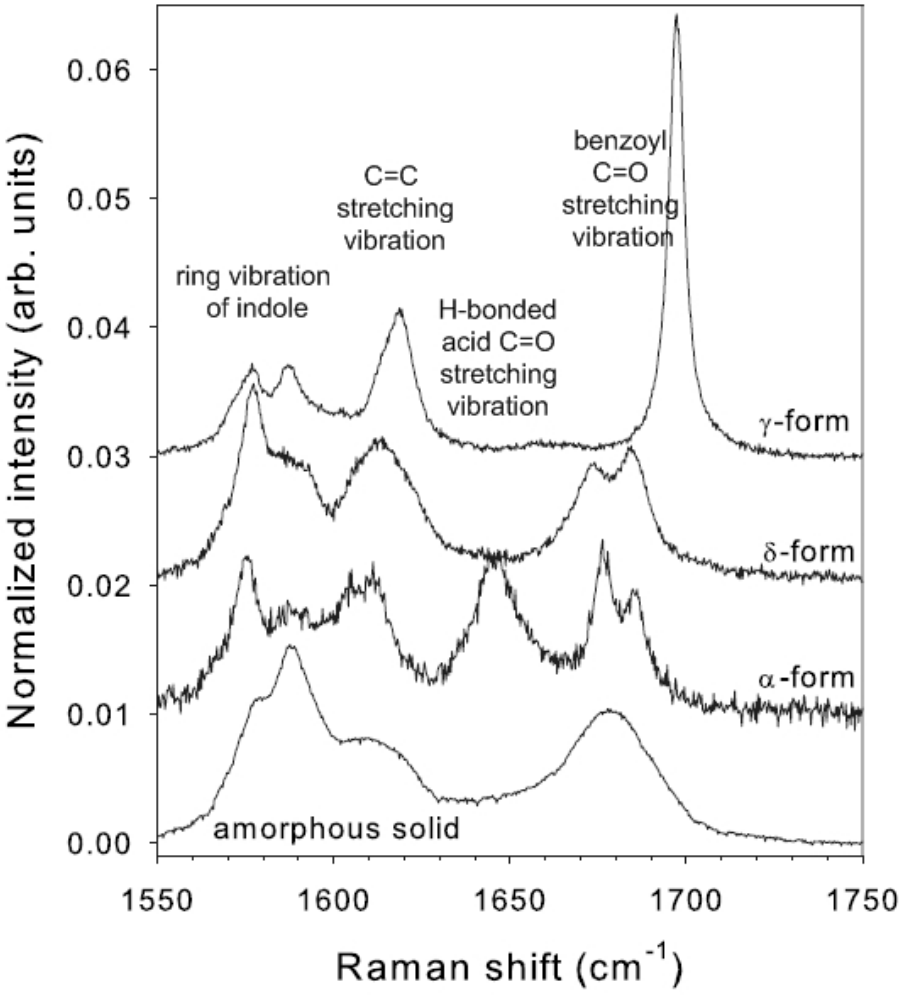

Figure 15. The Raman spectrum of α, γ, δ, and amorphous IMC in the carbonyl stretching region (adapted from [126]).

The spectral data of δ IMC reported is conflicting; according to Joshi [98], the peak at 1649 cm^{-1} is present in the Raman spectrum of δ IMC, but the peak was not observed by Hédoux *et al*. [126]. The probable reason is that the authors used different methods for producing δ IMC. In the former case, δ IMC was obtained upon desolvation of methanolate, in the latter case supercooled liquid was isothermally aged at 353 °C. The peak at 1649 cm^{-1} has probably been caused by the presence of α form which may have been formed instead of methanolate if supersaturation has been reached a high level locally due to the unevenness of evaporation.

The Raman spectra of the non-stoichiometric solvates of IMC have not been published. The difficulty of producing pure solvates and the disturbing fluorescence are the main problems in the analysis. The Raman spectra obtained during the solubility study can be roughly divided into five different types: γ form, α form, and 3 different solvate spectra. Typical examples of these spectra are presented in figure 16. It has to be emphasized that the spectra shown are not fully representative spectra of the pure forms, since all of the samples include likely desolvated forms, degradation products or traces of other polymorphs in some extend.

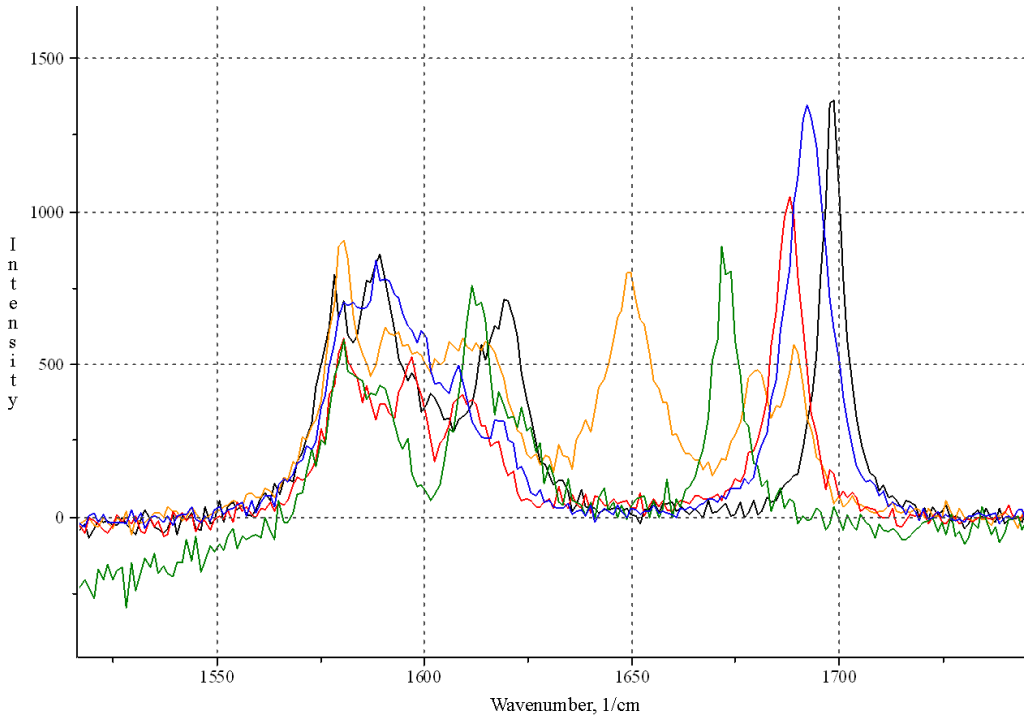

Figure 16 Raman spectrum of IMC γ form (black), α form (orange), methanolate (blue), solvate 1 (red), and EtOAc solvate (green).

The spectrum of methanolate agreed well with the one presented by Joshi [98]. DCM, acetone and ethanol solvates showed identical Raman spectra. In figure 16, the spectrum is denoted solvate 1. Surprisingly, also the excess solids from pure methanol and from the DCM–ethanol 2:3 mixture resulted in this spectrum. The spectrum of the proposed ethyl acetate solvate observed in one of the samples differed much from all the other spectra, and its interpretation is risky, since the strong fluorescence indicates degradation of IMC.

In the spectra of the solvates, the band of the benzoyl C=O vibration is shifted to a lower wavelength compared to the γ form. This indicates that the vibration of the benzoyl groups is hindered for some reason. Hydrogen bonding is a typical reason for the shift of a band to a lower frequency [127]. The polymorphs α and δ both have hydrogen bounded and non-bounded benzoyl groups in their structures, which produces two separate peaks in the benzoyl C=O vibration region [126]. In the amorphous form, these two peaks have melted into one broad peak [128]. In the spectra of the solvated forms, however, only a single, quite narrow peak can be observed.

Towler and Taylor [116] have presented spectra of IMC in ethanol and in nitromethane. In spite of the formation of the metastable α-form of IMC in a supersaturated ethanol solution, the Raman spectrum does not show a peak at 1650 cm^{-1}, which is inherent for the solid-state spectrum of α IMC. The peak at 1650 cm^{-1} represents the hydrogen bond between amide carbonyl and carboxylic acid. According to Towler and Taylor [116], it seems that the solvent-solute interactions are dominating the spectra of solutions containing solid aggregates.

The spectrum observed for the “solvate 1” in the present work (figure 16) bears a resemblance to the spectra presented by Towler and Taylor. That kind of spectrum can be thought to present the interactions of IMC with any adsorbed organic solvent. Then the appearance of that spectrum in the case of the filter cake samples from methanol and a DCM–ethanol mixture could be explained with the solvent residuals that remaining in the samples due to insufficient drying. The presence of solvent residuals would have been, however, observed in the TG analysis. In the light of the DTA curve, the samples were desolvated methanolate which contained all the three polymorph forms of IMC, δ being the dominating form. Nevertheless, the spectrum was not in agreement with either of the spectra presented for the δ form in references [98, 126]. Furthermore, it remains unclear why the DCM and acetone solvates show similar spectrum as the desolvated methanolate.

8.1.3 Problems in the solubility measurement

IMC showed up to be a challenging model compound due to its polymorphism and the formation of various solvates. As a consequence, a special attention had to be paid on the characterization of the solid phase already during the solubility measurements.

It has to be emphasized that the study was of qualitative nature, and the aim was not to produce pure solvated forms or polymorphs. Therefore, the determination of the compositions of IMC solvates based on the mass losses observed in TG analysis might give erroneous results even in the case of pure solvents, since it is very likely that the samples are mixtures of solvates and non-solvated IMC polymorphs. Furthermore, it is probable that desolvation has already occurred partially upon vacuum drying of the samples. There was also quite much deviation in the results. For instance, the TG mass losses observed upon desolvation varied between the samples taken from the same solvent mixture.

Due to the above mentioned difficulties in the determination of the exact compositions of IMC solvates, it is not easy to take the solvate formation into account in the solubility calculations. Furthermore, the presence of other forms than the most stable γ-form in the cake samples impugns the solubility results. The determination of the true equilibrium solubility of a polymorphic compound presumes namely that the excess solids are in the most stable form that always has the lowest solubility [129]. On the other hand, based on the Le Chatelier's principle, a solvate is less soluble in the solvent from which it is formed than the original solid.

It has to be admitted that there are several possible error sources in the solubility measurements. Since the dissolution curves versus time were not determined, it is not completely sure if the experiment time of 24 h was sufficient for obtaining the equilibrium. Some times the equilibration time was even shorter since a bit more IMC was added if the excess solids were totally dissolved when the samples were checked during the experiment. If the equilibrium is not achieved, the amount of

excess solids may, furthermore, affect the apparent solubility as Kawakami *et al*. [130] have presented using IMC as a model compound.

Romero *et al*. [62] have presented saturation curves vs. time which show that several days or even weeks may be required to reach the final equilibrium state. Similar long-time experiments could be recommended for IMC. The first appearance of a region of constant concentration in the saturation curve might not give the true solubility, since the saturation curves of IMC could possibly show plateau regions attributed to a metastable form due to the strong tendency for solvate formation and polymorphism.

Another weakness of the solubility experiments was the lack of reliable analysis for the possible degradation of IMC. Solvent induced degradation is typical for pharmaceuticals. Furthermore, the cake samples were not protected from light during the drying, which may have induced photolytic degradation of IMC. In the case of IMC methyl ester, a typically formed degradation product in the pholysis of IMC in methanol, the melting peak is overlapping with the endotherm of desolvation, since the melting point of the methyl ester is reported to be 85–87 °C [104] and the desolvation and the evaporation of the solvent usually occurred at the temperature range of 80–90 °C.

Similarly to the thermal analysis, also Raman spectroscopy fails to give any clear evidence of the decomposition of IMC. The presence or absence of the degradation products could be determined, for instance, using HPLC with a UV-detector [131]. In fact, HPLC is a widely used technique in solubility measurements. One example of the superiority of HPLC over other methods from this point of view is that it enabled Nti-Gyabaah *et al*. [132] to observe degradation of lovastatin in methanol, which has not been noticed by Sun *et al*. [133], who had used a laser monitoring observation technique.

Optimization of the drying conditions and time would significantly improve the quality of the results. In addition to the drying temperature and pressure, the geometry of the sample container has a substantial effect on the drying process. It could be observed with a naked eye that the shape of the crystals formed on the

walls of the container often differed from that of the crystals in the bottom, where the crystallization occurred more slowly than on the walls.

Besides drying, there were no process steps that would have significantly exposed the samples to degradation or polymorphic transformations. The analysis techniques used in this study needed only a little sample preparation. Nevertheless, the mechanical strength used in the sampling may have slightly induced solid state transformations in some of the dried samples because, depending on its crystal form, the re-crystallized IMC was very hard. Transformation to the more stable form may also have been induced by the very small amounts of solid IMC from previous experiments which may have been left into the sample bottles after washing.

Despite the deficiency of the solubility measurements, the obtained results were valuable in the design of the drug loading experiments and, furthermore, gave better understanding of the molecular structure of IMC and the interactions between IMC and the solvents.

8.2 Loading experiments

Based on the measured solubilities, the observed solvate formation tendency and the health and safety issues, the following solvent mixtures were selected for the loading experiments:

- DCM–methanol,
- Acetone–ethanol, and
- Ethyl acetate–ethanol.

The composition of each mixture was selected to be equal to the one which showed the maximum solubility, and the concentration of the solution was fixed to be 0.8 times the measured saturation concentration. This high concentration was selected since surface fraction has not been detected in IMC loaded PSi samples in earlier experiments [134].

The degree of loading was determined based on the mass loss observed in TG analysis. The true drug load can be calculated by subtracting the possible fraction

of the crystalline drug on the surface of PSi particles determined using DSC and the possible solvent residuals observed as a mass loss at low temperatures below 100 °C. The experimental results together with the theoretical minimum loads calculated using equation (12) are presented in table XII. The maximum loading calculated using equation (24) was 54 % for TOPSi particles and 64 % for TCPSi particles. The TG curves are presented in appendix C.

Table XII Degree of loading obtained from the selected loading solutions and the calculated theoretical minimum values for TOPSi and TCPSi particles.

Solvent	Experimental loading, w-%		Theoretical minimum loading, w- %	
	TOPSi	TCPSi	TOPSi	TCPSi
DCM-methanol	25.1±1.5	26.8±0.7	17.5	23.9
Acetone-ethanol	9.3 ±2.6	11.3±0.3	9.2	13.1
Ethyl acetate-ethanol	7.7±0.1	8.9±0.6	6.6	9.5

The highest drug load was achieved using TCPSi particles and the mixture of DCM and MeOH as a loading solvent. The drug loads obtained with the other solvents were minor. For some of the samples the deviations of the results were quite high which implies that the drug load is not very homogeneous.

Comparison of the experimental results with the theoretical ones it seems that IMC has higher affinity towards TOPSi surface than towards TCPSi surface. In the case of TCPSi particles the drug loads were not higher than the theoretical minimum values. This implies that there are not attractive forces between IMC and TCPSi surface at all. Higher drug loads were, however, obtained with TCPSi due to the larger pore volume. The calculated theoretical minimum loads seem to predict the experimental drug loads quite well. Thus it can be concluded that the concentration of the loading solution is the dominating factor determining the drug load and there are no strong repulsive or attractive interactions affecting the adsorption process.

The TG curves of the loaded samples were compared with the curves obtained with the original unloaded PSi particles. This comparison may, however, be slightly misleading, since the structure and the chemical composition of PSi particles may have changed during the loading process. The oxidation of PSi has been reported at least in MeOH [135]. Even though TOPSi and TCPSi are more stable than as-anodized PSi, they are probably vulnerable for this kind of oxidation. No residual moisture in the unloaded TOPSi and TCPSi particles was observed in the TG analysis.

As can be seen from the figures of appendix C, the TG curves of unloaded PSi particles are slightly sloped upwards. In the case of the IMC loaded particles, the mass increase is strongly accelerated after the decomposition of the drug, probably because of the evolved oxygen contained in decomposition products. Even when an inert purge gas is used, it is typical that an increase in the TG curve at 500–600 °C is observed due to oxidation of PSi [134]. If the PSi particles are being constantly oxidized during the TG measurement, the mass increase related to oxidation is compromising the mass loss caused by the evaporation of the decomposition products of IMC. The determined drug loads will be thus underestimated.

The possible presence of solvent residuals is hard to determine based on the TG curve, since the buoyancy effect in the beginning of the measurement together with the oxidation of PSi masks the possible mass loss.

Another interfering issue in the interpretation of the results is the possible reaction of PSi with the alumina crucible. Silicon has some sort of compatibility problems with the majority of crucible materials available. Graphite would be a suitable crucible material for analyzing PSi, but it might be easily oxidized because of the evolved decomposition products.

It is not completely sure if the final temperature was satisfactory for the complete removal of IMC from the sample. The bulk IMC is totally decomposed already at temperatures below 500 °C, but it seems that the evaporation of the decomposition products from the pores of PSi is a slow process. Maybe a better

way would be to heat the sample to 500 °C and keep it in isothermal conditions for some time.

Surface fraction was not observed for the samples loaded from neither acetone-EtOH nor EtOAc-EtOH solutions. Nevertheless, crystalline IMC was present in the samples loaded from the DCM-MeOH solution. DSC curves of the samples containing crystalline IMC are presented in figure 17. As can be seen, all the three IMC polymorph forms are present in the samples. The melting endotherm of δ IMC at around 130 °C is followed by a small re-crystallization exotherm.

As already discussed in chapter 8.1.2, δ form IMC is formed upon desolvation of IMC methanolate. It is not sure whether the desolvation has occurred already during drying, during the storage of the samples, or just when the sample was heated in the analysis. Even though no significant mass loss was observed in the TG analysis, it is possible that at least small amount of residual methanol is present in the sample, and more of an effort should be made to ensure absence of solvent residuals after drying of the sample. The high drying temperature used might be disadvantageous since the possible crystallization during the drying is likely to result in metastable forms if the evaporation rate of the solvent is too high for formation of stable crystals.

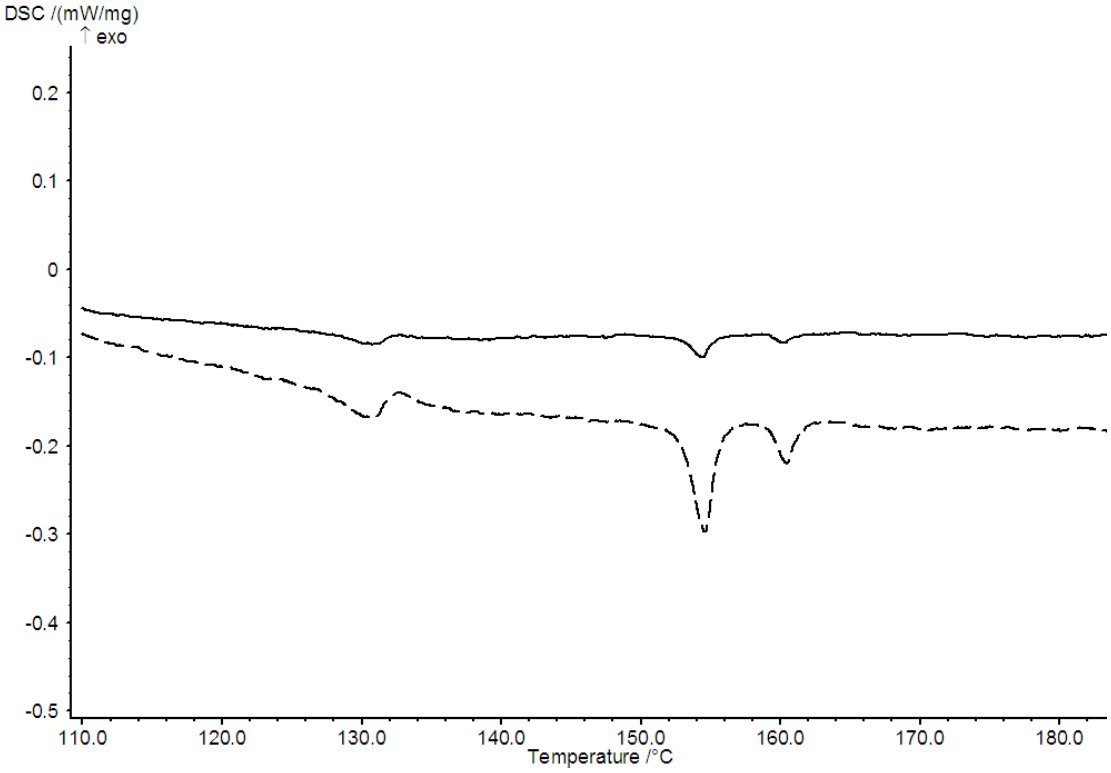

Figure 17. DSC curves for the IMC loaded TOPSi (dashed line) and TCPSi (solid line) particles when a 4:1 mixture of DCM-MeOH was applied as a loading solvent.

The presence of metastable polymorphs makes the determination of the amount of crystalline IMC difficult. All the polymorphs present should be produced as pure for the reference measurements. If the crystallinity is estimated based on the enthalpy of fusion of the stable γ form, the crystalline fraction is below 1 % in the both of the samples but that is an underestimate because the true enthalpies of fusion of the metastable forms are lower than that of the most stable form.

Since the presence of even a minor fraction of crystalline form should be avoided, it is recommended to decrease the concentration of the loading solution. Maybe the results of the solubility measurements gave a bit too high value for the DCM-MeOH mixture in question, or the temperature dependency of solubility is very strong. Crystallization may have occurred during the filtration step as the solutions may have become supersaturated when they have slightly cooled down during the treatment. The very small pore size of the filter medium has enabled even the smallest crystals to remain in the filter cake. It would be preferable to

carry out the filtration in thermostated conditions at the same temperature as used in loading.

It is likely that the strong affinity between IMC and the solvents, which even leads to solvate formation, hinders the drug loading and perhaps a longer loading time would have been needed. Another possibility would be to increase the temperature and thus accelerate the movement of the API molecules which might significantly increase the adsorption rate. Since the strength of the solute–solvent interactions affects on the adsorption kinetics, it would be important to carry out kinetic experiments in all the loading solvents and select the loading time based on those results. Even if the most important criterion probably is that the loading time selected is long enough to reach the equilibrium, extra time is not favorable. Too long loading time might impose the drug to degradation or increase the fraction of the drug crystallized on the surface of the particles.

The main reason for ignoring the loading kinetics is that the kinetic experiments are laborious and time consuming. Since thermal analysis is the most relevant method for determination of both the surface fraction and the loaded amount, in-line monitoring of the loading process is not feasible. As keeping the composition of the loading system constant upon sampling from a batch is extremely difficult, the simplest method is to repeat the loading experiment several times using equal amounts of constituents but varying the loading time.

8.3 Characterization of the loaded drug

Micro-Raman measurements of the IMC loaded silica particles gave information on the uniformity of the drug load and enabled the determination of the solid form of IMC in the samples. Indomethacin loaded SBA-15 and MCM-41 samples with slightly varying drug loads were studied. Also the changes after annealing the samples for 3 months in high temperature and humidity (30 °C, relative humidity 60 %) and after exposing them to liquid nitrogen temperature (-196 °C) were investigated. The Raman spectra of the loaded silica particles are presented in appendix D. Similar characterization of the drug load was not possible in the case of loaded PSi-particles because of the strong fluorescence background of PSi.

Both amorphous and γ-IMC were observed in the first SBA-15 sample. The main difference in the spectra of the original sample and the sample measured with the Tristar nitrogen sorption method, in which the sample is exposed to the temperature of -196 °C, was that in the case of the Tristar-sample, the baseline was more skewed. Fluorescence may result in a skewed baseline or a partially or completely saturated Raman signal. One source of fluorescence is the yellow color of amorphous IMC [136]. The increased fluorescence may, however, suggest partial degradation of the loaded IMC. This should be, however, verified with some other analysis technique.

It is possible that thermal stress induces structure defects in amorphous material, which might promote crystallization or even degradation. Nevertheless, Vyazovkin and Dranca [137] observed no changes in the amorphous IMC after it had been exposed to liquid nitrogen temperature. The thermal stress in their study was, however, not as harsh as the one to which the loaded silica samples were imposed, since the samples were stored in a freezer prior to the treatment.

The strongest fluorescence was observed with the sample that had been stressed at 30 °C and relative humidity 60 % for 3 months. Interestingly, the spectrum of α-IMC was observed in the stressed sample. Also the amount of γ-IMC seemed to have increased. Amorphous IMC loaded into silica particles is not stable in the studied storage conditions.

Crystallization of amorphous IMC at different conditions has been studied intensively [124, 137-140]. Typically, stable γ-IMC is formed below the glass transition temperature of IMC but crystallization at higher temperatures will yield both α and γ forms. The preparation method may also affect to the stability of the amorphous form. The storage temperature of the IMC loaded silica particles was below the T_g of IMC but the high humidity level may have induced the formation of metastable α-IMC.

A significant amount of α-IMC was present in the second SBA-15 sample. This sample had been treated at the liquid nitrogen temperature in the Tristar-analysis but since α-IMC was not observed in any of the other Tristar-measured samples it

is more probable that α-IMC has already formed during the drying process, not because of the Tristar-analysis. The stressed sample was already decomposed. The degradation was observed also as a change of the color of the sample from pale cream to brownish. The difference between the stabilities of the two SBA-15 samples is probably related to the different crystal forms of IMC. The metastable α form is more sensitive towards decomposition than the more stable γ form.

IMC loaded MCM-41 particles resulted in quite similar spectra as the SBA-15 particles. No α form was present in either of the samples; only the characteristic spectra of the amorphous IMC and γ form were detected. Strong fluorescence in the sample MCM+indo(4) caused difficulties in the baseline correction. Again, the increased fluorescence indicates the decomposition of IMC. The main difference in the two loaded MCM-41 samples was the particle size. It is probable that the size of the particles has an influence on the stability of the loaded drug; the higher surface area of smaller particles results in accelerated degradation.

Both of the stressed samples were already decomposed to some extent. Despite the fact that the non-uniform color of the sample suggested only a partial decomposition, the full analysis of the samples with Raman mapping was not reasonable. It is not clear why only one of the samples showed quite good stability in the stressing experiment and the others were readily decomposed. Further study is needed for determination of suitable storing conditions for drug loaded silica particles and it would be also necessary to develop methods for improving the stability.

The laser beam readily burned the IMC in the Tristar-measured samples. Probably this could have been prevented by increasing the distance between the measurement points. If the measurement points were partially overlapping, the same point was induced to the laser beam for a longer time and thus the temperature in that point might have increased too much. For some reason the other samples than those measured with Tristar were less vulnerable to the laser induced degradation. It might be possible that the drug on the surface of the sample is more easily decomposed than that inside the pores. Perhaps distribution

of the drug in the sample is changed during the Tristar-measurement. It is, however, not possible to draw any conclusions without further evidence on this.

The analysis did not draw a distinction between the drug on the surface and inside the pores. By adjusting the depth of the measurement it might be possible to characterize the differences between the drug inside the pores and on the particle surface. Unfortunately, the small size of the particles makes this kind of analysis difficult. It is preferred to use a single particle in the measurement, since if a cake of many particles is measured, one cannot be sure if the measurement point is truly inside a particle or on the surface of another particle. The spot size of the focusing point of the laser is not allowed to exceed the size of the sample, though. Thus in the case of particles with a diameter below 100 μm it is necessary to use more than one particle in the analysis, which reduces the reliability of the results.

The drug load in the sample SBA+indo(5) is illustrated in figure 18. The visualization of drug load was based on the intensities of the characteristic peaks of different IMC solid forms. These characteristic peaks were selected in such a way that their overlapping was minimal. Wavenumbers examined were 1650 cm^{-1} for α form, 1698 cm^{-1} for γ form, and 1681 cm^{-1} for amorphous form. The variation total amount of IMC was evaluated based on the intensity of the overlapping peaks at 1589 cm^{-1}. It should be emphasized that the analysis was of qualitative nature, since a calibration model would have been required for quantitation.

Figure 18 shows that the relative amount of IMC varies among the measurement points, but it is difficult to estimate the significance of this variation. Several lighter points in the map suggest the presence of crystalline γ form. Any large crystalline clusters are, however, not observed. Similar kind of visualization of the drug load as presented for SBA+indo(5) was prepared for each sample. Due to the high level of fluorescence the maps of other samples were not very illustrative and thus not presented herein.

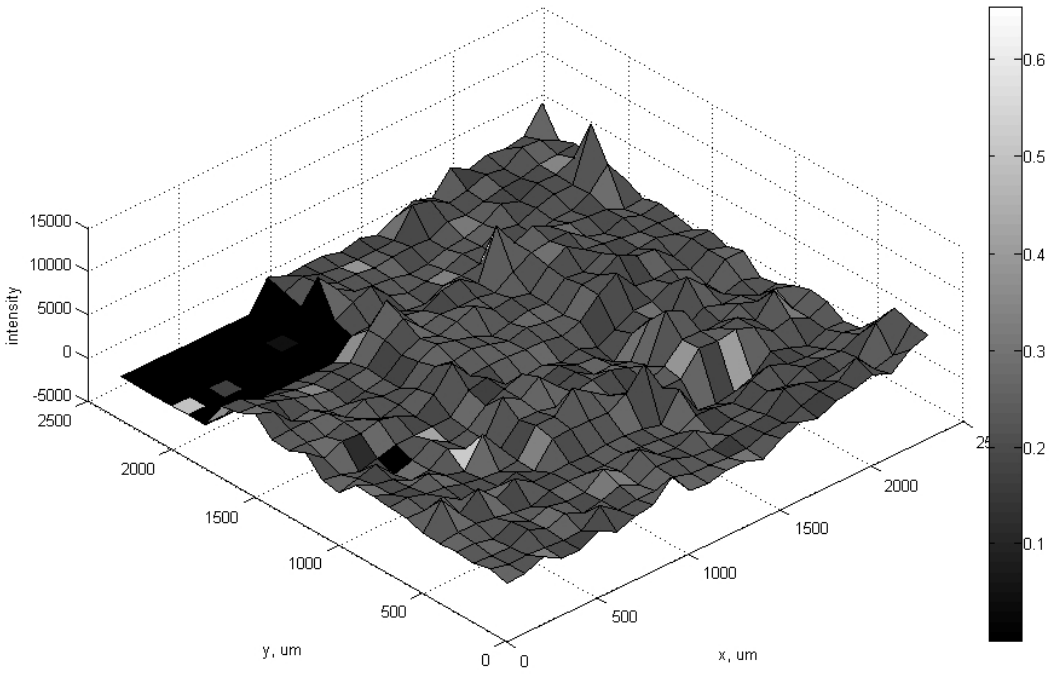

Figure 18 Distribution of the drug in IMC loaded SBA-15 silica particles (sample “SBA+indo(5)”). Z-axis indicates the total amount of IMC. The color shade illustrates the crystallinity of IMC: the lighter the color, the higher the probability of the occurrence of crystalline γ-IMC in the measurement point. Black color suggests increased fluorescence and the presence of decomposed IMC.

9 Summary and conclusions

Loading of indomethacin into mesoporous silicon from various binary solvent mixtures was studied. The aim was to investigate the molecular interactions in the loading system, since understanding these interactions is a key factor in the optimization of the loading process.

The 4:1 mixture of DCM and methanol revealed to be the best loading solvent among the studied binary solvent mixtures of dichloromethane, acetone and ethyl acetate with methanol and ethanol. The drug loads obtained were from 7.7 w-% to 26.8 w-%. In the samples with the highest drug loads, IMC was, unfortunately, not totally in amorphous form as desired.

Unfortunately, the solid form of the loaded drug in PSi-particles cannot be detected with Raman spectroscopy due to the strong background spectrum of PSi. However, the method is applicable for IMC loaded silica particles. Raman spectrum reveals the polymorph form and the uniformity of the drug load can be investigated by collecting a large number of spectra from different measurement points. In the light of the results of the present study, the stability of the amorphous drug in the loaded samples at high temperature and humidity is not satisfactory.

Optimization of the drug loading process still requires a lot of investigation, since many important factors had to be left beyond the scope of this work. The solubility of a compound that has several polymorphs and pseudo-polymorphs is already a complex issue, especially in mixed solvents. The tendency to solid state transformations hampered the analysis of the loaded samples. Furthermore, the amount of the loading experiments had to be limited due to the scarce amount of PSi available.

Mesoporous silicon is a promising drug carrier material. Even though the drug loads achieved in this study remained low, the experiments gave valuable

information of the interactions involved in the drug loading. The continuation of the study is recommended.

9.1 Interactions in the loading system

Since the main differences among the drug loads obtained in present study seem to be resulted from the concentration differences in the loading solutions, not much information could be achieved from the intermolecular forces in the drug loading system. It would be interesting to repeat the experiments using equal concentrations, but in that case the concentration of the loading solution would remain very low, and thus the drug loads would probably remain unsatisfactory low.

Based on the strong solvate formation of IMC, it can be assumed that IMC is typically associated with the solvent molecules also in the solution phase. The microenvironment sensitivity of IMC in ethanol–water mixtures has also been reported; depending on the composition of the solvent mixture, fluorescent or non-fluorescent complexes can be formed [141]. Solvation, i.e. the complex formation in the solution phase, affects the diffusivities of the compounds. It is likely to slow down the adsorption process significantly, since mass transfer is typically the rate limiting step. If the pore size of the adsorbent is small, solvation might practically prevent the adsorption inside the pores completely.

The fact that IMC had higher affinity towards TOPSi surface than towards TCPSi surface suggests that the polarity of the adsorbent surface is preferable for adsorption. The interactions between IMC and PSi surface are thus probably of polar nature. TOPSi surface is akin to silica surface, but the amount of silanol-groups is lower on the TOPSi surface. Furthermore, the effective surface area of PSi is typically lower than that of silica. This might be the reason for the lower drug loads in the case of drug loading of PSi particles compared to silica particles.

Watanabe *et al*. [142, 143] have revealed that IMC may chemically react with silica surface under mechanical stress. It might be possible, that the reaction occurs also during the drug loading if the conditions are too harsh. This kind of

chemisorption has probably a negative effect on the dissolution rate. Since the affinity between IMC and PSi seemed to be quite low, probably this kind of strong chemical interactions did not occur.

The results of the solubility and loading experiments and the spectral data are helpful when one tries to elucidate interactions occurring in the loading system. In order to obtain a complete, reliable picture of all the interactions, it would be, however, highly recommended to use several analysis techniques, e.g. FTIR for the liquid phase and ATR (Attenuated Total Reflectance) FTIR for wet powder as Teychene *et al*. [120] have used.

9.2 Optimization of drug loading

In the light of the results of the present study, the selection of the loading solvent is one of the most crucial factors in the optimization of a drug loading process. Unfortunately, there are no easy “ad hoc” methods for the selection of the loading solvent, since many factors must be taken into consideration in the solvent selection, for example the possibility of solvate formation. A single solubility parameter is not sufficient even for the preliminary solvent screening, since it does not even manage to predict the solubilities in binary solvent mixtures very well. The development of the computational methods for solubility prediction will facilitate solvent selection in the future and be a significant step towards the detailed modeling of a multi-component system such as the one in the drug loading process.

The concentration of the loading solution can be selected to be quite near to the saturation concentration, since the formation of surface fraction seems not to be a big problem with TOPSi and TCPSi particles as it typically is with silica particles. The high concentration increases the drug load. The ratio of the loading solvent and adsorbent particles in the loading used in this work was very high. Probably the ratio can be selected to be much lower without significantly compromising the loading efficiency; in the case of an industrial scale process it is an imperative to minimize the solvent use.

Higher IMC solubilities and drug loads are obtained using solvents with high vapor pressure. It might be that the pressure in the vessel increases in the case of these solvents, since the operating temperatures are quite near to the boiling point of the solvent. This suggests that high pressure would be advantageous to the drug loading. At least it might enhance the wetting of the particles. As far as reproducibility of the loading experiments is concerned, it would be recommendable to carry out the experiments in controlled pressure even though it makes the experiment setup much more complicated.

Drying conditions should be selected in such a way which ensures the desolvation if solvates are likely to be formed. The drying procedure used (1 h at 85 °C) was satisfactory for the samples prepared in this work, but the optimal drying time and temperature depends on several parameters such as the vapor pressure of the loading solvents, the sensitivity of the drug compound, and the pore properties of the adsorbent. Thermogravimetry is a good tool in the determination of a sufficient drying time. The optimization experiments should be carried out using real loaded PSi-samples, since the evaporation of the solvent from the pores is slower than that from a solution, for instance.

9.3 Proposals and recommendations for further study

The scope of this work was not sufficient for the final optimization of the loading solvent, and the number of the studied solvents had to be limited. Better loading efficiency could probably be achieved using solvents that are not forming solvates as easily as the solvents used in this study. For example, acetonitrile could be a favorable loading solvent, since it does not form solvates with IMC [97]. In order to get reliable solubility data for the basis of the solvent selection, attention must be paid to the dissolution kinetics and to the solvate formation.

In addition to the loading solvent, there are several other important loading parameters which need to be investigated in more extend. Effect of temperature on drug loading, for example, is an interesting issue. Maybe even more crucial factor is the loading time, so a study on the adsorption kinetics is absolutely necessary. Mixing is also one of the most important factors in the loading process, and its

significance increases when the ratio of the loading solvent and the adsorbent particles is reduced. Magnetic stirring may not be the best method to ensure constant, effective mixing of the heterogeneous system. Therefore, the development of mixing is one important task in the design of the loading process, especially on larger scale. Modeling may be a useful tool for that. The scale-up of the loading is, however, a prerequisite for the final optimization.

One problem in the drug loading might be the inefficient wettability of the PSi particles. The wettability could be perhaps increased using a surfactant or a higher pressure in the loading process, or by a suitable pre-treatment of the particles. The issue of PSi wettability is under research at the moment.

The drying of the loaded PSi is one of the most crucial steps in the loading process. Harsh drying conditions cannot be used for pharmaceuticals, since they are usually highly vulnerable to degradation, but on the other hand, the complete removal of solvents is an imperative. The optimization of drying would be valuable for both solubility measurements and loading experiments. The modeling of solvent evaporation and desolvation in the case of solvent mixtures would be one interesting task, and investigation of the effect of the drying conditions, e.g. temperature and pressure, should be included in the study.

One important task is the development of analysis methods. It would be preferable to analyze the loading *in-situ*. The main problems are the small scale of the loading and the difficulty to determine the surface fraction with other techniques than DSC. When the procedure for the drug loading and the analysis has been developed to a certain level, the loading of various pharmaceutical compounds can be investigated fast and the results can be compared easily.

After successful loading experiments, dissolution tests are needed to demonstrate the performance of the product. It is also important to make sure, e.g. by HPLC analysis, that no degradation of IMC has occurred during drug loading. Toxicity tests both *in vitro* and *in vivo* are also of an essence. The stability tests are of great importance to ensure the adequate shelf-life the drug product. Also, it is important to determine the effect of storage conditions, e.g. temperature and humidity, on

the stability. Modern techniques of thermal analysis, e.g. thermogravimetry at controlled humidity, could be utilized.

Even if the stability of an amorphous drug can be significantly enhanced using PSi as a carrier, it might be that the stability is still not satisfactory to meet the requirements set for pharmaceutical products. Furthermore, it is typical that even if the amorphous form is stable when stored in low-humidity conditions, it rapidly converts to the stable crystalline form upon administration because the transformation kinetics are much faster in the aqueous environment [144]. The solid state transformations of amorphous IMC during dissolution were recently studied using *in situ* Raman spectroscopy, and the results showed that crystallization indeed occurs during the dissolutions process but the dissolution rate still remains significantly higher than that of bulk IMC due to the slow crystallization kinetics [136]. Better stability could be, however, obtained with nanosized crystals and the kinetic solubility would still be at a high level compared to the bulk API. Therefore, it would be also important to study the methods applicable for the crystallization of the amorphous drug inside the pores. In the case of a drug with various polymorphs this will also require a precise optimization.

Due to the fairly high costs of the drug loading experiments and analysis, it is recommendable to endeavor to develop mathematical models for the prediction of the applicability of different loading solvents and for optimization of loading process conditions. It is a very demanding task to create a sophisticated model for a complex multicomponent system, and the occurrence of specific interactions such as hydrogen bonding makes it even more challenging. Since the study of drug loading will probably be mainly based on experimental work for long, a careful experiment design is a key issue.

As a final conclusion, the application of PSi particles in oral drug delivery has a great potential but a lot of further study on the subject is required. Besides the optimization of the drug loading process, one of the major challenges is to find convenient analysis methods for the reliable determination of the drug load. Better

characterization of PSi materials may also open new opportunities for their application in separation processes and in various drug delivery formulations.

References

1. Ambrogi, V., Perioli, L., Marmottini, F., Accorsi, O., Pagano, C., Ricci, M. and Rossi, C., Role of mesoporous silicates on carbamazepine dissolution rate enhancement. *Micropor. Mesopor. Mater.* **113**(2008), 1–3, 445–452.

2. C. H. Lau, M. Totolici and C. Barnett. Enhanced Dissolution of Poorly Soluble Drugs Using Mesoporous Silicon, Poster presentation, AAPS Annual Meeting and Exposition, San Antonio, Texas, 28.10.–2.11.2006.

3. Brayden, D.J., Controlled release technologies for drug delivery. *Drug Discovery Today* **8**(2003), 21, 976–978.

4. Lipinski, C.A., Lombardo, F., Dominy, B.W. and Feeney, P.J., Experimental and computational approaches to estimate solubility and permeability in drug discovery and development settings. *Advanced Drug Delivery Reviews* **23**(1997), 1–3, 3–25.

5. Hancock, B.C. and Parks, M., What is the True Solubility Advantage for Amorphous Pharmaceuticals? *Pharm.Res.* **17**(2000), 4, 397–404.

6. Sugano, K., Okazaki, A., Sugimoto, S., Tavornvipas, S., Omura, A. and Mano, T., Solubility and Dissolution Profile Assessment in Drug Discovery. *Drug Metabolism and Pharmacokinetics* **22**(2007), 4, 225–254.

7. Stegemann, S., Leveiller, F., Franchi, D., de Jong, H. and Lindén, H., When poor solubility becomes an issue: From early stage to proof of concept. *Eur. J. Pharm. Sci.* **31**(2007), 5, 249–261.

8. Charman, W.N., Porter, C.J.H., Mithani, S. and Dressman, J.B., Physicochemical and physiological mechanisms for the effects of food on drug absorption: The role of lipids and pH. *J.Pharm.Sci.* **86**(1997), 3, 269–282.

9. Mellaerts, R., Mols, R., Kayaert, P., Annaert, P., Van Humbeeck, J., Van den Mooter, G., Martens, J.A. and Augustijns, P., Ordered mesoporous silica induces pH-independent supersaturation of the basic low solubility compound itraconazole resulting in enhanced transepithelial transport. *Int. J. Pharm.* **357**(2008), 1–2, 169–179.

10. Kaukonen, A.M., Laitinen, L., Salonen, J., Tuura, J., Heikkilä, T., Limnell, T., Hirvonen, J. and Lehto, V.-P., Enhanced in vitro permeation of furosemide loaded into thermally carbonized mesoporous silicon (TCPSi) microparticles. *European Journal of Pharmaceutics and Biopharmaceutics* **66**(2007), 3, 348–356.

11. Bahl, D. and Bogner, R., Amorphization of Indomethacin by Co-Grinding with Neusilin US2: Amorphization Kinetics, Physical Stability and Mechanism. *Pharm.Res.* **23**(2006), 10, 2317–2325.

12. Salonen, J., Laitinen, L., Kaukonen, A.M., Tuura, J., Björkqvist, M., Heikkilä, T., Vähä-Heikkilä, K., Hirvonen, J. and Lehto, V.-P., Mesoporous silicon microparticles for oral drug delivery: Loading and release of five model drugs. *Journal of Controlled Release* **108**(2005), 2–3, 362–374.

13. Foraker, A.B., Walczak, R.J., Cohen, M.H., Boiarski, T.A., Grove, C.F. and Swaan, P.W., Microfabricated Porous Silicon Particles Enhance Paracellular Delivery of Insulin Across Intestinal Caco-2 Cell Monolayers. *Pharm.Res.* **20**(2003), 1, 110–116.

14. Hirvonen, J., Laaksonen, T., Peltonen, L., Santos, H., Lehto, V.-P., Heikkilä, T., Riikonen, J., Mäkilä, E. and Salonen, J., Feasibility of silicon-based mesoporous materials for oral drug delivery applications. *Dosis* **24**(2008), 2, 129–149.

15. Madieh, S., Simone, M., Wilson, W., Mehra, D. and Augsburger, L., Investigation of drug-porous adsorbent interactions in drug mixtures with selected porous adsorbents. *J.Pharm.Sci.* **96**(2007), 4, 851–863.

16. Cullis, A.G., Canham, L.T. and Calcott, P.D.J., The structural and luminescence properties of porous silicon. *J.Appl.Phys.* **82**(1997), 3, 909.

17. Wang, S., Ordered mesoporous materials for drug delivery. *Micropor. Mesopor. Mater.* (in press, corrected proof).

18. Väänänen, E., The chemistry, processing and applications of silica based materials, Licentiate Thesis, Lappeenrannan teknillinen korkeakoulu, Lappeenranta, 2000.

19. Kresge, C.T., Leonowicz, M.E., Roth, W.J., Vartuli, J.C. and Beck, J.S., Ordered mesoporous molecular sieves synthesized by a liquid-crystal template mechanism. *Nature* **359**(1992), 6397, 710–712.

20. Beck, J.S., Vartuli, J.C., Roth, W.J., Leonowicz, M.E., Kresge, C.T., Schmitt, K.D., Chu, C.T.W., Olson, D.H., Sheppard, E.W. et al., A new family of mesoporous molecular sieves prepared with liquid crystal templates. *J. Am. Chem. Soc.* **114**(1992), 27, 10834–10843.

21. Andersson, J., Rosenholm, J., Areva, S. and Linden, M., Influences of Material Characteristics on Ibuprofen Drug Loading and Release Profiles from Ordered Micro- and Mesoporous Silica Matrices. *Chem. Mater.* **16**(2004), 21, 4160–4167.

22. Vallet-Regi, M., Ramila, A., del Real, R.P. and Perez-Pariente, J., A New Property of MCM-41: Drug Delivery System. *Chem. Mater.* **13**(2001), 2, 308–311.

23. Charnay, C., Bégu, S., Tourné-Péteilh, C., Nicole, L., Lerner, D.A. and Devoisselle, J.M., Inclusion of ibuprofen in mesoporous templated silica: drug loading and release property. *European Journal of Pharmaceutics and Biopharmaceutics* **57**(2004), 3, 533–540.

24. Davidson, A., Modifying the walls of mesoporous silicas prepared by supramolecular-templating. *Current Opinion in Colloid & Interface Science* **7**(2002), 1–2, 92–106.

25. Jansen, J.C., Shan, Z., Maschmeyer, T., Marchese, W., Zhou, W. and van der Puil, N., A new templating method for three-dimensional mesopore networks. *Chem.Commun.*(2001), 713–714.

26. Salonen, J., Kaukonen, A.M., Hirvonen, J. and Lehto, V., Mesoporous silicon in drug delivery applications. *J.Pharm.Sci.* **97**(2008), 2, 632–653.

27. Salonen, J., Studies on porous silicon oxidation and structure, Ph.D. dissertation, University of Turku, Department of Physics, Turku, 1999.

28. Anglin, E.J., Cheng, L., Freeman, W.R. and Sailor, M.J., Porous silicon in drug delivery devices and materials. *Adv. Drug Deliv. Rev.* **60**(2008), 11, 1266–1277.

29. Salonen, J. and Lehto, V., Fabrication and chemical surface modification of mesoporous silicon for biomedical applications. *Chemical Engineering Journal* **137**(2008), 1, 162–172.

30. Lehmann, V. and Gosele, U., Porous silicon formation: A quantum wire effect. *Appl.Phys.Lett.* **58**(1991), 8, 856.

31. Fathauer, R.W. and George, T., Visible luminescence from silicon wafers subjected to stain etches. *Appl.Phys.Lett.* **60**(1992), 8, 995.

32. Noguchi, N. and Suemune, I., Luminescent porous silicon synthesized by visible light irradiation. *Appl.Phys.Lett.* **62**(1993), 12, 1429.

33. Li, Y.Y., Kollengode, V.S. and Sailor, M.J., Porous-Silicon/Polymer Nanocomposite Photonic Crystals Formed by Microdroplet Patterning. *Adv Mater* **17**(2005), 10, 1249–1251.

34. Limnell, T., Riikonen, J., Salonen, J., Kaukonen, A.M., Laitinen, L., Hirvonen, J. and Lehto, V.-., Surface chemistry and pore size affect carrier properties of mesoporous silicon microparticles. *Int. J. Pharm.* **343**(2007), 1–2, 141–147.

35. Buriak, J.M. and Allen, M.J., Lewis Acid Mediated Functionalization of Porous Silicon with Substituted Alkenes and Alkynes. *J. Am. Chem. Soc.* **120**(1998), 6, 1339–1340.

36. Buriak, J.M., Organometallic Chemistry on Silicon and Germanium Surfaces. *Chem. Rev.* **102**(2002), 5, 1271–1308.

37. Stewart, M.P. and Buriak, J.M., Photopatterned Hydrosilylation on Porous Silicon. *Angewandte Chemie International Edition* **37**(1998), 23, 3257–3260.

38. Lees, I.N., Lin, H., Canaria, C.A., Gurtner, C., Sailor, M.J. and Miskelly, G.M., Chemical Stability of Porous Silicon Surfaces Electrochemically Modified with Functional Alkyl Species. *Langmuir* **19**(2003), 23, 9812–9817.

39. Melo, R.A.A., Giotto, M.V., Rocha, J. and UrquietaGonzlez, E.A., MCM-41 ordered mesoporous molecular sieves synthesis and characterization. *Materials Research* **2**(1999), 173.

40. Frasch, J., Lebeau, B., Soulard, M., Patarin, J. and Zana, R., In Situ Investigations on Cetyltrimethylammonium Surfactant/Silicate Systems, Precursors of Organized Mesoporous MCM-41-Type Siliceous Materials. *Langmuir* **16**(2000), 23, 9049–9057.

41. Heikkilä, T., Salonen, J., Tuura, J., Hamdy, M.S., Mul, G., Kumar, N., Salmi, T., Murzin, D.Y., Laitinen, L., Kaukonen, A.M., Hirvonen, J. and Lehto, V.-P., Mesoporous silica material TUD-1 as a drug delivery system. *Int. J. Pharm.* **331**(2007), 1, 133–138.

42. *Ullmann's encyclopedia of industrial chemistry,* Vol A23, B. Elvers, S. Hawkins, W. Russey and G. Schulzed., 5th ed., VCH, Weinheim, 1993.

43. Zhao, X.S., Audsley, F. and Lu, G.Q., Irreversible Change of Pore Structure of MCM-41 upon Hydration at Room Temperature. *J. Phys. Chem. B* **102**(1998), 21, 4143–4146.

44. Jugdaohsingh, R., Anderson, S.H., Tucker, K.L., Elliott, H., Kiel, D.P., Thompson, R.P. and Powell, J.J., Dietary silicon intake and absorption. *Am. J. Clin. Nutr.* **75**(2002), 5, 887–893.

45. Canham, L.T., Reeves, C.L., Loni, A., Houlton, M.R., Newey, J.P., Simons, A.J. and Cox, T.I., Calcium phosphate nucleation on porous silicon: factors influencing kinetics in acellular simulated body fluids. *Thin Solid Films* **297**(1997), 1–2, 304–307.

46. Desai, T.A., Hansford, D.J., Kulinsky, L., Nashat, A.H., Rasi, G., Tu, J., Wang, Y., Zhang, M. and Ferrari, M., Nanopore Technology for Biomedical Applications. *Biomed.Microdevices* **2**(1999), 1, 11–40.

47. pSivida Ltd: Oncology, http://www.psivida.com/application/oncology.asp, 4.6. 2008.

48. Rosenholm, J.M. and Lindén, M., Towards establishing structure–activity relationships for mesoporous silica in drug delivery applications. *Journal of Controlled Release* **128**(2008), 2, 157–164.

49. Kinoshita, M., Baba, K., Nagayasu, A., Yamabe, K., Shimooka, T., Takeichi, Y., Azuma, M., Houchi, H. and Minakuchi, K., Improvement of

solubility and oral bioavailability of a poorly water-soluble drug, TAS-301, by its melt-adsorption on a porous calcium silicate. *J.Pharm.Sci.* **91**(2002), 2, 362–370.

50. Nakai, Y., Yamamoto, K. and Izumikawa, S., Interaction of Medicinals and Porous Powder. III. : Effects of Pore Diameter of Porous Glass Powder on Crystalline Properties. *Chem. Pharm. Bull.* **37**(1989), 2, 435–438.

51. Mäkilä, E., Lääkemolekyylien adsorptiosta mesohuokoiseen piihin, Master's Thesis, University of Turku, Department of Physics, Turku, 2007.

52. Salonen, J., Determination of drug load in porous silicon microparticles by calorimetry. *Physica status solidi. A, Applied research* **202**(2005), 8, 1629.

53. Griesser, U.J., The Importance of Solvates, in Hilfiker, R., ed. *Polymorphism.* Wiley-VCH Verlag GmbH & Co. KGaA, Weinheim, 2006, p. 211–233.

54. Bernstein, J., *Polymorphism in molecular crystals,* Clarendon Press, Oxford, 2002.

55. Ambrogi, V., Perioli, L., Marmottini, F., Giovagnoli, S., Esposito, M. and Rossi, C., Improvement of dissolution rate of piroxicam by inclusion into MCM-41 mesoporous silicate. *Eur. J. Pharm. Sci.* **32**(2007), 3, 216-222.

56. *CRC handbook of solubility parameters and other cohesion parameters,* A. F. M. Barton, ed., 2nd ed., CRC Press cop, Boca Raton (FL), 1991.

57. Bhattachar, S.N., Deschenes, L.A. and Wesley, J.A., Solubility: it's not just for physical chemists. *Drug Discovery Today* **11**(2006), 21–22, 1012–1018.

58. Bennema, P., van Eupen, J., van der Wolf, B.M.A., Los, J.H. and Meekes, H., Solubility of molecular crystals: Polymorphism in the light of solubility theory. *Int. J. Pharm.* **351**(2008), 1–2, 74–91.

59. Pacheco, D.P., Manrique, Y.J. and Martínez, F., Thermodynamic study of the solubility of ibuprofen and naproxen in some ethanol + propylene glycol mixtures. *Fluid Phase Equilibria* **262**(2007), 1–2, 23–31.

60. Perlovich, G.L., Kurkov, S.V. and Bauer-Brandl, A., Thermodynamics of solutions: II. Flurbiprofen and diflunisal as models for studying solvation of drug substances. *Eur. J. Pharm. Sci.* **19**(2003), 5, 423–432.

61. Perlovich, G.L., Kurkov, S.V., Kinchin, A.N. and Bauer-Brandl, A., Thermodynamics of solutions III: comparison of the solvation of (+)-naproxen with other NSAIDs. *European Journal of Pharmaceutics and Biopharmaceutics* **57**(2004), 2, 411–420.

62. Romero, S., Bustamante, P., Escalera, B., Mura, P. and Cirri, M., Influence of solvent composition on the solid phase at equilibrium with

saturated solutions of quinolones in different solvent mixtures. *Journal of Pharmaceutical and Biomedical Analysis* **35**(2004), 4, 715–726.

63. Tsinman, K., Tsinman, O., Berger, C., Avdeef, A. and Holland, M., Aqueous Solubility Measurement - Kinetic vs. Thermodynamic Methods.

64. Hancock, B.C., York, P. and Rowe, R.C., The use of solubility parameters in pharmaceutical dosage form design. *International Journal of Pharmaceutics* **148**(1997), 1, 1–21.

65. Gordon, L.J. and Scott, R.L., Enhanced Solubility in Solvent Mixtures. I. The System Phenanthrene–Cyclohexane–Methylene Iodide. *J. Am. Chem. Soc.* **74**(1952), 16, 4138–4140.

66. Smith, E.B., Walkley, J. and Hildebr, J.H., Intermolecular Forces Involving Chlorofluorocarbons. *J. Phys. Chem.* **63**(1959), 5, 703–704.

67. Bustamante, P., Navarro, J., Romero, S. and Escalera, B., Thermodynamic origin of the solubility profile of drugs showing one or two maxima against the polarity of aqueous and nonaqueous mixtures: Niflumic acid and caffeine. *J.Pharm.Sci.* **91**(2002), 3, 874–883.

68. Joyban-Gharamaleki, A., Romero, S., Bustamante, P. and Clark, B.J., Multiple Solubility Maxima of Oxolinic Acid in Mixed Solvents and a New Extension of Hildebrand Solubility Approach. *Chem.Pharm.Bull.* **48**(2000), 2, 175–178.

69. Peña, M.A., Reíllo, A., Escalera, B. and Bustamante, P., Solubility parameter of drugs for predicting the solubility profile type within a wide polarity range in solvent mixtures. *Int. J. Pharm.* **321**(2006), 1–2, 155–161.

70. Romero, S., Reíllo, A., Escalera, B. and Bustamante, P., The Behavior of Paracetamol in Mixtures of Amphiprotic and Amphiprotic-Aprotic Solvents. Relationship of Solubility Curves to Specific and Nonspecific Interactions. *Chem. Pharm. Bull.* **44**(1996), 5, 1061–1064.

71. Marcus, Y., On the preferential solvation of drugs and PAHs in binary solvent mixtures. *Journal of Molecular Liquids* **140**(2008), 1–3, 61–67.

72. Jouyban, A., Chan, H., Chew, N.Y.K. and Khoubnasabjafari, M., Solubility Prediction of Paracetamol in Binary and Ternary Solvent Mixtures Using Jouyban-Acree Model. *Chem. Pharm. Bull.* **54**(2006), 4, 428–431.

73. Jouyban, A., Chew, N.Y.K., Chan, H., Sabour, M. and Acree, J.,William E., A Unified Cosolvency Model for Calculating Solute Solubility in Mixed Solvents. *Chem. Pharm. Bull.* **53**(2005), 6, 634–637.

74. Jouyban, A., Review of the cosolvency models for predicting solubility of drugs in water-cosolvent mixtures. *J. Pharm. Pharmaceut. Sci.* **11**(2008), 1, 32–58.

75. Frank, T.C., Downey, J.R. and Gupta, S.K., Quickly Screen Solvents for Organic Solids. *Chem. Eng. Prog.* **95**(1999), 12, 41–61.

76. Millard, J.W., Alvarez-Núñez, F.A. and Yalkowsky, S.H., Solubilization by cosolvents: Establishing useful constants for the log–linear model. *International Journal of Pharmaceutics* **245**(2002), 1–2, 153–166.

77. Ali, S.H., Measurement and prediction of pyrene solubility in pure, binary, ternary and quaternary solvent systems. *Fluid Phase Equilibria*, **264**(2008), 1–2, 29–44.

78. Lohmann, J., Joh, R. and Gmehling, J., From UNIFAC to Modified UNIFAC (Dortmund). *Ind. Eng. Chem. Res.* **40**(2001), 3, 957–964.

79. Klamt, A., Conductor-like Screening Model for Real Solvents: A New Approach to the Quantitative Calculation of Solvation Phenomena. *J. Phys. Chem.* **99**(1995), 7, 2224–2235.

80. Eckert, F. and Klamt, A., Fast solvent screening via quantum chemistry: COSMO-RS approach. *AIChE J.* **48**(2002), 2, 369–385.

81. Song, J.H. and Sailor, M.J., Dimethyl Sulfoxide as a Mild Oxidizing Agent for Porous Silicon and Its Effect on Photoluminescence. *Inorg. Chem.* **37**(1998), 13, 3355–3360.

82. Constable, D.J.C., Jimenez-Gonzalez, C. and Henderson, R.K., Perspective on Solvent Use in the Pharmaceutical Industry. *Org. Process Res. Dev.* **11**(2007), 1, 133–137.

83. Gani, R., Jiméz-González, C., ten Kate, A., Crafts, P.A., Jones, M., Powell, L., Atherton, J.H. and Cordiner, J.L., A modern approach to solvent selection. *Chemical Engineering* **113**(2006), 3, 30–43.

84. IHC Guidance for Industry - Q3C Impurities: Residual Solvents (1997).

85. IHC Guidance for Industry - Q3C Tables and List (2003).

86. Sanganwar, G.P. and Gupta, R.B., Dissolution-rate enhancement of fenofibrate by adsorption onto silica using supercritical carbon dioxide. *Int. J. Pharm.* **360**(2008), 1–2, 213–218.

87. Saig, A., Finkelstein, Y., Danon, A. and Koresh, J.E., Sensing the Physicochemical Nature of He and Ne in Micropores by Adsorption Measurements. *J. Phys. Chem. B* **109**(2005), 22, 11180–11185.

88. Horiba Jobin Yvon - Raman tutorial, http://www.jobinyvon.com/Raman/Raman-Resource/Raman-Tutorial/1-3, 17.6.2008.

89. Abramof, P.G., Miranda, C.R.B., Beloto, A.F., Ueta, A.Y. and Ferreira, N.G., An investigation of natural oxidation process on stain-etched

nanoporous silicon by micro-Raman spectroscopy. *Applied Surface Science*, **253**(2007), 17, 7065–7068.

90. Laserna, J.J., ed., *Modern techniques in Raman spectroscopy*, Wiley cop, Chichester, 1996.

91. Šašić, S., *Pharmaceutical applications of Raman spectroscopy*, Wiley-Interscience cop, Hoboken (NJ), 2008.

92. Brown, M.E., *Introduction to thermal analysis techniques and applications*, Kluwer Academic Publishers cop, Dordrecht, 2001.

93. Taylor, L.S. and Zografi, G., Spectroscopic Characterization of Interactions Between PVP and Indomethacin in Amorphous Molecular Dispersions. *Pharm.Res.* **14**(1997), 12, 1691–1698.

94. Watanabe, T., Wakiyama, N., Kusai, A. and Senna, M., A molecular orbital study on the chemical interaction across the indomethacin/silica interparticle boundary due to mechanical stressing. *Powder Technology* **141**(2004), 3, 227–232.

95. Kavvada, K.M., Murray, J.G., Moore, V.A., Coombes, A.G.A. and Hanson, P.J., High permeability of the anionic form restricts accumulation of indomethacin by cultured gastric surface epithelial cells exposed to low apical pH. *European Journal of Pharmacology* **549**(2006), 1–3, 41–49.

96. Legendre, B. and Feutelais, Y., Polymorphic and Thermodynamic Study of Indomethacin. *Journal of Thermal Analysis and Calorimetry* **76**(2004), 1, 255–264.

97. Slavin, P.A., Sheen, D.B., Shepherd, E.E.A., Sherwood, J.N., Feeder, N., Docherty, R. and Milojevic, S., Morphological evaluation of the γ-polymorph of indomethacin. *J. Cryst. Growth* **237–239**(2002), Part 1, 300–305.

98. Joshi, V., Physical transformations in solvated pharmaceuticals, Ph.D. Dissertation, Purdue University, Ann Arbor (MI), 1999.

99. Hamdi, N., Feutelais, Y., Yagoubi, N., de Girolamo, D. and Legendre, B., Solvates of Indomethacin. *Journal of Thermal Analysis and Calorimetry* **76**(2004), 3, 985–1001.

100. Crowley, K.J. and Zografi, G., Cryogenic grinding of indomethacin polymorphs and solvates: Assessment of amorphous phase formation and amorphous phase physical stability. *J.Pharm.Sci.* **91**(2002), 2, 492–507.

101. Archontaki, H.A., Kinetic study on the degradation of indomethacin in alkaline aqueous solutions by derivative ultraviolet spectrophotometry. *The Analyst* **120**(1995), 2627–2634.

102. Garcia, B., Hoyuelos, F.J., Ibeas, S. and Leal, J.M., Hydrolysis Mechanisms for Indomethacin and Acemethacin in Perchloric Acid. *J. Org. Chem.* **71**(2006), 10, 3718–3726.

103. Li, M., Conrad, B., Maus, R.G., Pitzenberger, S.M., Subramanian, R., Fang, X., Kinzer, J.A. and Perpall, H.J., A novel oxidative degradation pathway of indomethacin under the stressing by hydrogen peroxide. *Tetrahedron Letters* **46**(2005), 20, 3533–3536.

104. Wu, A., Cheng, H., Hu, C., Chen, F., Chou, T. and Chen, C., Photolysis of indomethacin in methanol. *Tetrahedron Letters,* **38**(1997), 4, 621–622.

105. Chao, S., Wu, A., Lee, C., Chen, F. and Wang, C., Anti-inflammatory Effects of Indomethacin's Methyl Ester Derivative and Induction of Apoptosis in HL-60 Cells. *Biol.Pharm.Bull.* **28**(2005), 12, 2206–2210.

106. Trask, A.V., Shan, N., Jones, W. and Motherwell, W.D.S., Indomethacin methyl ester. *Acta Cryst.* **E60**(2004), o508–o509.

107. Savolainen, M., Heinz, A., Strachan, C., Gordon, K.C., Yliruusi, J., Rades, T. and Sandler, N., Screening for differences in the amorphous state of indomethacin using multivariate visualization. *Eur. J. Pharm. Sci.* **30**(2007), 2, 113–123.

108. Liu, H., Finn, N. and Yates, M.Z., Encapsulation and Sustained Release of a Model Drug, Indomethacin, Using CO2-Based Microencapsulation. *Langmuir* **21**(2005), 1, 379–385.

109. Forster, A., Hempenstall, J., Tucker, I. and Rades, T., Selection of excipients for melt extrusion with two poorly water-soluble drugs by solubility parameter calculation and thermal analysis. *Int. J. Pharm.* **226**(2001), 1–2, 147–161.

110. Poling, B.E., Prausnitz, J. M. and O'Connell, J. P. *The properties of gases and liquids,* McGraw-Hill, Boston, 2001.

111. Boublík, T., Fried, V. and Hála, E. *The vapour pressures of pure substances selected values of the temperature dependence of the vapour pressures of some pure substances in the normal and low pressure region,* Elsevier cop, Amsterdam, 1984.

112. Majer, V. and Svoboda, V. *Enthalpies of vaporization of organic compounds a critical review and data compilation,* Pergamon Press, Oxford, 1985.

113. Marcus, Y., *The properties of solvents,* Wiley, Chichester, 1999.

114. Heinz, A., Savolainen, M., Rades, T. and Strachan, C.J., Quantifying ternary mixtures of different solid-state forms of indomethacin by Raman and near-infrared spectroscopy. *Eur. J. Pharm. Sci.* **32**(2007), 3, 182–192.

115. Chieng, N., Aaltonen, J., Saville, D. and Rades, T., Physical characterization and stability of amorphous indomethacin and ranitidine hydrochloride binary systems prepared by mechanical activation. *European Journal of Pharmaceutics and Biopharmaceutics* **(**in press, accepted manuscript).

116. Towler, C.S. and Taylor, L.S., Spectroscopic Characterization of Intermolecular Interactions in Solution and Their Influence on Crystallization Outcome. *Cryst. Growth Des.* **7**(2007), 4, 633-638.

117. Krestov, G.A., *Thermodynamics of solvation solution and dissolution, ions and solvents, structure and energetics,* Ellis Horwood cop, New York, 1991.

118. Durov, V.A., Modeling of supramolecular ordering in mixtures: Structure, dynamics and properties. *Journal of Molecular Liquids* **103-104**(2003), 41–82.

119. Romero, S., Escalera, B. and Bustamante, P., Solubility behavior of polymorphs I and II of mefenamic acid in solvent mixtures. *International Journal of Pharmaceutics* **178**(1999), 2, 193–202.

120. Teychene, S., Autret, J.M. and Biscans, B., Determination of solubility profiles of eflucimibe polymorphs: Experimental and modeling. *J.Pharm.Sci.* **95**(2006), 4, 871–882.

121. Sato, K., Sugimoto, K. and Nakane, T., Separation of ethanol/ethyl acetate mixture by pervaporation at 100–130 °C through NaY zeolite membrane for industrial purpose. *Micropor. Mesopor. Mater.* **115**(2008), 1–2, 170–175.

122. Iliuta, M.C. and Thyrion, F.C., Vapour-liquid equilibrium for the acetone-methanol-inorganic salt system. *Fluid Phase Equilibria* **103**(1995), 2, 257–284.

123. *Thermodynamisches Gleichgewicht siedender Gemische,* Vol 3, J. Weishaupt and H. Hausened., 6th ed., Springer, Berlin, 1975.

124. Andronis, V. and Zografi, G., Crystal nucleation and growth of indomethacin polymorphs from the amorphous state. *Journal of Non-Crystalline Solids,* **271**(2000), 3, 236–248.

125. Chen, X., Morris, K.R., Griesser, U.J., Byrn, S.R. and Stowell, J.G., Reactivity Differences of Indomethacin Solid Forms with Ammonia Gas. *J. Am. Chem. Soc.* **124**(2002), 15012–15019.

126. Hedoux, A., Guinet, Y., Capet, F., Paccou, L. and Descamps, M., Evidence for a high-density amorphous form in indomethacin from Raman scattering investigations. *Physical Review B (Condensed Matter and Materials Physics)* **77**(2008), 9, 094205.

127. Socrates, G., *Infrared and Raman characteristic group frequencies tables and charts,* 3rd ed., Wiley cop, Chichester, 2001.

128. Schmidt, A.G., Wartewig, S. and Picker, K.M., Polyethylene oxides: protection potential against polymorphic transitions of drugs? *J.Raman Spectrosc.* **35**(2004), 5, 360–367.

129. Fioritto, A.F., Bhattachar, S.N. and Wesley, J.A., Solubility measurement of polymorphic compounds via the pH-metric titration technique. *Int. J. Pharm.* **330**(2007), 1–2, 105–113.

130. Kawakami, K., Miyoshi, K. and Ida, Y., Impact of the Amount of Excess Solids on Apparent Solubility. *Pharm.Res.* **22**(2005), 9, 1537–1543.

131. Nováková, L., Matysová, L., Havlíková, L. and Solich, P., Development and validation of HPLC method for determination of indomethacin and its two degradation products in topical gel. *Journal of Pharmaceutical and Biomedical Analysis* **37**(2005), 5, 899–905.

132. Nti-Gyabaah, J., Chmielowski, R., Chan, V. and Chiew, Y.C., Solubility of lovastatin in a family of six alcohols: Ethanol, 1-propanol, 1-butanol, 1-pentanol, 1-hexanol, and 1-octanol. *Int. J. Pharm.* **359**(2008), 1–2, 111–117.

133. Sun, H., Gong, J. and Wang, J., Solubility of Lovastatin in Acetone, Methanol, Ethanol, Ethyl Acetate, and Butyl Acetate between 283 K and 323 K. *J. Chem. Eng. Data* **50**(2005), 4, 1389–1391.

134. Teemu Heikkilä. Personal Communication, 7.10.2008.

135. Razi, F., Rahimi, F. and Iraji zad, A., Fourier transform infrared spectroscopy and scanning tunneling spectroscopy of porous silicon in the presence of methanol. *Sensors and Actuators B: Chemical,* **132**(2008), 1, 40–44.

136. Savolainen, M., Kogermann, K., Heinz, A., Aaltonen, J., Peltonen, L., Strachan, C. and Yliruusi, J., Better understanding of dissolution behaviour of amorphous drugs by in situ solid-state analysis using Raman spectroscopy. *European Journal of Pharmaceutics and Biopharmaceutics* (in press, corrected proof).

137. Vyazovkin, S. and Dranca, I., Effect of Physical Aging on Nucleation of Amorphous Indomethacin. *J. Phys. Chem. B* **111**(2007), 25, 7283–7287.

138. Andronis, V., Yoshioka, M. and Zografi, G., Effects of sorbed water on the crystallization of indomethacin from the amorphous state. *J.Pharm.Sci.* **86**(1997), 3, 346-351.

139. Andronis, V. and Zografi, G., The Molecular Mobility of Supercooled Amorphous Indomethacin as a Function of Temperature and Relative Humidity. *Pharm.Res.* **15**(1998), 6, 835–842.

140. Patterson, J.E., James, M.B., Forster, A.H., Lancaster, R.W., Butler, J.M. and Rades, T., The influence of thermal and mechanical preparative techniques on the amorphous state of four poorly soluble compounds. *J.Pharm.Sci.* **94**(2005), 9, 1998–2012.

141. Ghatak, A., Mandal, P.C. and Sarkar, M., Indomethacin: A NSAID sensitive to micro heterogeneity in alcohol–water mixtures. *Chemical Physics Letters* **460**(2008), 4–6, 521–524.

142. Watanabe, T., Wakiyama, N., Usui, F., Ikeda, M., Isobe, T. and Senna, M., Stability of amorphous indomethacin compounded with silica. *International Journal of Pharmaceutics* **226**(2001), 1–2, 81–91.

143. Watanabe, T., Hasegawa, S., Wakiyama, N., Usui, F., Kusai, A., Isobe, T. and Senna, M., Solid State Radical Recombination and Charge Transfer across the Boundary between Indomethacin and Silica under Mechanical Stress. *Journal of Solid State Chemistry* **164**(2002), 1, 27–33.

144. Aaltonen, J., Allesø, M., Mirza, S., Koradia, V., Gordon, K.C. and Rantanen, J., Solid form screening – A review. *European Journal of Pharmaceutics and Biopharmaceutics* (in press, corrected proof).

A Pore size distributions of TOPSI and TCPSI based on nitrogen adsorption measurements (by T. Heikkilä, University of Turku)

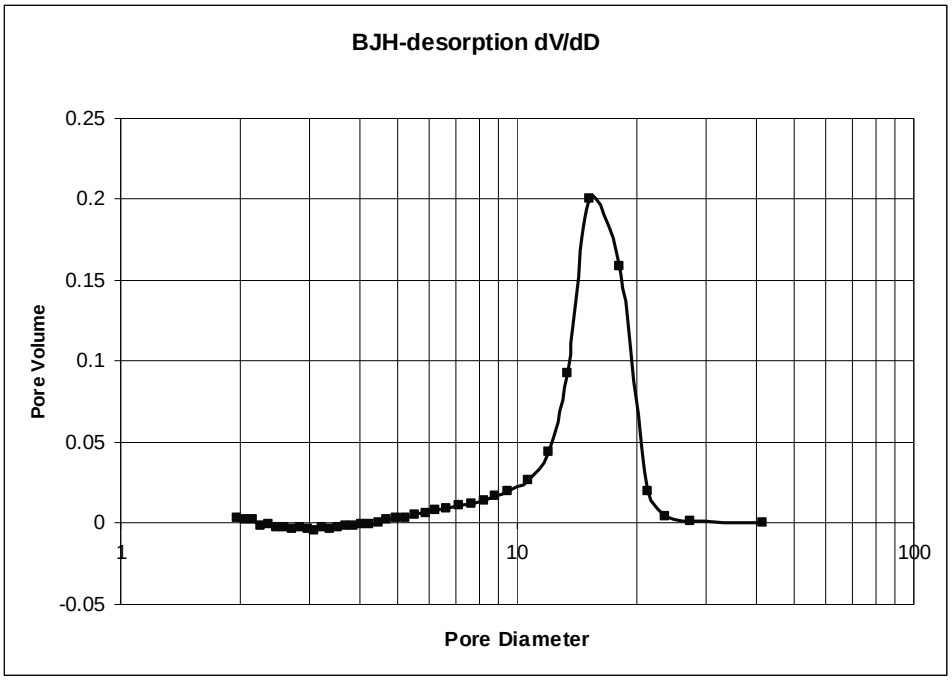

Figure A1 Pore size distribution of TCPSi particles.

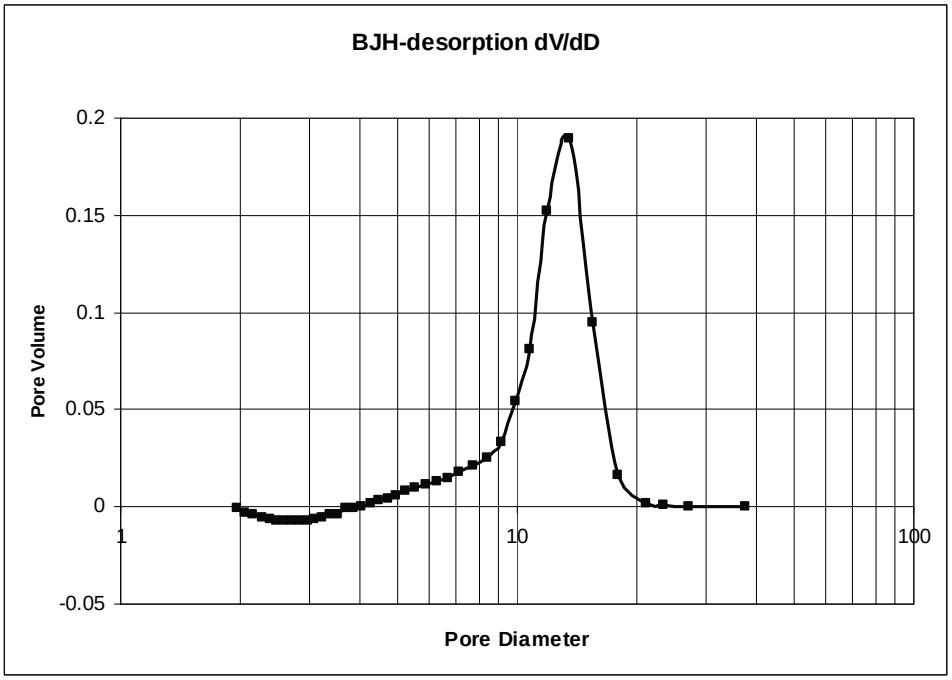

Figure A2 Pore size distribution of TOPSi-particles.

B Solubility curves

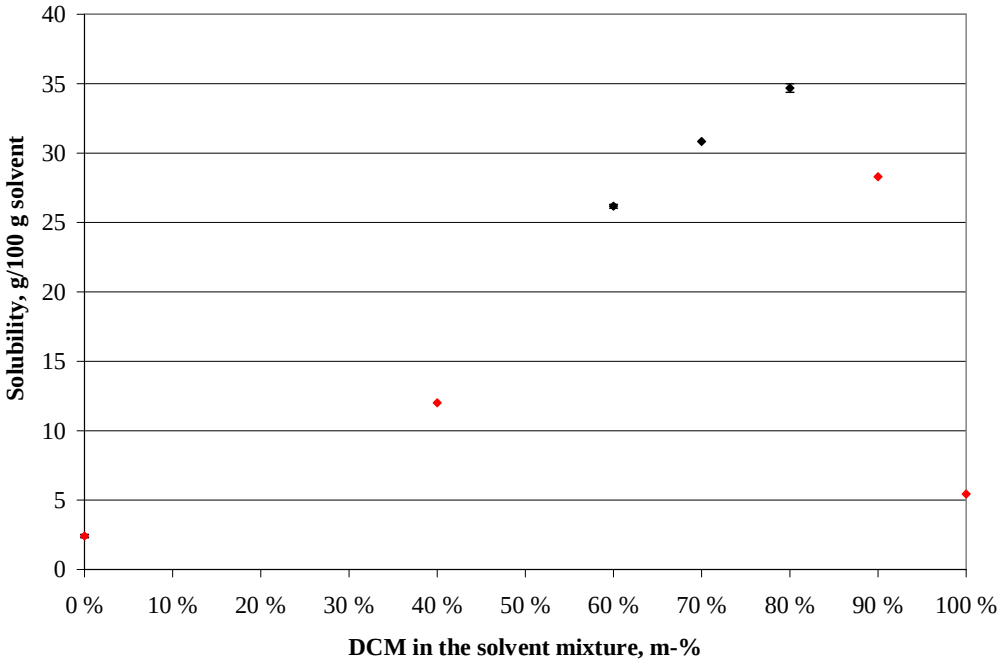

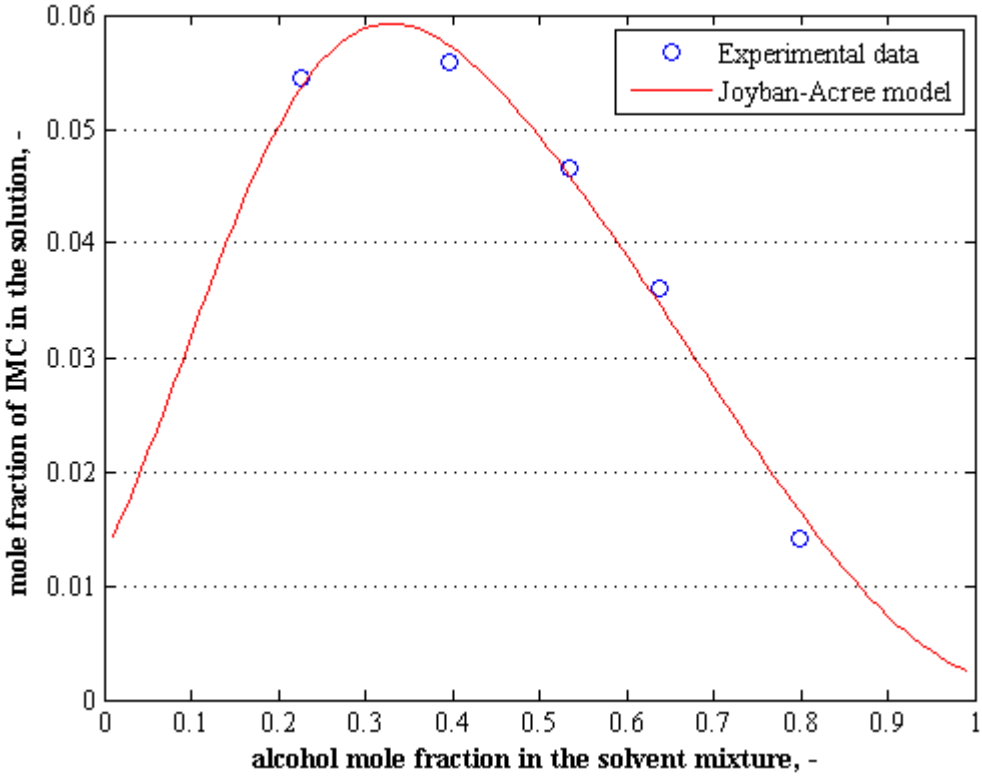

Figure B1 The solubility of of IMC in DCM–methanol mixtures. Red points denote the presence of solvates in the solid phase.

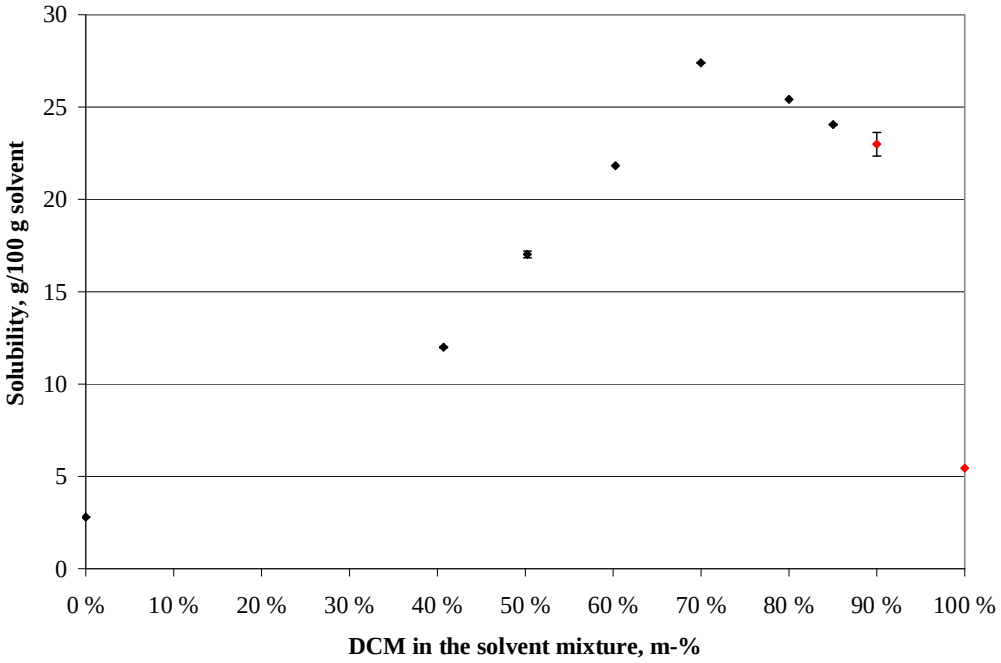

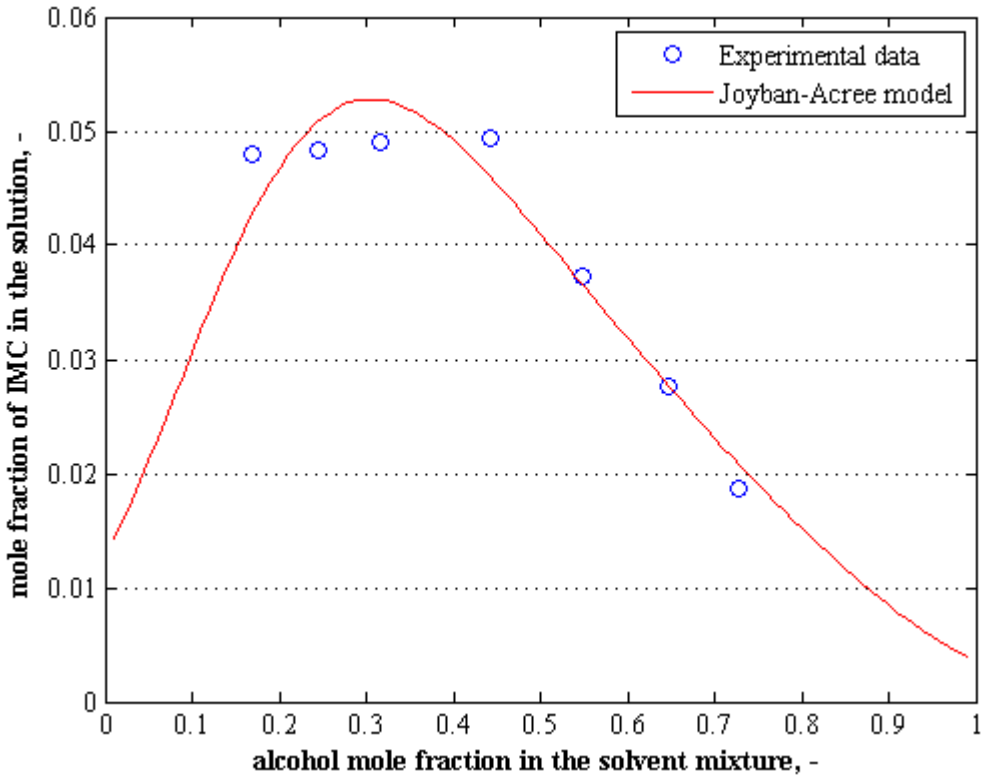

Figure B2 The solubility of of IMC in DCM–ethanol mixtures. Red points denote the presence of solvates in the solid phase.

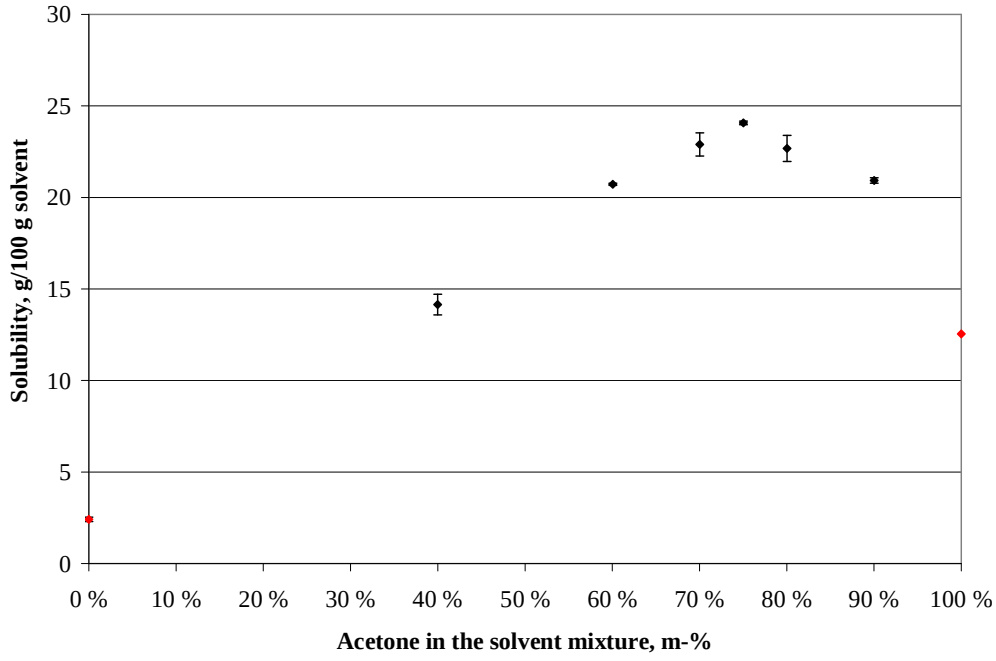

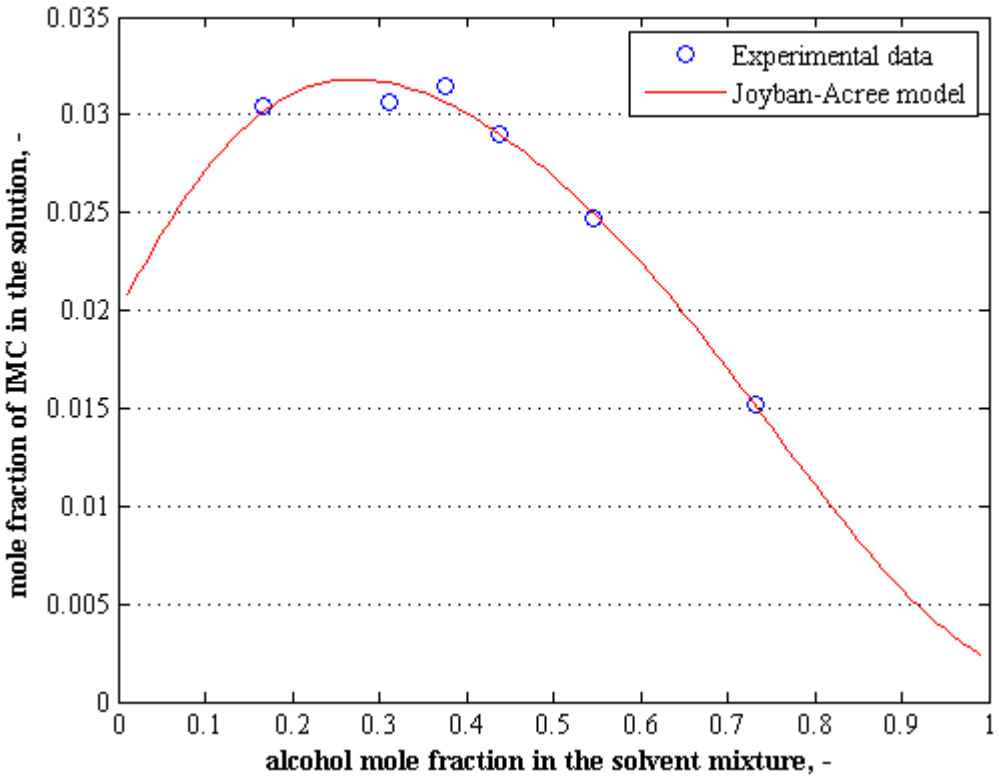

Figure B3 The solubility of of IMC in acetone–methanol mixtures. Red points denote the presence of solvates in the solid phase.

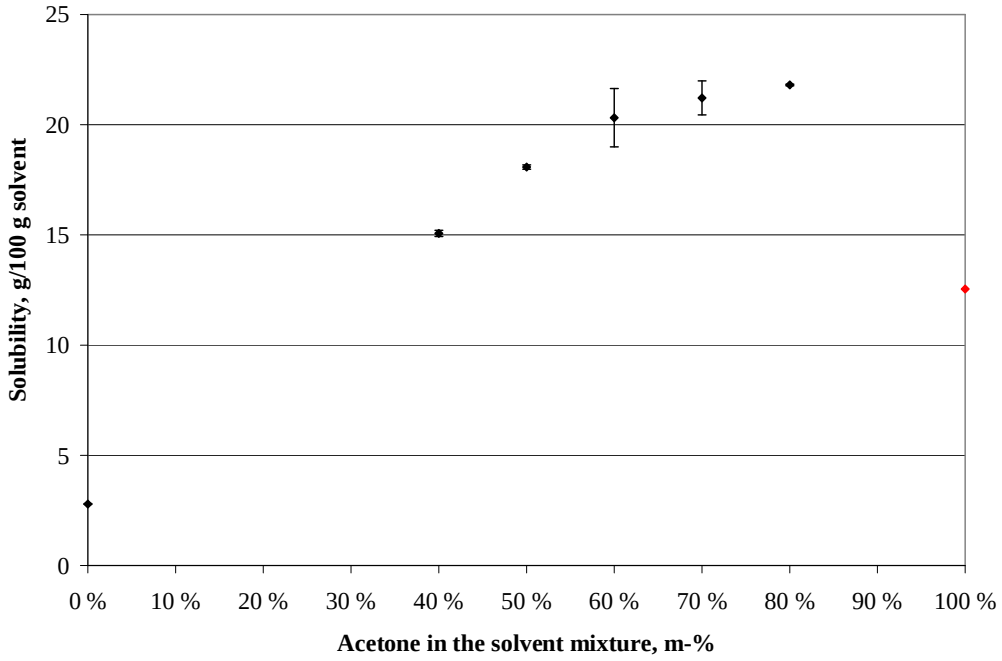

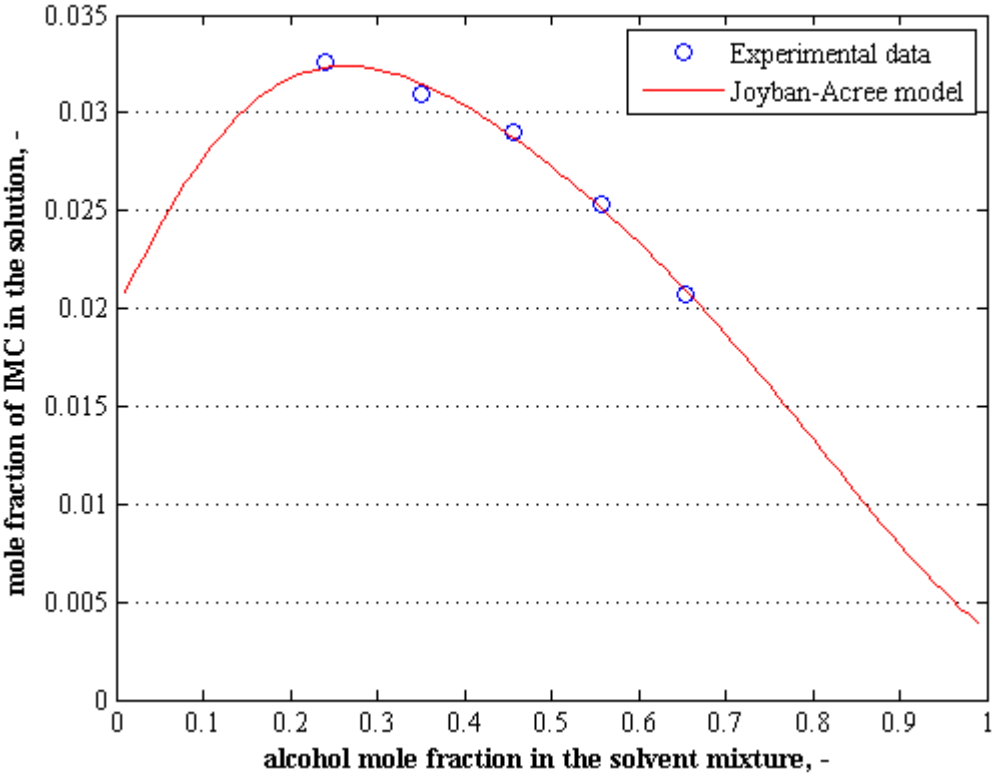

Figure B4 The solubility of of IMC in acetone–ethanol mixtures. Red points denote the presence of solvates in the solid phase.

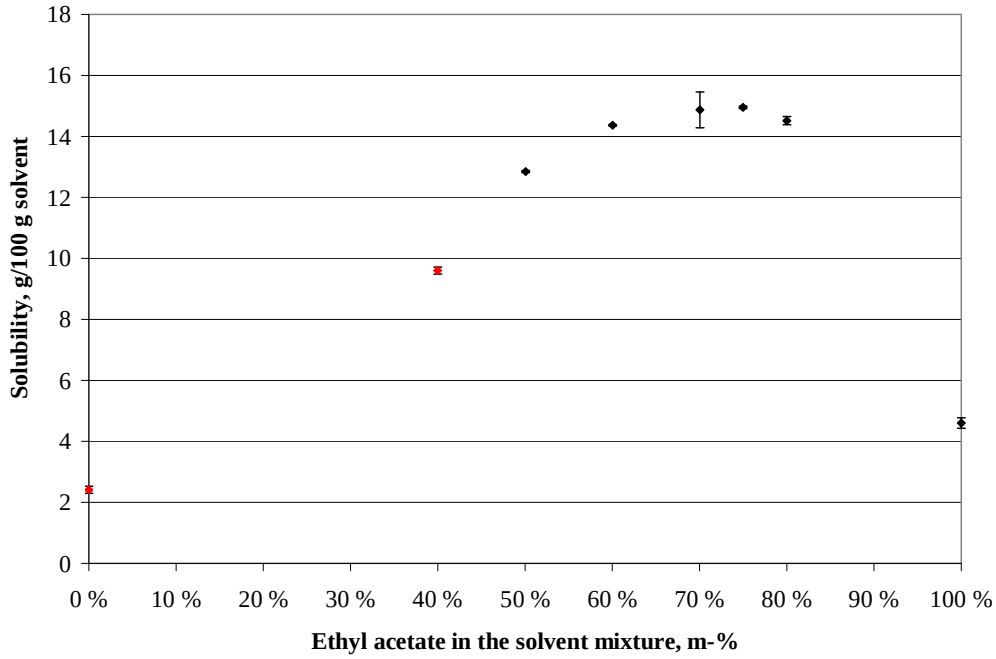

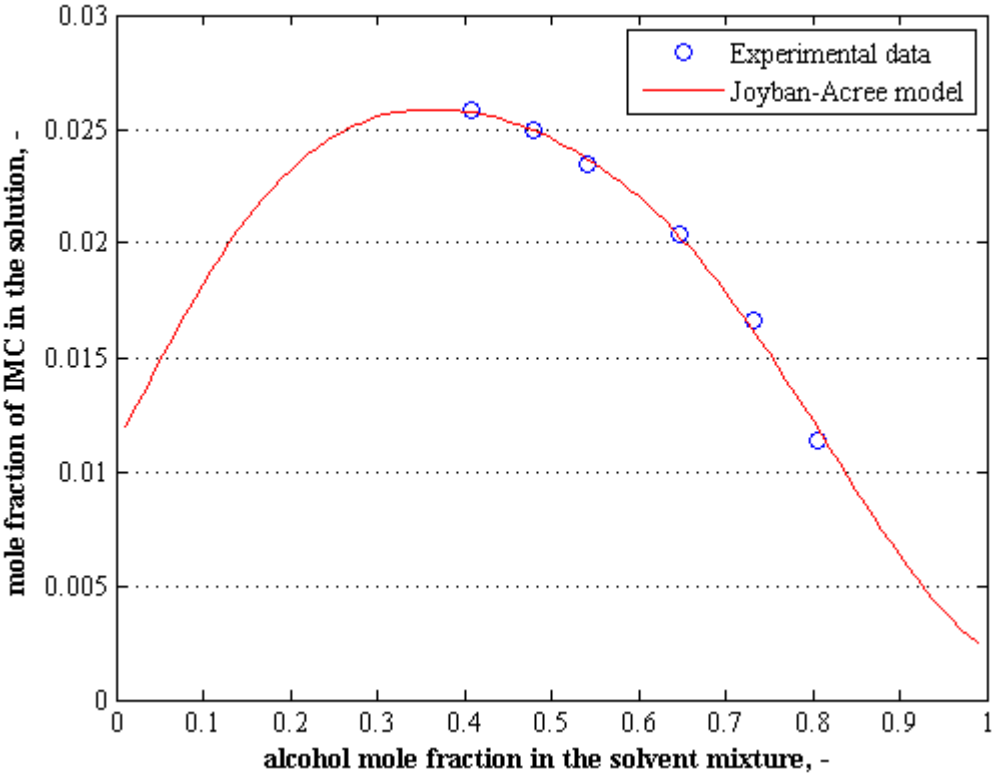

Figure B5 The solubility of of IMC in EtOAc–methanol mixtures. Red points denote the presence of solvates in the solid phase.

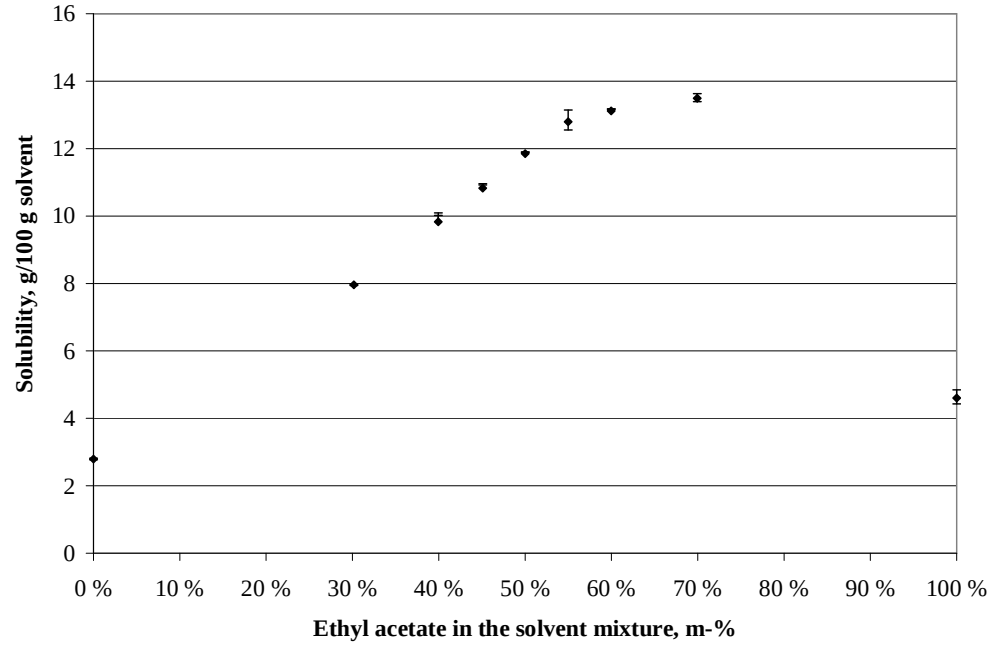

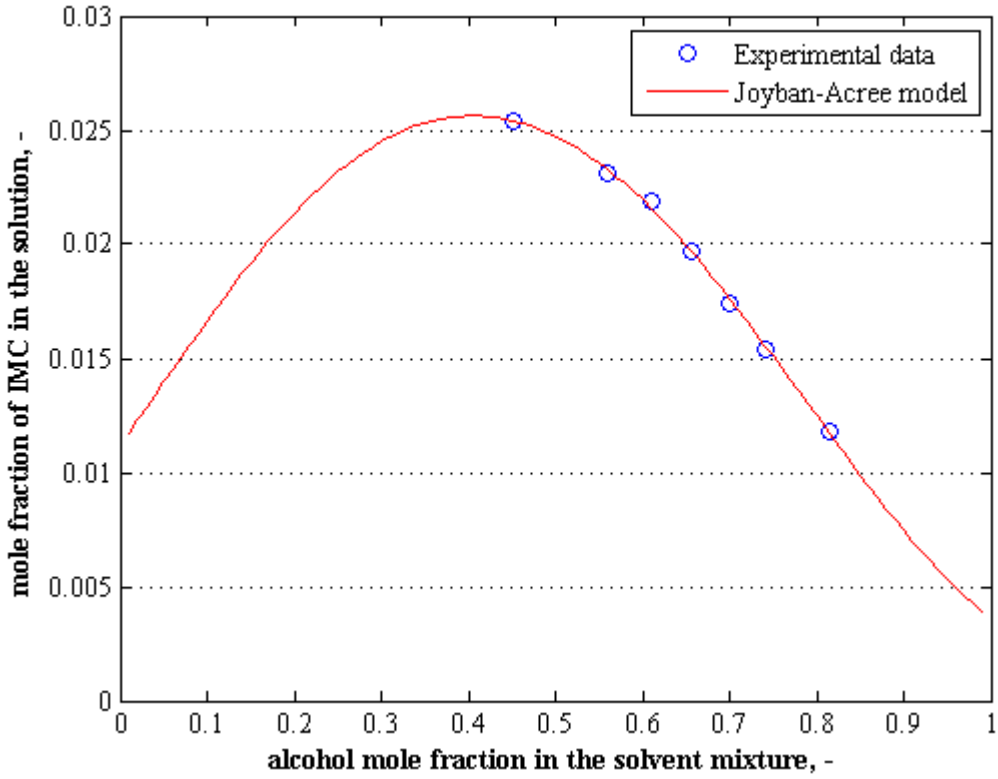

Figure B6 The solubility of of IMC in EtOAc–methanol mixtures.

C TG curves

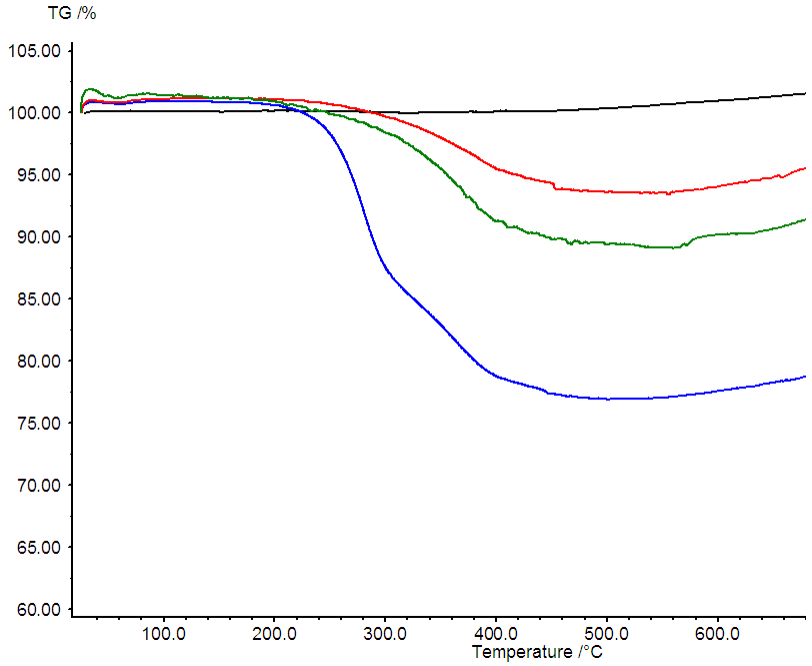

Figure C1 TG curves of the IMC loaded TOPSi particles from DCM-MeOH solution (blue), acetone-EtOH solution (green), EtOAc-EtOH solution (red), and unloaded TOPSi particles (black).

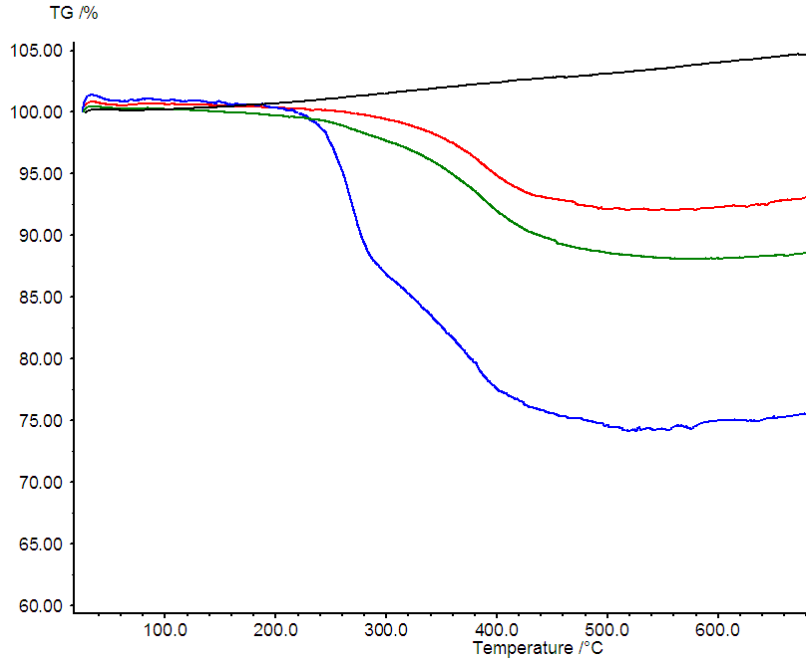

Figure C2 TG curves of the IMC loaded TCPSi particles from DCM-MeOH solution (blue), acetone-EtOH solution (green), EtOAc-EtOH solution (red), and unloaded TCPSi particles (black).

D Raman spectra of the loaded silica samples

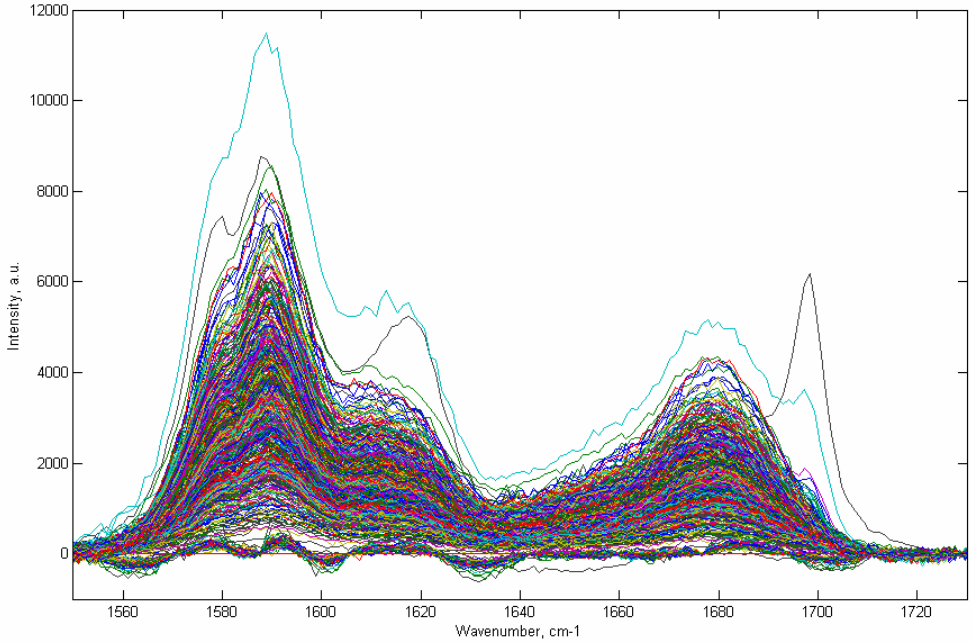

Figure D1 SBA+indo(5)

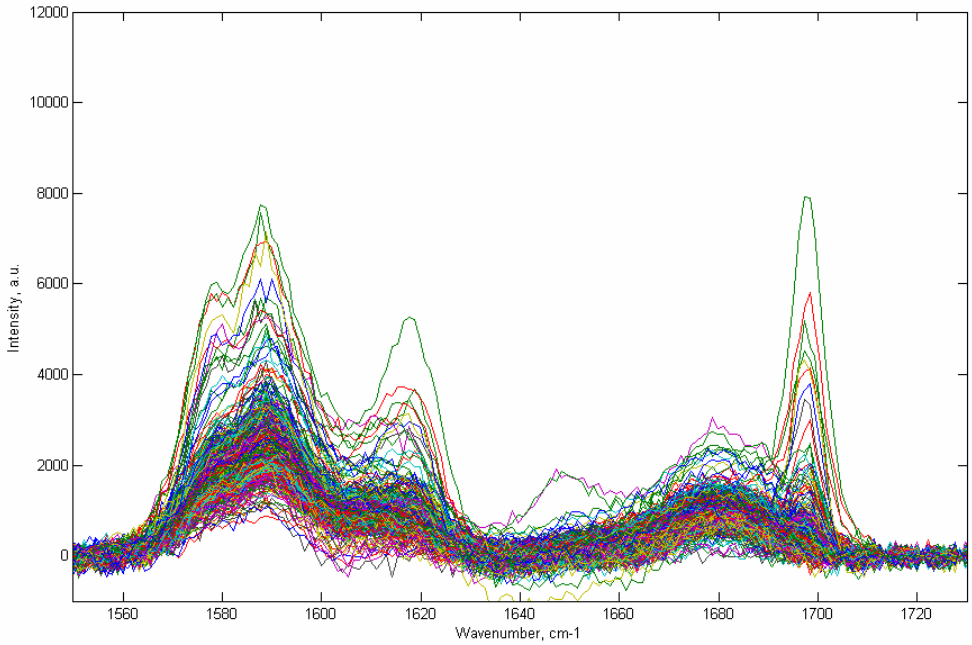

Figure D2 SBA+indo(5) stressed

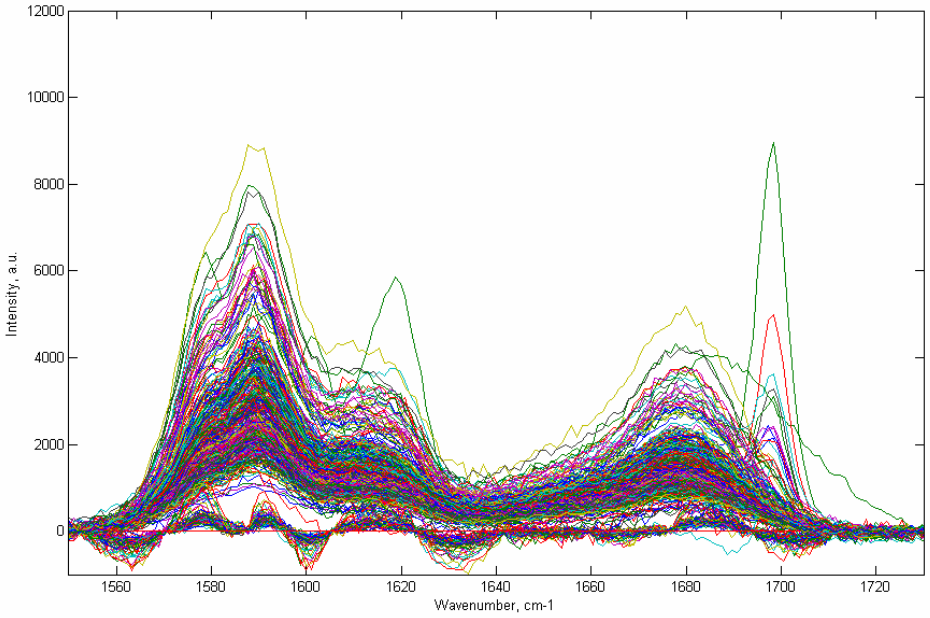

Figure D3 SBA+indo(5)-TRISTAR

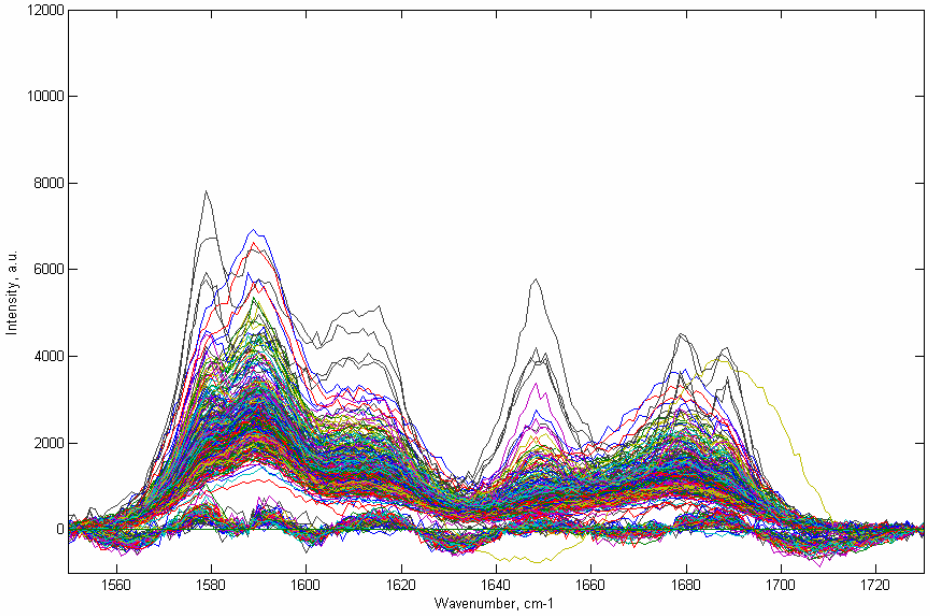

Figure D4 SBA+indo(6)-TRISTAR

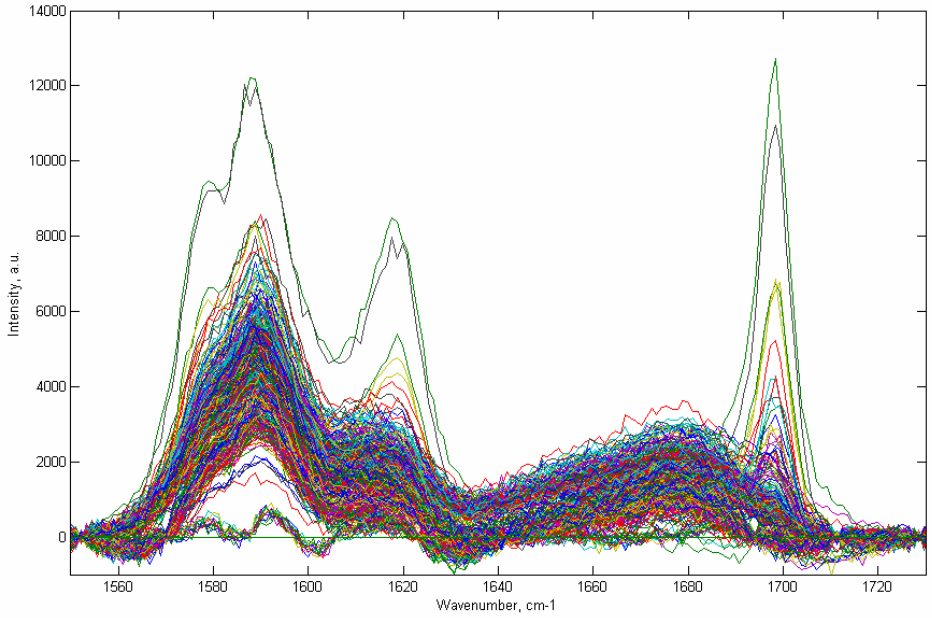

Figure D5 MCM+indo(3)-TRISTAR

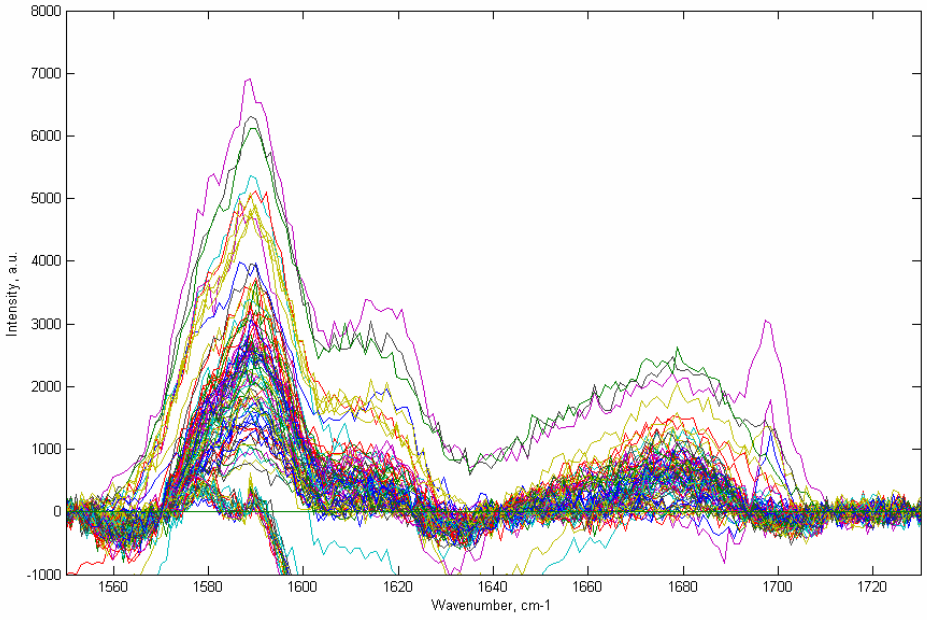

Figure D6 MCM+indo(4)-TRISTAR